

United Kingdom Atomic Energy Authority

**HARWELL**

## **U.K. Nuclear Data Progress Report**

**January - December 1984**

D J S Findlay and J A Cookson

NDS LIBRARY COPY

Nuclear Physics Division  
Harwell Laboratory, Oxfordshire

June 1985



UNCLASSIFIED

UKNDC(85)P112

NEANDC(E)262 Vol.8

INDC(UK)-039/LN

U.K. NUCLEAR DATA PROGRESS REPORT

JANUARY - DECEMBER 1984

Editors: D.J.S. Findlay and J.A. Cookson

Nuclear Physics Division  
AERE Harwell

June 1985

HL85/1489

# CONTENTS

	<u>Accelerator*</u>	<u>Page No.</u>
Contents		2
Preface		8
<u>1984 NUCLEAR DATA FORUM</u>		9
DIMPLE criticality experiments (G. Ingram)		10
The potential use of criticality benchwork experiments in nuclear data evaluation (R.J. Brissenden)		19
The use of benchwork experiments for the validation of nuclear data (A.K. McCracken)		26
CINDA-type index		29
1. <u>NUCLEAR PHYSICS DIVISION, AERE HARWELL</u>		31
Introduction		31
1.1 HELIOS - The new machine for the electron linac laboratory	E	32
1.2 Neutron transmission measurements on HELIOS in the energy range 0.01 to 10 eV	E	32
1.3 Measurements of $\eta(^{235}\text{U})$ in the energy range below 1 eV	E	35
1.4 Work related to the NEANDC Task Force investigating the discrepant resonance parameters in $^{238}\text{U}$ above 1.15 keV		36
1.5 Calculation of the neutronics characteristics of the Fast Neutron Target of HELIOS	E	37
1.6 High resolution transmission measurements on natural iron	E	38
1.7 Resonance neutron capture in $^{54}\text{Fe}$ and $^{62}\text{Ni}$	E	39
1.8 The $^{93}\text{Nb}(n,n')^{93\text{m}}\text{Nb}$ reaction		41
1.9 Fission chambers for the intercomparison of fast neutron flux density measurements	I	42
1.10 Studies of neutron induced charged particle reactions: Development of a 'phoswich' detector	D,I	43

\*For key see p.31

## CONTENTS

	<u>Accelerator*</u>	<u>Page No.</u>
1.11 Nuclear standard reference data		45
1.12 Neutron energy standards		45
1.13 Nuclear data computer codes		45
1.13.1 The computer code NJOY		45
1.13.2 FISPIN on the Harwell computer		46
1.14 Nuclear materials assay		47
1.14.1 Fissile material assay by neutron interrogation		47
1.14.1.1 Matrix effects in the assay of fissile material in 200 litre drums		47
1.14.1.2 The assay of fissile material in 200 litre drums: spatial variability of response		51
1.14.1.3 Monitoring of 500 litre drums by neutron interrogation		51
1.14.1.4 Pulsed neutron source development		52
1.14.2 Fast shuffler		53
1.14.3 Evaluation of possible methods of monitoring the $^{235}\text{U}$ enrichment of centrifuge plants operating at low pressure		53
1.14.4 The effects of neutron multiplication on neutron coincidence counter measurements		55
1.15 Neutron diagnostics for JET		57
1.15.1 Neutron yield monitors (time resolved)		57
1.15.2 Neutron yield calibration		57
1.15.3 Time-integrated neutron yield monitor	I	57
1.15.4 Neutron spatial emission profile monitor		59

\*For key see p. 31

## CONTENTS

	<u>Accelerator*</u>	<u>Page No.</u>
1.15.5 2.5 MeV neutron spectrometer for deuterium plasmas		60
1.15.6 14 MeV neutron spectrometers for deuterium-tritium plasmas		60
1.15.6.1 Si diode spectrometer	A,I	60
1.15.6.2 Annular radiator proton recoil spectrometer		63
1.15.6.3 Design of shielded enclosure for both spectrometers		64
2. <u>CHEMICAL NUCLEAR DATA</u>		66
2.1 Introduction		66
2.2 Measurement work		66
2.2.1 Nuclear reaction studies designed to test methods for the measurement of data for reactor development and isotope production		66
2.2.2 On-line chemical separations of short-lived nuclides in fission and other nuclear reactions		67
2.2.3 Transfer reactions in the system $^{92}\text{Mo} + ^{16}\text{O}$		70
2.2.4 Direct transfer reactions in the heavy ion systems $^{12}\text{C}$ , $^{14}\text{N}$ , $^{16}\text{O} + ^{197}\text{Au}$		73
2.2.5 Integral nuclear reaction rate measurements of transactinium nuclides in defined neutron spectra		77
2.2.6 Participation by AERE in the IAEA Co-ordinated Research Programme on the Measurement and Evaluation of Transactinium Nuclear Decay Data		77
2.2.7 Transactinium half-life, alpha energy and emission probability measurements		79
2.3 CNDC Data Library Sub-committee		80
2.3.1 Data library development		80

\*For key see p.31

## CONTENTS

	<u>Page No.</u>
2.3.2 Fission yields	83
2.3.3 Joint Evaluated File (JEF)	84
2.3.4 CASCADE	84
3. <u>REACTOR PHYSICS DIVISION, AEE WINFRITH</u>	85
3.1 Nuclear data evaluation and validation	85
3.1.1 Fission product data	85
3.1.1.1 Fission product yields	85
3.1.1.2 Decay heat	85
3.1.2 IAEA Co-ordinated Research Programme on transaction decay data	85
3.1.3 Few-group capture cross-sections of $^{231}\text{Pa}$ and $^{230}\text{Th}$ in FISPIN	85
3.1.4 Three-group actinide cross-sections	86
3.1.5 Benchwork testing of the JEF-1 library	86
3.2 Theoretical methods	86
3.2.1 Level statistics in the unresolved resonance region	86
3.3 Cross-section processing codes	86
3.3.1 NJOY/SIGAR	86
3.3.2 NJOY/ACER	86
3.3.3 Code implementation and testing on the Harwell computers	86
4. <u>DIVISION OF RADIATION SCIENCE AND ACOUSTICS, NATIONAL PHYSICAL LABORATORY</u>	87
4.1 Californium neutron source emission rate intercomparisons	87
4.2 Fast neutron fluence intercomparisons	87
4.3 Investigation of the $^{45}\text{Sc}(p,n)^{45}\text{Ti}$ reaction	87
4.4 Neutron yield from the spontaneous fission of $^{252}\text{Cf}$	88

## CONTENTS

	<u>Page No.</u>
4.5 The ratio of hydrogen to manganese thermal neutron capture cross-sections and its impact on the measurement of neutron source emission rates by manganese bath techniques	89
4.6 The thermal neutron capture cross-section of $^{55}\text{Mn}$	90
4.7 Nuclear decay scheme measurements	90
5. <u>DEPARTMENT OF PHYSICS RADIATION CENTRE, UNIVERSITY OF BIRMINGHAM</u>	92
5.1 Delayed neutron measurements	92
5.1.1 Further delayed neutron spectrum measurements	92
5.1.2 Comparison of existing data	92
5.1.3 Improved utilisation of data from delayed neutron measurements	92
6. <u>DEPARTMENT OF PHYSICS, UNIVERSITY OF EDINBURGH</u>	94
6.1 The use of a deuterated scintillator for in situ neutron spectrometer	94
7. <u>DEPARTMENT OF MATHEMATICS AND PHYSICS, UNIVERSITY OF ASTON IN BIRMINGHAM</u>	97
7.1 Multiple neutron scattering effects in $^7\text{Li}$	98
8. <u>DEPARTMENT OF PHYSICS, UNIVERSITY OF EDINBURGH</u>	102
8.1 The polarisation and differential cross-section for elastic scattering of 3 MeV neutrons	102
8.2 Polarisation of neutrons from the $^7\text{Li}(\text{d},\text{n})^8\text{Be}$ reaction	102
8.3 2.5 MeV neutron elastic and inelastic differential scattering cross-sections	102
8.4 Inelastic scattering of 14 MeV neutrons by Bi	102
9. <u>NUCLEAR PHYSICS LABORATORY, UNIVERSITY OF OXFORD</u>	103
9.1 Neutron inelastic scattering	103
9.1.1 The inelastic scattering of neutrons by $^{238}\text{U}$	103
9.1.2 The inelastic scattering of neutrons by $^{232}\text{Th}$	103
9.2 The neutron optical potential	103



## CONTENTS

	<u>Page No.</u>
9.3 Neutron reaction cross-section calculations	104
9.3.1 Neutron scattering and reactions on $^{59}\text{Co}$ from 1 to 20 MeV	104
9.3.2 Neutron scattering and reactions on $^{93}\text{Nb}$ from 1 to 20 MeV	104
9.4 Pre-equilibrium processes	104
9.4.1 Pre-equilibrium processes in the reactions of neutrons on $^{59}\text{Co}$ and $^{93}\text{Nb}$	104
9.4.2 Pre-equilibrium processes in nuclear reactions	105
10. <u>DEPARTMENT OF PHYSICS, UNIVERSITY OF LIVERPOOL</u>	106
10.1 Nuclear data evaluation	106

## PREFACE

This report is prepared at the request of the United Kingdom Nuclear Data Committee (UKNDC) and summarises nuclear data research in the UK between January and December 1984.

Nuclear data are presented by laboratory. There are contributions this year from the Harwell and Winfrith Laboratories of the UKAEA, the National Physical Laboratory, the Birmingham Radiation Centre, the University of Birmingham, the University of Aston in Birmingham, the University of Edinburgh, the University of Oxford, and the University of Liverpool.

This report includes work from various collaborations involving Harwell, Winfrith, the Universities of Oxford, Birmingham and Manchester, the National Physical Laboratory, the Physikalisch-Technische Bundesanstalt (Braunschweig, W. Germany) and Hammersmith Hospital. Contributions on Chemical Nuclear Data are gathered by the Chemical Nuclear Data Committee (CNDC) and grouped under that heading.

Contributions to the report on nuclear data topics are welcome from all sources, and we extend an invitation to researchers in other laboratories of industry, government, universities and polytechnics to use this medium.

Where the work is clearly relevant to requests in WRENDA 83/84 (INDC(SEC)-88/URSF), request numbers are given after the title of the contribution.

## 1984 NUCLEAR DATA FORUM

The eighteenth Nuclear Data Forum took place at AEE Winfrith on 18 December 1984. Three invited lectures were delivered: on DIMPLE criticality experiments (G. Ingram, AEE Winfrith), on the potential use of criticality benchmark experiments in nuclear data evaluation (R.J. Brissendon, AEE Winfrith) and on the use of benchmark experiments for the validation of nuclear data (A.K. McCracken, AEE Winfrith). These three lectures are reproduced in this report. Those were eight contributed talks:

Evaluation of the thermal neutron constants of  $^{233}\text{U}$ ,  $^{235}\text{U}$ ,  $^{239}\text{Pu}$  and  $^{241}\text{Pu}$  and the fission neutron yield of  $^{252}\text{Cf}$   
E.J. Axton

Integral adjustments to nuclear data in the thermal energy region  
M.J. Halsall (AEE Winfrith)

Report on the NEANDC Task Forces on the resonance parameters and capture cross-section of  $^{238}\text{U}$  and resonance parameters of the 1.15 keV resonance in  $^{56}\text{Fe}$   
M.C. Moxon and M.G. Sowerby (AERE Harwell)

Summary report of the IAEA Group Meeting on Nuclear Standards Reference Data (Geel, November 1984)  
A.J. Deruytter (CBNM, JRC-Geel)

Iron filtering of reactor neutrons  
K.G. Harrison, R. Birch, L.H.J. Peaple, J.H. Delafield and C.A. Perks (AERE Harwell)

Report on the IAEA Co-ordinated Research Programme on transactinium isotope decay data  
A.J. Fudge (AERE Harwell)

Measurements of gamma-ray intensities following resonance neutron capture in  $^{54}\text{Fe}$  and  $^{62}\text{Ni}$   
J.P. Mason and B.H. Patrick (AERE Harwell)

The  $(\gamma, f)$  and  $(\gamma, n)$  reactions in  $^{232}\text{Th}$  and  $^{238}\text{U}$  between 5 and 10 MeV  
D.J.S. Findlay, N.P. Hawkes, M.R. Sené and G. Edwards (AERE Harwell)

## DIMPLE Criticality Experiments

G. Ingram

Reactor Physics Division, AEE Winfrith

Lecture given at the Nuclear Data Forum, AEE Winfrith, Dec. 1984

### 1. Introduction

DIMPLE is a water-moderated zero-power reactor, located at AEE Winfrith. Ten to twenty years ago it was used to validate water reactor calculational methods and, in particular, to support the design of the Winfrith Steam Generating Heavy Water Reactor. Recently the plant has been refurbished to validate the methods and data applied to assess criticality hazards arising in the manufacture, transport, storage and reprocessing of reactor fuel. Operation of the reactor in its new role began in Sep. 1983. Descriptions of the plant, the first series of experiments and future plans are outlined below.

### 2. Description

The overall layout of the plant is illustrated in Fig. 1. The reactor consists essentially of a large aluminium tank, 2.6 m in diameter and 4 m high. It is enclosed in a steel-lined concrete block shield, which provides a secondary containment. Stainless steel pipes link the reactor tank, through dump valves, to dump tanks located in a pit. These accommodate the moderator when the reactor is shut down and are also enclosed in a steel-lined secondary containment. Additional circuits allow heating, cooling and clean-up of the moderator.

To maintain clean core geometries in the present work, the reactor is controlled by water level alone. Initially, water is added to the reactor tank by means of a coarse pump. This is inhibited at a predetermined level, below the fuel, and water is then added or removed in precisely regulated amounts by a fine pump. A weir, external to the reactor tank, dictates the maximum water level that can be achieved. The depth is monitored by a range of probes, the most accurate of these giving readings to  $\pm 0.1$  mm.

The reactor power level is monitored by a series of boron detectors located in submersible pods adjacent to the core. These cover the range of seven decades from shut-down up to the maximum operating power, which corresponds to a peak power density of 20 watts  $\text{kg}^{-1}$  of  $^{235}\text{U}$ . If the reactor power exceeds this maximum value or if the rate of change of reactor

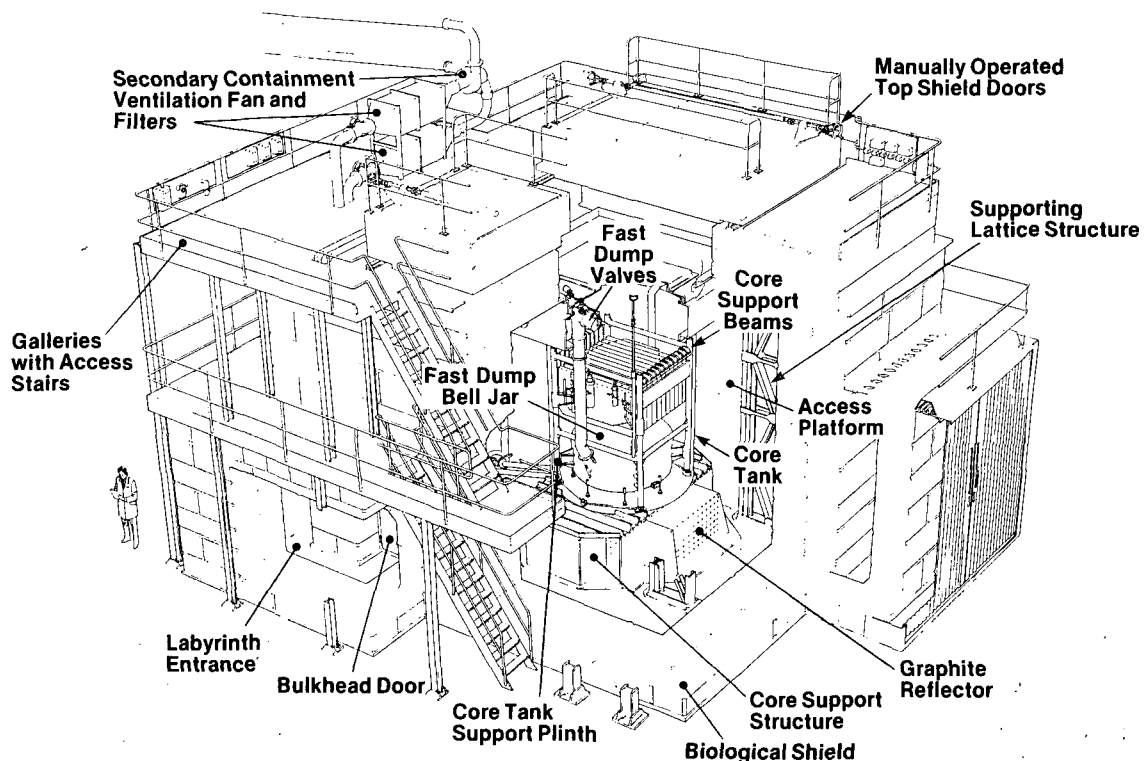


Fig. 1 General view of DIMPLE reactor

power exceeds a pre-set level the reactor is automatically shut down.

Shut-down is achieved by means of a fast dump system. This lowers the water level in the reactor tank by 30 cm in about 1 s, which is sufficient to compensate for the most extreme transients which could be induced by incorrect operation of the plant. The principal features of the fast dump system are illustrated in Fig. 2. It consists essentially of a bubble of air, trapped in a 2 m diameter stainless steel bell jar located under the core. To shut down, the bubble is vented through fast dump valves to the air space at the top of the reactor tank. Draining of the reactor tank, via partial dump and main dump valves, then follows automatically.

Approximately 4 tonnes of uranium oxide fuel, in the form of 10 mm diameter sintered pellets, is available for use in DIMPLE. The enrichments range from 2% to 7%, with most of the fuel being at 3% enrichment. Some mixed-oxide fuel is also available to provide a simulation of irradiated



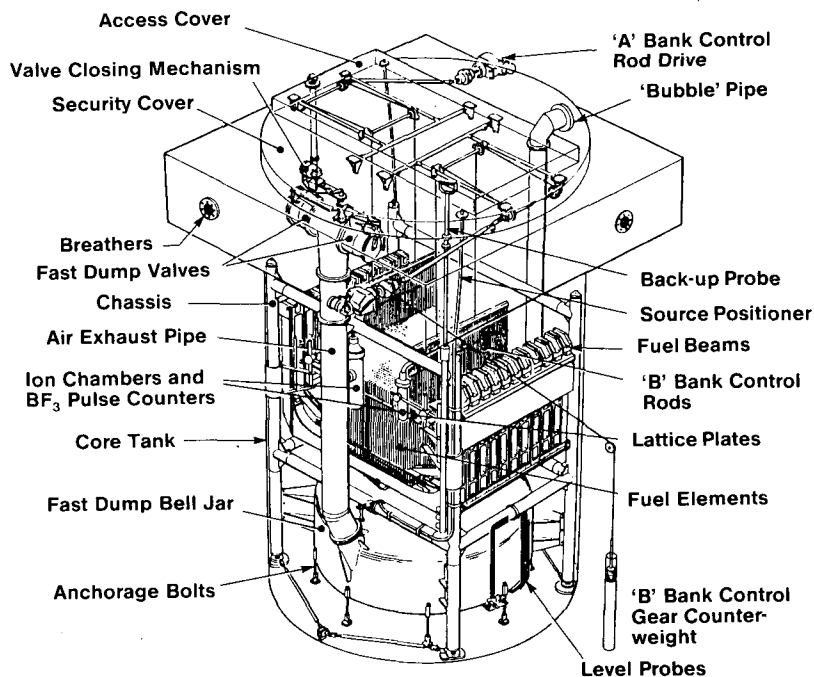


Fig. 3 General arrangement of core

virtually no extreme accident simulations and little diagnosis of the sensitivity of the calculated results to any residual deficiencies in the nuclear data in the codes. Thus if the demands of a cost-conscious industry to reduce margins in error are to be met, then further high accuracy experiments guided by calculation and backed up by diagnostic measurements are important. To meet these requirements, the primary aims of the DIMPLE experimental programme are then to:

- (a) validate the methods under development for criticality predictions and to establish realistic estimates of the associated uncertainties;
- (b) define benchmarks in areas where experimental data are sparse and where the need for precise data is likely to become of increasing importance to designers;
- (c) undertake close simulation of particular designs, under normal and accident conditions, to minimise uncertainties in the assessments for these designs.

Experiments will be designed not only to establish the critical size or k-value, but also to probe for possible compensating errors in the methods

and data applied in the predictions. This is important if the conclusions from the relatively idealised geometry of the experiments are to be applied, with a high level of confidence, to the more complex geometries normally encountered in plant and flask designs. These additional experiments will include measurements of the reaction rates of prime importance to the neutron balance, fine structure measurements and reaction rate distributions through the assemblies. The programme will include both critical and subcritical experiments to extend the range of lattice parameters and to allow mock-ups of practical configurations. This subcritical work provides an ideal opportunity to pursue a further aim of investigating the feasibility of developing a reliable, mobile plant instrument for monitoring subcriticality.

### 3.2 Assembly S01

The first series of experiments in this new programme was based on arrays of steel clad 3% enriched uranium oxide pins in light water. For the first assembly, a rebuild of an earlier<sup>(1)</sup> DIMPLE benchmark R1/100H, the pins were arranged in a simple cylindrical configuration, with a high neutron leakage (about 20% of the neutrons leaking from the core). These studies served a dual purpose: they allowed the benchmark data to be reassessed using up-to-date experimental techniques; and they also provided a clean geometry reference assembly for the subsequent programme, where about 20% of the neutrons were absorbed in a boron steel walled CAGR skip. The lattice loading for assembly S01, which is illustrated in Fig. 4, comprises an array of 1565 pins with a fuel length of just under 700 mm on a square 13.2 mm pitch. The results from this first assembly are currently being compared with prediction and have been instrumental in identifying a number of errors in standard calculation methods. Some preliminary values are shown in Table 1, where it can be seen that the most striking difference between the present and earlier values is in the measurement of the  $^{238}\text{U}$  capture rate relative to the fission rate in  $^{235}\text{U}$ . Investigation has revealed that this difference, which is just over 3%, is due to an underestimate of the fission product correction to the  $^{238}\text{U}$  capture results.

At the request of BNF plc some measurements of the worth of hafnium were included in the programme. These show good agreement with WIMS data within the accuracy of the measurements (see Table 2).



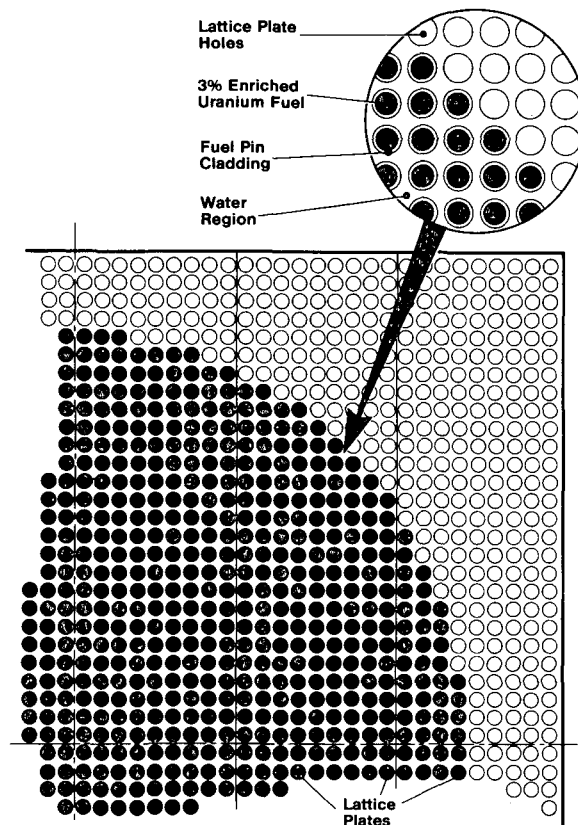


Fig. 4 One quarter of cylindrical geometry pin lattice, 3% enriched uranium, 13.2 mm pitch

### 3.3 Assembly S02

The second DIMPLE assembly S02 makes use of a 20 compartment, boron steel walled CAGR skip insert. This provides a realistic environment for generic studies and for the development of subcritical monitoring techniques. Similar skips are used by the CEGB for the transport of irradiated fuel, and BNF plc is assessing their use for the long term storage of CAGR fuel.

The first of the CAGR skip configurations, a critical array with 3% enriched uranium oxide pins, was loaded in March this year. This represented a gross overloading of a flask and provided a suitable reference for the subsequent subcritical studies, which are more typical of normal transport and storage arrangements.

Table 1

Preliminary comparison of SOL results with the R1/100H values  
and WIMS predictions

Parameter	R1/100H	SOL	C/E (SOL)
Critical water height (cm)	48.8 ± 0.1	49.4 ± 0.1	
Axial buckling (m <sup>-2</sup> )	24.51 ± 0.19	24.09 ± 0.10 (fission chamber)  24.20 ± 0.20 (activation foils)	
k-value			1.000 ± 0.001
Water height coeff. (dk/k per cm)	0.248 ± 0.011	0.243 ± 0.012	1.082 ± 0.054
Central reaction rate ratios:			
<sup>238</sup> U fission/ <sup>235</sup> U fission	0.0029 ± 0.0003	0.00307 ± 0.00015	0.928 ± 0.046
<sup>238</sup> U capture/ <sup>235</sup> U fission (lattice/thermal)	4.15 ± 0.03	4.29 ± 0.02	0.973 ± 0.006
<sup>239</sup> Pu fission/ <sup>235</sup> U fission (lattice/thermal)	1.589 ± 0.010	1.607 ± 0.010	0.989 ± 0.006
<sup>235</sup> U fission fine structure (relative to fuel):			
fuel can	1.130 ± 0.009	1.112 ± 0.007	1.008 ± 0.006
moderator	1.261 ± 0.013	1.221 ± 0.007	1.013 ± 0.006

- Notes: (1) Both modified diffusion theory GOG and transport theory TWOTRAN using two-dimensional models with the experimental buckling applied yielded the same C/E for the k-value.
- (2) The water height coefficient was calculated using GOG, the central reaction rate ratios were obtained with TWOTRAN, and CACTUS was used for the fine structure calculations.

Table 2

Comparison of central reactivity worth measurements  
with LWR WIMS predictions

Sample	Percentage change in reactivity		
	measured	calculated	C/E
four fuel pins out	$+0.219 \pm 0.007$	+0.237	$1.08 \pm 0.03$
one 10 mm diameter boron/aluminium rod in	$-0.374 \pm 0.039$	-0.395	$1.06 \pm 0.10$
one 5 mm diameter hafnium rod in	$-0.265 \pm 0.019$	-0.268	$1.01 \pm 0.07$
four 1 mm diameter hafnium wires in	$-0.104 \pm 0.012$	-0.113	$1.09 \pm 0.12$

Note: Only the random errors are shown above. There is also a systematic error of about  $\pm 5\%$ , arising from delayed neutron uncertainties in the absolute reactivity calibration.

A total of seven fully flooded subcritical arrays, with simulated fuel clusters, have been studied so far. These have been used for investigating the influence of cluster size and, at the request of BNF plc, the influence of the radial location of the cluster within a compartment. The Modified Source Multiplication technique<sup>(2)</sup> has been used throughout to establish the k-values, which are in the range of 0.8 to 0.9, and the experimental uncertainties in the k-values are currently estimated to be about 0.01. Some exploratory cross-correlation and auto-correlation noise analyses have also been completed to cross-check the k-values obtained.

Preliminary comparisons of the results obtained so far with WIMS and MONK6 predictions show reasonable agreement (to within  $\pm 0.02$  in the k-value) although there is some evidence that calculation tends to overestimate the reactivity changes as the clusters are moved radially within the compartments.

### 3.4 Future Experiments

The programme with the skip insert has aroused wide interest, and measurements will continue next year. This future work will include the

introduction of voids between the clusters and the boron steel walls which can produce large increases in reactivity, the introduction of boron poisoning in the water and the use of higher enrichment fuel. The feasibility of introducing severe power distribution asymmetries by simulating a major loading error in the skip, with 7% enriched uranium oxide pins, is also under investigation. These experiments are being planned in collaboration with the CEA (Fontenay-au-Roses and Valduc) and are expected to attract CEC funding.

Other experiments in the criticality field which are currently under investigation include measurements with hafnium in a plutonium environment and studies of the influence of fuel burn-up. The first of these relates to plutonium separation column design. The second, although meeting a specific request for information relevant to the design of fast reactor fuel dissolvers, represents an area that is likely to expand and become of increasing importance in future criticality assessments. To meet other requests, future feasibility studies will also include uranium and plutonium solutions and mixed-oxide fuels with small amounts of hydrogen moderation.

#### 4. Conclusion

The DIMPLE plant and the current programme of criticality experiments have been outlined. The response of the nuclear industry to this work has been encouraging and confirms the need for a continuing programme in this area.

---

- (1) W.A.V. Brown et al. report AEEW-R 502.
- (2) J.M. Stevenson et al. Experience with Sub-Critical Monitoring in Large Critical Assemblies, Symposium on Fast Reactor Physics, Aix-en-Provence, 1979.

The Potential Use of Criticality Benchmark Experiments  
in Nuclear Data Evaluation

R.J. Brissenden

Reactor Physics Division, AEE Winfrith

Lecture given at the Nuclear Data Forum, AEE Winfrith, Dec. 1984

1. Introduction

The presence of significant systematic errors even in the latest nuclear data compilations can be shown by making Monte Carlo calculations for critical systems. In the present work, calculations have been made for forty-four critical systems. Modelling errors, which used to plague such calculations, have been eliminated, and discrepancies between calculated and experimental eigenvalues of critical systems can now be confidently ascribed to errors in the nuclear data. The Monte Carlo code MONK is particularly suitable for these calculations.

2. Monte Carlo Computer Code MONK6

MONK6 is now the standard UK criticality code and is used extensively to establish the criticality condition of various proposed assemblies. The quantity computed is  $k_{\text{eff}}$ , the fundamental eigenvalue of the multiplying system. When the system is critical  $k_{\text{eff}} = 1$ ; subcritical systems have  $k_{\text{eff}} < 1$ . MONK6 stands out because of its point energy capability and because of its superior geometrical representation. MONK6 uses a collision-processing system called DICE which is able to use very detailed point energy representations of the nuclear data. This system is coded as a standard module which fits also into MCBEND, the UK standard shielding code. In addition, MONK6 already has the geometrical and compositional input data prepared for many high-quality critical experiments so that evaluators can try out different versions of the nuclear data very easily. There are also comprehensive facilities for making small adjustments to the data to see the effects of such changes on the eigenvalues.

An example of the representation of nuclear data used by MONK6 is the  $^{239}\text{Pu}$  fission cross-section between 0.1 eV and 0.1 MeV. The cross-section values come from the 1972 evaluation of MacDougall, which based on the resonance parameters of Ribon and Lecoq (1971), the resonances being resolved up to 600 eV. Above the resolved region the resonance structure is formed as a random ladder of s- and p-wave resonances. These have been

sampled using mean parameters in appropriate theoretical distributions. The mean parameters are estimated from the resolved region, appropriate penetration factors and statistical spin factors being assigned by theory; the distribution theory includes the channel theory of fission and the strong interference effects described by Lynn in about 1965. There are also corrections for distant levels and phase shift factors. Above a few hundred eV the ultra-fine detail of the resonance structure is smoothed by a sub-grouping algorithm, the data merely preserving sufficient oscillations to deal with self-shielding effects in neutronics calculations at constant temperature. Above the ladder region, at about 25 keV and ranging up to about 700 keV, a statistical sub-group algorithm is used to apply a self-shielding oscillation to the mean cross-section from the evaluation by MacDougall. The mean parameters for the Gaussian distributions used in this treatment are derived from the oscillations at around 25 keV in the ladder sub-groups.

Using point-energy cross-sections and proper energy-dependent treatment of all secondary neutron production processes does slow down the MONK6 code from speeds achievable with multigroup data. There is also a big increase in the amount of fast core required. However the penalties are not too excessive, and one can normally achieve an accuracy of about 0.5% in 10 - 20 mins. on the IBM computer at Harwell using about 6 Mbyte of fast core.

There is not much point in using very accurately modelled nuclear data if one cannot treat the geometry also in great detail. However MONK6 has the most comprehensive geometry package of any Monte Carlo code available for general use: the geometry package can deal with cuboids, cylinders, spheres, truncated cones, wedges, prisms and even tori as explicit body shapes, and they may be combined in various ways: overlapping partially or completely to form composite bodies, or lined up into regular arrays and lattices of various sorts. In addition in MONK there is a HOLE geometry facility which allows the introduction of surfaces beyond the range of first and second degree algebraic equations such as screws, helical blades, spiral shapes and so on; shapes may be configured in forms much more irregular than simple lattices and arrays; and hundreds of bodies may be used without undue loss of speed.

The comprehensive facility for making temporary changes to the nuclear data to study the effects on the calculations enables the strengths of nuclear reactions to be changed by multiplicative or additive factors, and

such changes may be made repeatedly in different energy ranges. The changes to the reaction may be offset in other nominated reactions to greater or lesser extent. The scattering laws and fission laws may also be subjected to the same sorts of changes. All the modifications proposed are held in a symbolic form in a separate file, the Symbolic-Change File. When the nuclear data are read in ready for a MONK run, the user may ask for these changes to be made to the nuclear data for the duration of the run, the actual data files remaining unchanged. The Symbolic-Change File may be altered and added to at any time between runs. This provides the evaluator with a powerful tool for studying the effects of any changes he is proposing to make. MONK6 has a development programme, part of which is to install a perturbation option. If this is successful it will be possible to compute the effects of changes more cheaply and more accurately.

Finally, MONK6 is rigorously checked out before use in criticality work, and all development work is carried out in versions of the code far removed from the production version. This means that users may proceed with confidence using a code which is run on average 15 times a day for serious production purposes.

### 3. Comparison of Monte Carlo calculations with criticality benchmark experiments

The work which will now be described concerns the existence of systematic errors and the potential inherent in the criticality benchmark experiments for helping with their elimination. This work has been reported more fully as ref. 1. The features of the cross-section and geometry modelling used in MONK6 mean that the modelling errors which used to arise from the use of group constants and simplified geometry with finite difference mesh over space and angle, have been eliminated. With few exceptions, which have been noted, the experiments we use are also very well documented and have been conducted with great care and attention to detail. Even so there are errors associated with the experimental eigenvalues and these can range from 0.2% for the best experiments up to perhaps 1% for some of the more difficult experiments. In some cases bad documentation has ruled out what would otherwise be a perfectly good experiment. Such cases are usually easy to spot and eliminate. A more complicated issue has been the recent debate about acid molarity measurements, which have thrown doubt on some work on experiments involving uranyl nitrate and plutonium nitrate solutions in nitric acid. However, the chemical problems are being resolved

and new and better experiments are becoming available. We are still left with a large usable body of  $k_{\text{eff}} = 1$  experiments of undoubted quality with errors well below the Monte Carlo noise of  $\pm 0.005$ .

Before comparing Monte Carlo calculations with criticality benchmark experiments, various  $^{235}\text{U}$  2200 m s<sup>-1</sup> parameters were considered. Table 1 presents values for five  $^{235}\text{U}$  2200 m s<sup>-1</sup> parameters  $\sigma_f$ ,  $\sigma_\gamma$ ,  $\bar{\nu}$ ,  $\eta$  and  $\alpha$  from different evaluations; from left to right there is a succession of adjustments more or less in chronological order of production, apart from the MONK6.2 numbers which are the unadjusted UKNDL values based on the 1958 and 1960 evaluations of Vogt. The concurrence of these values with the W235

Table 1  
2200 m s<sup>-1</sup>  $^{235}\text{U}$  parameters

	W235	W1235	W2235	ENDF/B-V	NNDC(82)	MONK6.2	Divadeenam and Stehn (1984)
$\sigma_f$	580.4	587.4	583.8	583.5	582.9	579.3	582.6 $\pm$ 1.1
$\sigma_\gamma$	100.5	93.5	98.7	98.4	98.6	100.4	98.3 $\pm$ 0.8
$\bar{\nu}$	2.430	2.430	2.430	2.437	2.430	2.424	2.4251 $\pm$ 0.0034
$\eta$	2.071	2.096	2.079	2.085	2.078	2.066	2.0751 $\pm$ 0.0033
$\alpha$	0.173	0.159	0.169	0.169	0.169	0.173	0.1687 $\pm$ 0.0015

values on the extreme left is hardly surprising since the original WIMS file W235 was also based on Vogt's work. The progression of the WIMS files: W235, W1235, W2235 arises from successive adjustments based on integral measurements. One can see that the last of these adjustments done by Askew in about 1971 anticipated evaluation workers by about 10 years, his answers being extraordinarily close to the recent NNDC values of 1982 and the 1984 values of Divadeenam and Stehn. We regarded this concurrence as so convincing that we forthwith adjusted our thermal values to agree with the NNDC(82) results.



### 3.1 $^{235}\text{U}$ resonance region above 0.5 eV

An adjustment process for the  $^{235}\text{U}$  resonance region above 0.5 eV was carried out using the homogeneous metal and homogeneous oxide results of Darrouzet and the LEMUR experiments of Sherwin. The results of the adjustment for  $^{235}\text{U}$  are:

- a 15% reduction in captures between 30 eV and 1 keV, 90% of the reduction being offset in the fissions; and
- a 10% reduction in fissions between 5 keV and 20 keV, all of this reduction being offset in the captures.

As a result we found the resonance integrals came into line with the ENDF/B-V evaluations; 6 b of capture were transferred to fissions bringing  $I_f$  up from 276 b to 282 b, the same as ENDF/B-V, and the capture integral  $I_\gamma$  was reduced from 147 b to 140 b, compared to the 139 b of ENDF/B-V. We found too that these new values corresponded fairly closely with the WIMS file 2235. We regarded this agreement as being supportive evidence for our adjustments, although quite obviously these adjustments concern only broad details of the cross-sections.

### 3.2 $^{238}\text{U}$ data

The adjustment of the  $^{238}\text{U}$  cross-sections were carried out in conjunction with the epithermal  $^{235}\text{U}$  adjustments described in sect. 3.1 because the two cannot be disentangled in experiments. There are significant problems with the detailed epithermal  $^{235}\text{U}$  cross-sections and it is unlikely that one could correct these faults entirely by integral measurements. Hopefully one can say what their effect will be in the worst category of criticality calculation.

The  $^{238}\text{U}$  data used was compiled by James in 1972 using resolved points of Rahn (1971). The capture width was taken to be 23 meV. The resonance integral of the  $^{238}\text{U}$  data we were using was too small and we could not put it right by simple scaling because it is mainly a deficiency in the peaks. A full account of this is available in ref. 1.

### 3.3 $^{239}\text{Pu}$ $\eta$ value

Table 2 shows the 2200 m s<sup>-1</sup>  $\eta$  values for  $^{239}\text{Pu}$ . There is a marked disparity between the adjusted value of 2.093 arrived at in the present work and the evaluated number  $2.1153 \pm 0.0052$ . One can see that the operational value used in WIMS is about 4 standard deviations away from the evaluated number with its quoted error. One can see also that the MONK6.1  $\eta$  value is in agreement with the evaluated data which is hardly surprising since it has

not been altered in any way. The consequence of using this high  $\eta$  value is a constant positive bias in the consideration of all critical experiments. It is suggested that evaluators focus their energies on this anomaly which is outstandingly large.

Table 2  
2200 m s<sup>-1</sup> <sup>239</sup>Pu parameters

	WIMSD	ENDF/B-V	MONK6.1	FD5	Divadeenam and Stehn 1984
$\eta$	2.093	2.119	2.122	-	$2.1153 \pm 0.0052$
$\alpha$	0.371	0.364	0.357	-	$0.3600 \pm 0.0032$
$\bar{\nu}$	2.869	2.890	2.879	2.8821	$2.8768 \pm 0.0057$

### 3.4 <sup>239</sup>Pu epithermal data

Table 3 gives all the <sup>239</sup>Pu fission resonance integrals in current use, but it is clear that there is virtually no agreement between any of the evaluations available to us. Crude adjustments from the present work are also shown in Table 3, but these are intended only as a stop-gap until better data are made available from JEF. However these adjustments produced substantial errors in the calculation of the HISS experiment performed at Winfrith.

Table 3  
<sup>239</sup>Pu fission and capture resonance integrals

	Resonance integrals (b)		$\alpha$
	fission	capture	
WIMS-3239	266	182	0.68
WIMS-5239	322.8	215.2	0.66
MONK-161	289.6	170.3	0.58
MONK-9161	235.5	171.6	0.73
ENDF/B-V 1399	303	193	0.64
MURALB-FD5	245	208	0.84
Present work	246	168	

## 4. Conclusion

Table 4 summarises the results of the adjustments made in the present work. Forty-four critical systems were considered, and they are all category 1 experiments carried out with meticulous attention to detail and have been minutely documented for calculational purposes. The systems range

from bare spheres of plutonium or uranium metal down to very highly thermalised systems consisting of large spheres filled with dilute solutions of the fissile nuclides. Also included are various arrangements of rods surrounded by moderator or surrounded by fissile solutions. These provide difficult challenges for the nuclear data. Clearly the eigenvalue predictions have been greatly improved.

Table 4

The effectiveness of making adjustments using critical experiments

	Calculated k-values	
	unadjusted	adjusted
19 uranium systems	$1.0022 \pm 0.0080$	$1.0060 \pm 0.0076$
10 plutonium systems	$1.0203 \pm 0.0202$	$1.0024 \pm 0.0077$
15 mixed systems	$1.0345 \pm 0.0255$	$1.0063 \pm 0.0098$

- 
- (1) R.J. Brissenden and N. Smith, The adjustment of the UKNDL nuclear database for MONK6.3, DIDWG paper no. 319 (1984).

## The Use of Benchmark Experiments for the Validation of Nuclear Data

A.K. McCracken

Reactor Physics Division, AEE Winfrith

Lecture given at the Nuclear Data Forum, AEE Winfrith, Dec. 1984

The adjustment of cross-section data to give improved statistical consistency between calculation and experiment is a long-established practice. Such exercises have most commonly been based upon so-called mock-up experiments in which a close simulation has been achieved of some feature or features of a particular reactor design; in zero energy experiments an entire reactor core is simulated. Adjustments made to data cannot be considered in isolation from the method of calculation used, and will clearly, in part at least, reflect inadequacies in the calculational method as well as in the data themselves. Such was the case with early work to improve calculational accuracy for Magnox reactors. Lack of modern computing power dictated the use of few-group approximate diffusion methods with a limited modelling capability. The refinements made served well their essential purpose of improving prediction of Magnox performance parameters, and no claim was made that the experiments gave much insight into the adequacy or otherwise of nuclear cross-sections involved in the calculations. Interest later moved to water reactors and fast reactors encompassed respectively by the WIMS and COSMOS schemes, and the latter is now briefly considered.

An extensive series of measurements in ZEBRA and other reactor criticals provided an experimental database for the adjustment of data for use in fast reactor predictions. Relatively powerful computers were by then available, and this made possible the use of much improved calculational algorithms. Campbell and Rowlands<sup>(1)</sup> used multigroup transport-corrected diffusion theory which was expected to provide a rather good description of neutron moderation and migration in fast reactor cores. They had moreover assembled some information, albeit rudimentary, about the uncertainty relationships which exist between items of nuclear data, information which is essential for the rigorous adjustment of data. Although some systematic error might have been introduced into their calculations caused by group-averaging of cross-sections and by a limited modelling capability, it is

reasonable to suppose that their calculational tools were of sufficient power to highlight deficiencies in the nuclear data rather than in the method of calculation. One of their findings, embodied in the data set FD5, was that the iron inelastic scattering cross-section in the UKNDL files DFN 906 and DFN 908 was too large at energies near the threshold.

McCracken and Grimstone<sup>(2)</sup> analysed the Winfrith iron benchmark experiment with the one-dimensional discrete ordinates code ANISN and its associated perturbation code SWANLAKE. Their calculations are subject to the same qualifications as those of Rowlands but are nevertheless expected to be of sufficient quality to expose major deficiencies in the iron cross-sections. Their findings were essentially similar to those of Rowlands.

In the USA workers analysed the iron penetration experiment at the Tower Shielding Facility using the same tools as McCracken and Grimstone. They concluded that, near the threshold energy, the iron inelastic scattering cross-sections given in ENDF/B-III (essentially the same compilation as DFN 906 and DFN 908) were too large and the revised file ENDF/B-IV took cognisance of this finding. Therefore, despite differences of detail, three sets of workers on different experiments came to broadly the same conclusion, viz. that a reduction of some 20% or more was required in the iron inelastic cross-section at energies near 1 MeV.

Since these analyses were performed, a Monte Carlo perturbation code DUCKPOND<sup>(3)</sup> has been incorporated into the Monte Carlo program MCBEND which utilises point-energy cross-section data and which has a very flexible and powerful modelling capability. The introduction of Monte Carlo statistics is a small price to pay for the essentially bias-free calculational ability afforded by these programs. The Winfrith iron benchmark experiment has been re-analysed using these tools and the adjustment code DATAK. The adjustments were applied to calculations which used in turn DFN 908 cross-sections and JEF (essentially ENDF/B-IV) cross-sections. The results are shown in Fig. 1, they reinforce strikingly the broad conclusions reached by independent workers using less powerful tools. They suggest that the iron inelastic data in JEF (and ENDF/B-IV) is considerably better than in the previously used files, and that the analyses described above, although not completely bias-free, were able to draw conclusions which were broadly valid about inadequacies in nuclear data employed in calculations.

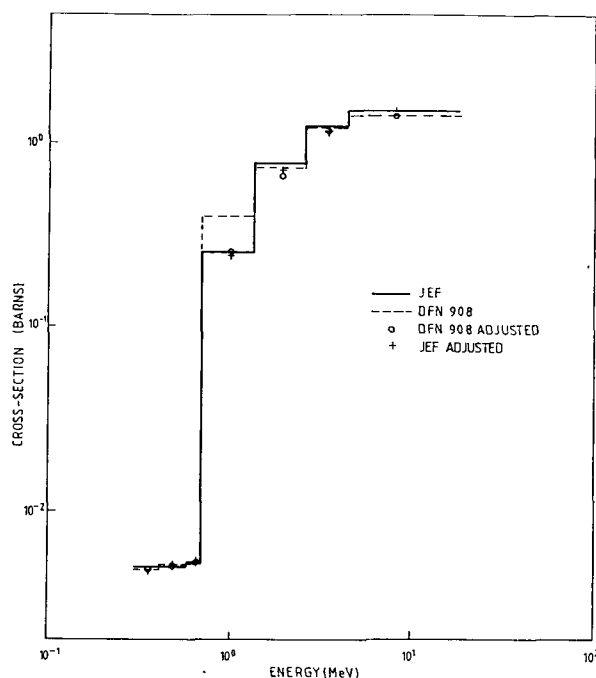


Fig. 1 A comparison of the iron DFN 908 adjusted and unadjusted nonelastic cross-sections with JEF adjusted and unadjusted nonelastic cross-sections

- 
- (1) J.L. Rowlands et al. The production and performance of the adjusted cross-section set FGL5, Proc. Int. Symp. on Physics of Fast Reactors, Tokyo, 1973.
  - (2) A.K. McCracken and M.J. Grimstone. Preliminary analysis of the Winfrith iron benchmark experiment. Proc. OECD Specialists' Meeting on Sensitivity Studies and Shielding Benchmarks, Paris, 1975.
  - (3) M.C.G. Hall DUCKPOND - A perturbation Monte Carlo code and its applications. Proc. OECD Specialists' Meeting on Sensitivity Studies and Shielding Benchmarks, Paris, 1975.

## CINDA-TYPE LISTING

Element Z	Quantity A	Type	Energy min	(eV) max	UKNDC (85)Pl12 (July 85) page no.	Lab	Comments
Li	7 n gamma	expt,prog	1.4 +7		98	BIR Cox + $\gamma$ prod from thick Li blanket	
C	nat total	" "	1.0 -1 1.0 +1		32	HAR Clare + meas total xsec below 10 eV	
Si	nat total	" "	1.0 -1 1.0 +1		32	HAR Clare + meas total xsec below 10 eV	
Mn	55 act xsec	" "	thermal		90	NPL Axton + therm capt xsec 13.41 $\pm 0.04$ b relative to H	
Fe	nat total	" "	3.0 +2 2.0 +5		38	HAR James +	
Fe	54 $\gamma$ spec	" "	3.0 +2 1.0 +5		39	HAR Mason + $\gamma$ spec from reson capt	
Fe	56 res parm	" "	1.1 +3		36	HAR Moxon + analysis of 1.1 keV Fe-56 reson for internat task force	
Co	59 eval	eval,prog	1.0 +6 2.0 +7		104	HAR Wilmore + calc using optical model	
Co	59 eval	" "	8.0 +6 1.4 +7		104	OXF Field + calc using compound and direct models	
Ni	62 $\gamma$ spec	expt,prog	3.0 +2 1.0 +5		39	HAR Mason + $\gamma$ spec from reson capt	
Nb	93 inelastic	" "	1.0 +6 6.0 +6		41	HAR Gayther +	
Nb	93 (n,2n)	eval,prog	8.0 +6 1.4 +7		104	OXF Field + calc using compound and direct models	
In	nat diff elas	expt,prog	3.0 +6		102	EDG Galloway + meas of polar and diff elas from 20 to 67° in progress	
Sn	nat diff elas	" "	3.0 +6		102	EDG Galloway + meas of polar and diff elas from 20 to 67° in progress	
Sb	nat diff elas	" "	3.0 +6		102	EDG Galloway + meas of polar and diff elas from 20 to 67° in progress	
Te	nat diff elas	" "	3.0 +6		102	EDG Galloway + meas of polar and diff elas from 20 to 67° in progress	
I	127 diff elas	" "	3.0 +6		102	EDG Galloway + meas of polar and diff elas from 20 to 67° in progress	
Eu	152 half life	" "			90	NPL Christmas + half life 4938 $\pm$ 4 d	
Eu	154 half life	" "			90	NPL Christmas + half life 3134 $\pm$ 2 d	
Th	230 eval	eval,prog			85	WIN Smith review of three group data	
Th	232 n inel	expt,prog	2.5 +6		103	OXF Hodgson + analysis of xsec data	
Pa	231 half life	" "			78	HAR Fudge + results sent for inclusion in CRP data sets	
Pa	231 eval	eval,prog			85	WIN Smith review of three group data	
Pa	233 half life	expt,prog			79	HAR Fudge + meas of $\gamma$ emiss prob in progress	
U	232 half life	" "			77	HAR Fudge + half life and $\gamma$ emiss prob	
U	235 eta	" "	5.0 -3 1.0 0		35	HAR Moxon +	
U	235 eval	eval,prog	thermal		22	WIN Brissenden adjustment of eval data	
U	235 delayed n	expt,prog	fast		92	BIR Owen + meas del neut groups using pulsed source	
U	237 half life	" "			78	HAR Fudge + data being analysed	
U	238 res parm	" "	1.4 +3 4.0 +3		36	HAR Moxon + analysis of U-238 transm data for internat task force	
U	238 n inel	" "	2.5 +6		103	OXF Hodgson + analysis of xsec data. To be published	

## CINDA-TYPE LISTING

Element Z	Quantity A	Type	Energy min	(eV) max	UKNDC (85)P112 (July 85) page no.	Lab	Comments
U	239 half life	expt,prog			79	HAR Fudge	+ meas of $\gamma$ emiss prob in progress
Np	235 half life	" "			79	HAR Wiltshire	+ meas in progress
Np	237 half life	" "			78	HAR Fudge	+ results sent for inclusion in CRP data sets
Np	237 half life	" "			79	HAR Fudge	+ work contin on half life and $\gamma$ emiss
Np	237 half life	" "			79	HAR Wiltshire	+ meas in progress
Np	239 half life	" "			79	HAR Fudge	+ meas of $\gamma$ emiss prob in progress
Pu	237 half life	" "			79	HAR Fudge	+ half life $45.86 \pm 0.10$ d
Pu	239 eval	eval,prog thermal			23	WIN Brissenden	adjustment of eval data
Pu	241 half life	expt,prog			78	HAR Fudge	+ examination of effects of Am-241 contamination
Am	reaction rates	" "	PFR spec		77	HAR Wiltshire	+ analysis in progress
Cm	reaction rates	" "	PFR spec		77	HAR Wiltshire	+ analysis in progress
Cm	242 half life	" "			79	HAR Fudge	+ half life $162.98 \pm 0.16$ d
Cm	242 half life	" "			79	HAR Wiltshire	+ half life $163.00 \pm 0.16$ d. Also $\alpha$ emiss meas in progress
Cm	244 half life	" "			79	HAR Fudge	+ work contin on half life and $\gamma$ emiss
Cf	252 nubar	" "			88	NPL Axton	+ $\bar{\nu} = 3.7509 \pm 0.0107$ n/fission



1. NUCLEAR PHYSICS DIVISION, AERE, HARWELL

(Division head: Dr. J.E. Lynn)

Introduction

Nuclear data measurements in Nuclear Physics Division are diverse and are performed on a variety of sources. Individual research items are labelled with a single letter indicating on which accelerator the experiments were performed. These labels are as follows:

Cockcroft-Walton Generator	A
3 MV pulsed Van de Graaff Generator IBIS	B
6 MV Van de Graaff Generator	C
14 MV Tandem Generator	D
136 MeV Electron Linear Accelerator	E
Variable Energy Cyclotron	G
500 kV Van de Graaff	I

In the contents pages there is a reference to the accelerator on which a measurement was made.

The material for this contribution is taken from the chapter on Nuclear Data and Technology for Nuclear Power in the 1984 Nuclear Physics Division Progress Report AERE PR/NP 32.

1.1E HELIOS - The new machine for the electron linac laboratory (J.E. Lynn, M.S. Coates, B.P. Clear, J. Down, R.A.J. Riddle and P.W. Swinden)

The year has seen extended and reliable routine use of the Harwell electron linear accelerator HELIOS for experiments in the Condensed Matter, Fast Neutron and Low Energy Cells, with a short interruption of ~2 weeks to complete the commissioning work on the Neutron Booster Cell referred to in UKNDC(84)P111 p.45. A Booster target power of 3 kW(e) was achieved and this marked essentially the final commissioning phase of the target beam lines on HELIOS.

A long-standing fault on one of the Booster mercury cooling circuits was rectified in the course of the commissioning work. A reduction in flow-rate had been noticed for some time and the evidence pointed to an accumulation of sediment in the flow channels, brought in somehow by the mercury. The fault was cured by draining the mercury and carrying out a wash with weakly acidulated water. On replacing the mercury the flow was found to be fully restored. The origin of the sediment is not fully understood.

A set-back was suffered to the progress with the pulse magnet system, also referred to in UKNDC(84)P111 p.45. During reliability tests a failure occurred on the water cooling system. The interlock protection device in use at the time did not act quickly enough to prevent severe damage to the coils of the pulse magnet. The magnet has been replaced and the protection system improved. Since then it has been established that a new heat exchanger is needed to allow operation of the system to steer an electron beam at the required conditions of 150 pps and 120 MeV. This work should be carried out in the early part of 1985.

1.2E Neutron transmission measurements on HELIOS in the energy range 0.01 to 10 eV (A.G. Clare (University of Reading), M.C. Moxon, J.B. Brisland and A.P. Guntrip)

Neutron transmission measurements have been carried out on several samples with the equipment described last year (UKNDC(84)P111 p.46). The main emphasis has been on high accuracy in the neutron energy region between ~ 0.1 and 20 eV. A statistical accuracy of better than  $\pm 0.0025$  in the transmission can be obtained on data averaged in 5% energy intervals in less than 24 hours running time. Uncertainties due to the background and normalisation each contribute a further  $\sim \pm 0.001$  to the overall error. However uncertainties in the impurity levels present in samples can often give rise to errors which are dominant. Measurements above 0.3 eV are

carried out normally with a permanent 0.002 inch thick gadolinium filter in the neutron beam. This is removed for measurements at lower energies. Two sets of filters are cycled in and out of the neutron beam, as well as the sample under investigation. The complete cycle consists of open, sample, resonance filter 1, sample + resonance filter 1, resonance filter 2, sample + resonance filter 2. (Resonance filter 1 consists of  $\sim 2$  mm of Hf and  $\sim 1$  mm Co and resonance filter 2  $\sim 2$  mm of Ag and 3 mm of Co.) The transmission of the sample is calculated from the ratio of the counts observed with the sample in and out of the neutron beam. The transmission calculated from the data between resonances when the resonance filters are in the neutron beam gives a good check on the accuracy of the extrapolation of the background for the non-filtered condition.

Figs. 1.1 to 1.4 show the observed total cross-sections in the energy range  $\sim 0.3$  to  $\sim 100$  eV for samples of graphite (Fig. 1.1), silicon (Fig. 1.2) and for two single crystals of silica cut along the a-axis (Fig. 1.3) and the b-axis (Fig. 1.4). The graphite cross-section, after corrections, is  $\sim 0.75\%$  lower than the presently recommended value of 4.740 b in ENDF/B-V. This will be investigated further in our next series of runs. The cross-section of silicon is about 10% lower than that recommended in BNL 325 (3rd edition, vol. 1). We believe the recommended value to be inaccurate. The measurements on the silica crystals show the expected decrease of the total cross section with decreasing energy.

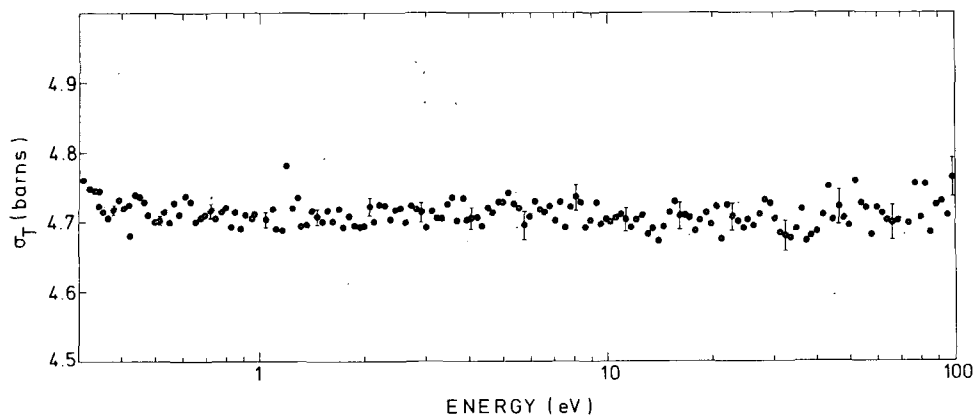


Fig. 1.1 Total neutron cross-section of graphite

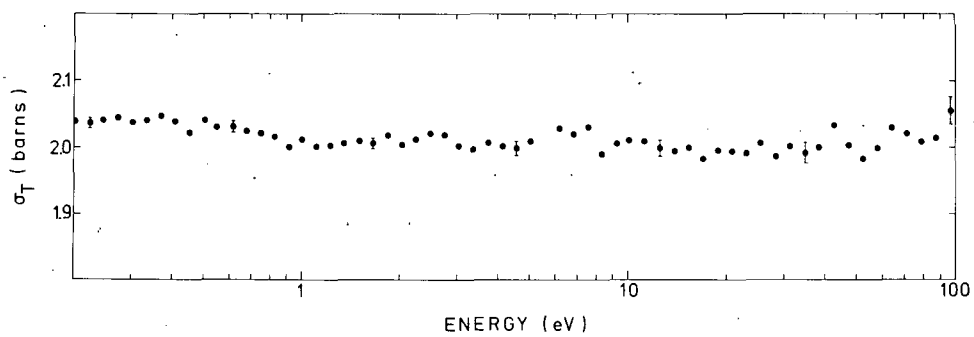


Fig. 1.2 Total neutron cross-section of silicon

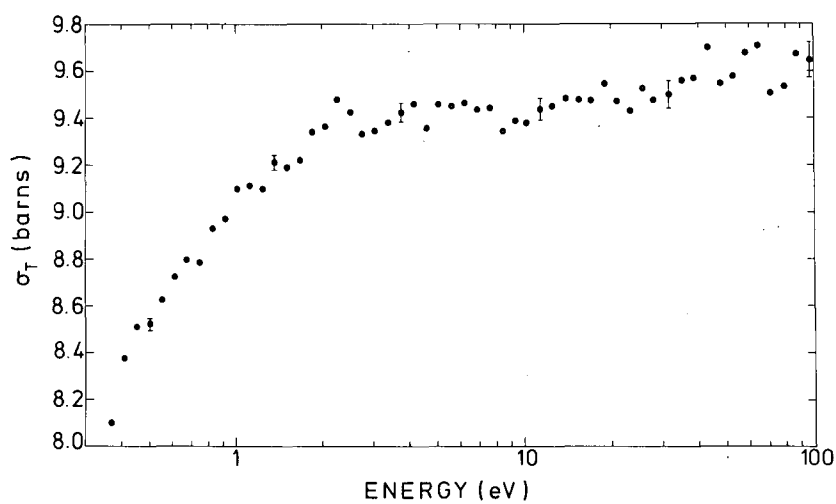


Fig. 1.3 Total neutron cross-section of a single crystal of  $\text{SiO}_2$  along the a-axis (barns per  $\text{SiO}_2$  "molecule")

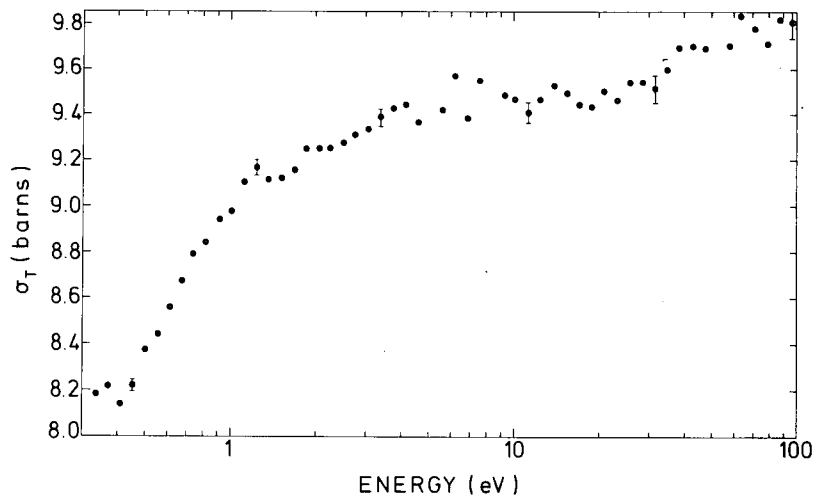


Fig. 1.4 Total neutron cross-section of a single crystal of  $\text{SiO}_2$  along the b-axis (barns per  $\text{SiO}_2$  "molecule")

1.3E Measurement of  $\eta(^{235}\text{U})$  in the energy range below 1 eV (M.C. Moxon, J.B. Brisland and A.P. Guntrip (WREDA 964-967))

In thermal reactor systems such as PWR with somewhat hard spectra there is still room for improvement of the basic data required for the precise understanding of core neutronics, particularly temperature coefficients. In particular a need exists for accurate measurements of both the energy dependence of  $\eta$  (the number of neutrons emitted per neutron absorbed) for  $^{235}\text{U}$  and the  $^{238}\text{U}$  capture cross-section in the thermal energy region. We have commissioned a 10 metre long neutron flight path on the Condensed Matter cell of HELIOS for this work, and the  $\eta(^{235}\text{U})$  measurements have begun. The experiment is a repeat of one with the old 45 MeV electron linac (UKNDC(76)P80 p.21) which HELIOS replaced, in which it turned out that background conditions were too poor to achieve the required measurement accuracy of  $\sim 1\%$ . The present experimental method is based on the use of the pulse shape discrimination technique to distinguish between high energy neutron events (fission) and gamma-ray events (fission and capture) detected in a liquid scintillation counter. Measurements on HELIOS began in December 1984, and it was established that background conditions are much improved on the new system. The background for the neutron events was negligible, while the gamma-ray events were dominated by the activity of the  $^{235}\text{U}$  samples. Pure capture samples such as Au or Ta gave signal-to-background ratios

greater than 100:1 in the black resonances and in the thermal region. The cross-talk between gamma-rays and neutrons for the pure capture samples was better than 600:1 below neutron energies of 10 eV.

1.4 Work related to the NEANDC Task Force investigation the discrepant resonance parameters in  $^{238}\text{U}$  above 1.15 keV (M.C. Moxon and D.B. Syme) (WREND 1067-1069)

The work reported last year (UKNDC(84)P111 p.48) has continued with an analysis of  $^{238}\text{U}$  neutron transmission data from ORNL<sup>(1)</sup>, JAERI<sup>(2)</sup> and CBNM<sup>(3)</sup>. The results, which were presents to a joint meeting of the  $^{238}\text{U}$  and Fe NEANDC Task Forces held in Paris during October 1984, are to be published shortly<sup>(4)</sup>. A brief summary of the work and its conclusions is given below.

The resonance parameters in the energy regions 4.0 to 3.8 keV, 2.74 to 2.47 and 1.82 to 1.42 keV, determined in least-squares fits to the ORNL transmission data, using the program REFIT<sup>(5)</sup>, agreed in general with the latest ORNL<sup>(6)</sup> analysis of ORNL data. The importance of the resolution function used in shape analysis has already been stressed (UKNDC(84)P111 p.48) and the technique used in REFIT provides a better physical model than the purely mathematical function used in other fitting programs. The resolution parameters determined from the fits to the ORNL data give similar shapes and energy dependences to those calculated by Monte Carlo techniques, but the resolution function is broader and more asymmetric than that given by the experimenters in their original report<sup>(1)</sup>. Similar conclusions were obtained from fits to the JAERI and CBNM transmission data. The main conclusion from the Task Force work is that the lack of knowledge and understanding of the neutron resolution function is the prime cause of the discrepancies in the values of the neutron width, and that in future the main components of the resolution function should be determined experimentally.

In order to improve resonance parameters with neutron widths less than 5 meV, capture yields were calculated from the ORNL transmission parameters using a radiation width of 23.5 meV and compared with capture yields measured at ORNL<sup>(7)</sup> and Harwell<sup>(8)</sup>. The calculated curves were ~ 15% and 4% respectively below the measurements. The good resolution of the ORNL data allows the use of area techniques to renormalise this data, giving a renormalisation factor of 0.885. The renormalisation removes some of the discrepancy in the neutron capture cross-section data. The need for

renormalisation can perhaps be explained by the presence of an unsuspected error in the shape of the incident neutron flux spectrum assumed in the measurements, but further work is needed before this can be stated with certainty. The much poorer resolution of the Harwell data does not enable us to carry out a comparable normalisation check over the whole energy region, but we propose to carry out some calculations in the energy region where the resonances are resolved.

- 
- (1) D.K. Olsen and G. de Saussure, ORNL/TM 8915 (1977); R.B. Perey et al. Nucl. Sci. Eng. 69 (1979) 202.
  - (2) Y. Nakajima et al., Proc. Conf. Neutron Cross-sections and Technology, Washington, 1975.
  - (3) F. Poortmans et al., Proc. Conf. Interactions of Neutrons and Nuclei, Lowell, 1976.
  - (4) M.C. Moxon, AERE-R 11642 (to be published).
  - (5) M.C. Moxon, Proc. Specialist's Meeting on Neutron Data for Structural Materials for Fast Neutrons, Geel, 1977.
  - (6) D.K. Olsen, ORNL/TM-9023 (1984).
  - (7) G. de Saussure et al., ORNL TM-4059 (1973).
  - (8) M.C. Moxon, AERE-R 6074 (1969).

1.5E Calculation of the neutronics characteristics of the Fast Neutron Target of HELIOS (D.B. Syme and R.B. Thom\*)

Measurements of the performance of the Fast Neutron Target of HELIOS were reported in UKNDC(84)P111 p.50. We have since begun Monte Carlo calculations of the target neutronics using the time dependent computer code MORSE<sup>(1)</sup>. The calculations are required to predict the emission spectra and source time distribution (resolution function) over the complete range of likely measurements (0.1 keV to 10 MeV). This is essential since the resolution function can only be directly measured below about 10 keV but is important at higher energies where the increasing resonance overlap makes the results of resonance analysis, and therefore the quality of reactor nuclear data, more strongly dependent on a knowledge of the resolution function. This was evident in the work of the task force on the discrepant

---

\* until July 1984

neutron resonance parameters of  $^{238}\text{U}$  (UKNDC(84)P111 p.48).

The present calculation should be an improvement over previous calculations because of its detailed description of target and moderator geometries and heterogeneity effects, a description achieved by using the calculated proper geometric distribution of neutron generation over the target and by using the valid (Alsmiller) spectrum for neutron emission. Early results have shown that these details do modify the target spectrum and source resolution function significantly, especially at higher energies, and that the  $\chi^2$  distribution approximation commonly used to represent the resolution function lineshape may only be valid below about 50 keV. This work is continuing.

---

(1) M.B. Emmett, ORNL 4972 (1975); also RSIC-CCC-203.

1.6E High resolution transmission measurements on natural iron (G.D. James, D.B. Syme and M.C. Moxon)  
(WRENDA 356)

The 150 m flight-path from the Fast Neutron Target of HELIOS has been used to measure the neutron transmission of natural iron for three sample thicknesses, 2, 5 and 15 mm. A minimum timing channel width of 10 ns and an electron pulse width of 30 ns were used. The observed neutron source was a 5% boron loaded polythene sheet 35 mm thick. The detected neutrons were stopped in a  $^{10}\text{B}$  plug from which the gamma rays were detected by a bismuth germanate (BGO) crystal 15 mm thick. The data, which cover a neutron energy range from well below 1 keV to several hundred keV, are of good statistical quality and have a low gamma and neutron background. Data processing computer programs to sum experimental runs and to deduce the neutron transmission have been completed and are being used. Twenty-five experimental runs have been reduced to four runs with self-consistent properties. Preliminary resonance analysis of the first of these has been carried out using REFIT. Neutron widths have been derived for s-wave resonances below 190 keV and agree well with the values obtained from an analysis<sup>(1)</sup> of transmission data measured on the Harwell synchrocyclotron. The resonance parameters have good statistical accuracy and the resultant fit to the transmission promises to be of higher quality than any obtained elsewhere. The next step in which all four runs are analysed simultaneously is about to start.

---

(1) M.C. Moxon and J.B. Brisland, Neutron Data of Structural Material for Fast Reactors, ed. K.H. Böckhoff (Pergamon, Oxford, 1979) p. 689.



1.7E Resonance neutron capture in  $^{54}\text{Fe}$  and  $^{62}\text{Ni}$  (J.P. Mason and B.H. Patrick)  
(WRENDA 391,486)

Last year it was reported (UKNDC(84)P111 p.58) that measurements of resonance neutron capture gamma-rays in structural materials were to be made using the Fast Neutron Target of HELIOS as a neutron source. The 12.5 m flight path for these measurements was completed successfully in February of this year and the first data were obtained in March. The two n-type Ge detectors used to observe the capture gamma-rays were interfaced so that their spectra were accumulated separately on a PDP-11/45 computer. Each event was recorded as two parameters, the neutron time-of-flight and the gamma-ray energy. Subsequent off-line analysis enables time-of-flight spectra to be observed for particular gamma-ray transitions, or alternatively the gamma-ray spectrum may be observed in a particular resonance by summing over the appropriate time channels.

The detector efficiencies were measured in situ at HELIOS by running the machine at a low pulse repetition rate and collecting the thermal capture gamma-ray spectra from Ti, Cr, Cl and N. The relative intensities of these gamma-rays are known, and these, together with measurements made using calibrated gamma-ray sources, allowed the relative efficiency to be deduced as a function of gamma-ray energy. A five parameter analytic function was found to be satisfactory in fitting the efficiency curves for each detector. Covariances were taken into account in the error analysis of the fitting.

Data were collected from capture in a 50 g sample of  $^{54}\text{Fe}$  over a period of two weeks running at 300 pps with an electron pulse width of 30 ns. The time-of-flight spectrum for all events for which the gamma-ray energy is greater than 2.5 MeV is shown in Fig. 1.5. The three s-wave resonances in this energy region can be seen together with several narrow p-wave resonances. The high energy part of the gamma-ray spectrum for events occurring in the 7.76 keV s-wave resonance is shown in Fig. 1.6. The relative transition strengths observed are compared with the predictions of the valence model in Table 1.1 and are seen to be in good agreement. Analysis is underway to produce absolute values for these transition strengths using values of the neutron flux which was measured by the Ge detectors using the  $^{10}\text{B}(n,\alpha\gamma)$  reaction. This will allow a more rigorous test of the valence model.

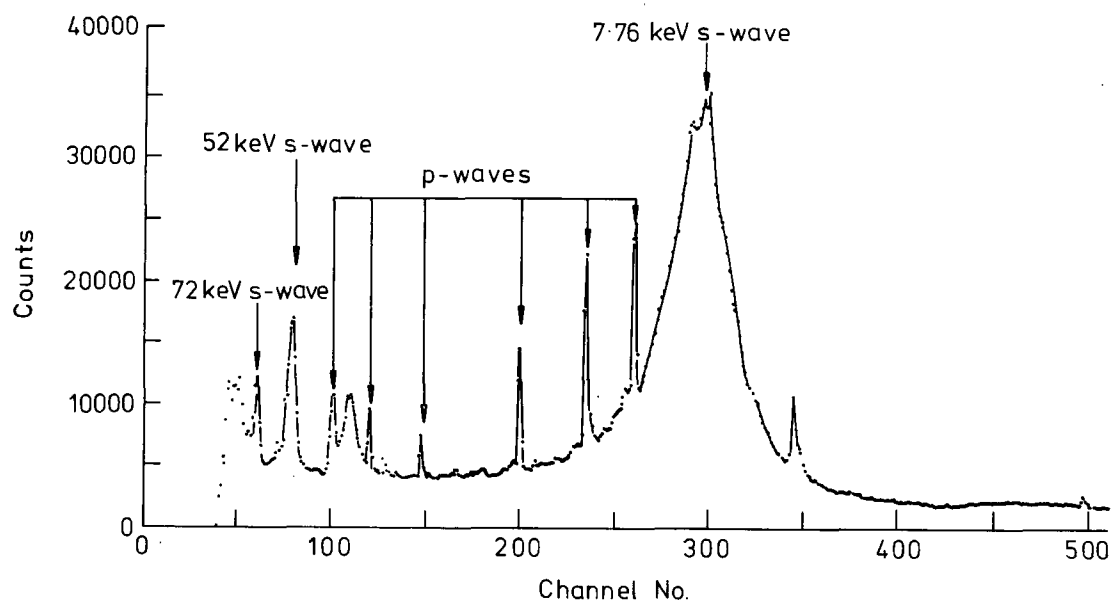


Fig. 1.5 Time-of-flight spectrum for  $^{54}\text{Fe}$  for events with gamma-ray energies greater than 2.5 MeV (the peaks at channels 110 and 340 are due to the aluminium canning)

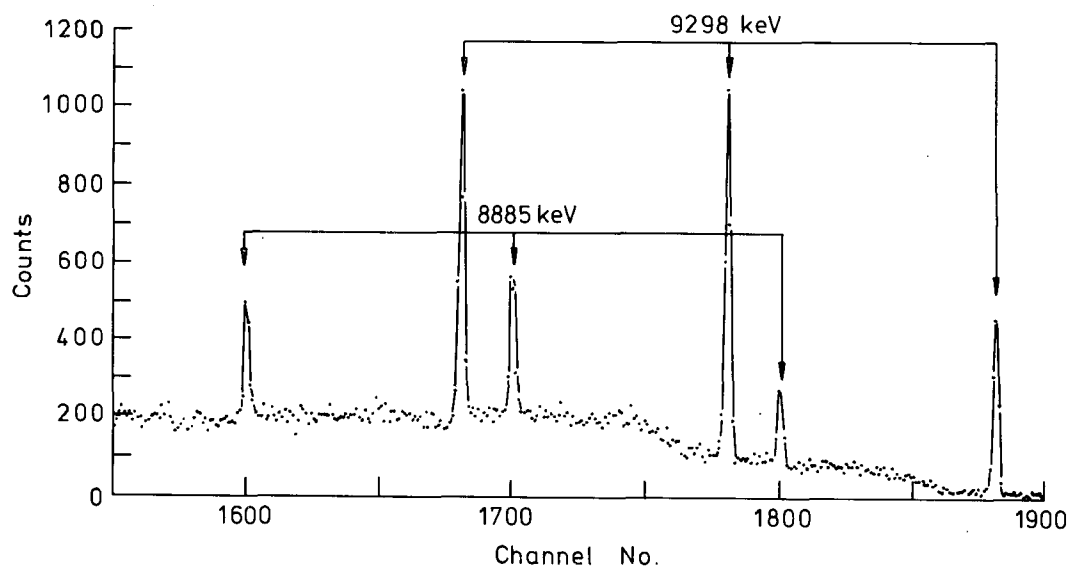


Fig. 1.6 Gamma-ray spectrum for  $^{54}\text{Fe}$  for events in the 7.76 keV s-wave resonance

Table 1.1

Measured transition intensities in the 7.76 keV  $^{54}\text{Fe}$  resonance compared with valence model predictions

Energy of transition (keV)	Relative intensity measured	Relative intensity valency model
9298	$100 \pm 10$	100
8885	$34 \pm 3$	38
7380	$4 \pm 1$	2.6
7243	$< 2$	5.2
6827	$6 \pm 1$	8.0
6268	$< 2$	1.3
5746	$< 2$	3.5
5508	$< 2$	7.1

Shortly more data will be collected with improved machine conditions (no moderator and a high pulse repetition rate) to allow observations of the 52 keV and 72 keV s-wave resonances.

Data have also been collected for capture in  $^{62}\text{Ni}$  and are currently being analysed.

1.8 The  $^{93}\text{Nb}(n,n')^{93\text{m}}\text{Nb}$  reaction (D.B. Gayther and C.A. Uttley, K. Randle (University of Birmingham), W.H. Taylor and M.F. Murphy (AEE, Winfrith))  
(WRENDA 563-569, 571-573, 582)

Preliminary values for the cross-section at the neutron energies mentioned in the last report (UKNDC(84)Pl11 p.60) are shown in Fig 1.7. The curve is the theoretical excitation function of Strohmaier et al.<sup>(1)</sup>, who also deduced the other cross-sections shown in Fig. 1.7 from  $(n,n'\gamma)$  measurements. While there is reasonable agreement between the present activation data and the theoretical cross-section at most energies, there is an indication that the predicted cross-section near 2.8 MeV may be too high. The planned measurement at 0.6 MeV has not yet been carried out, but a trial run with 400  $\mu\text{A}$  of 2.35 MeV protons on a 100 keV thick LiF target produced a sufficiently high neutro source intensity to accomplish an irradiation in abut 80 h.

---

(1) B. Strohmaier et al. Physics Data Series 13, 2 (1980) 62.

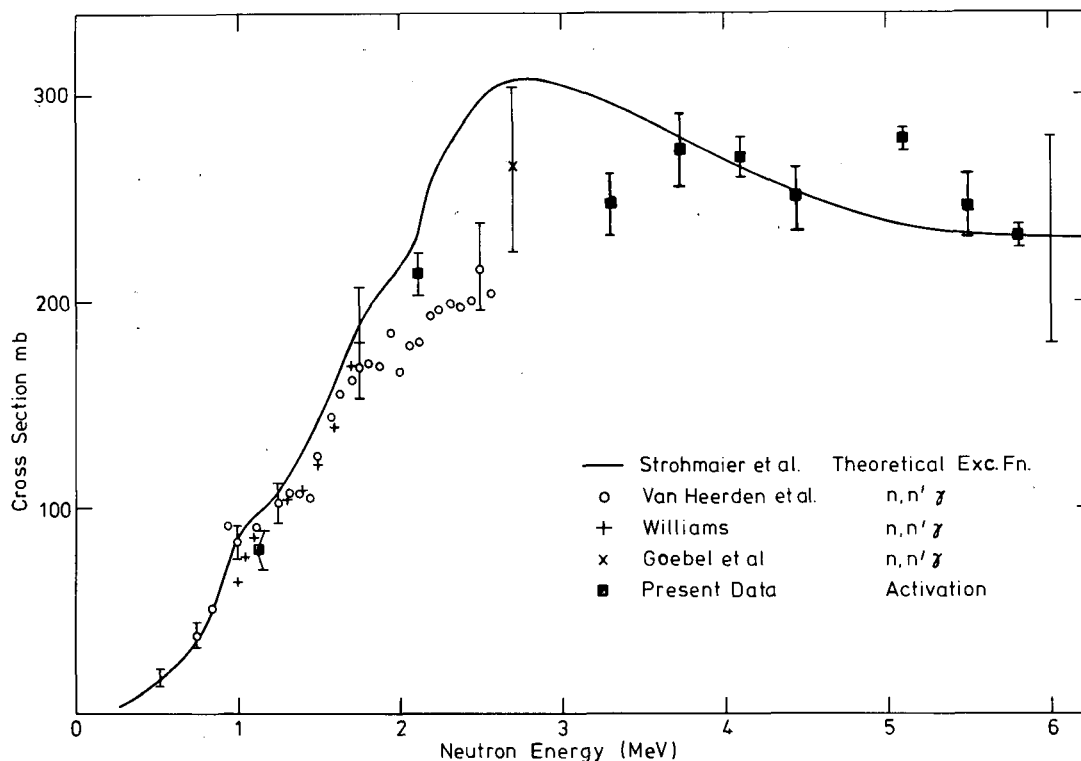


Fig. 1.7 The 30 keV isomer production cross section in  $^{93}\text{Nb}$  by inelastic neutron scattering

#### 1.9I Fission chambers for the intercomparison of fast neutron flux density measurements (D.B. Gayther)

The chambers were at the Bureau International des Poids et Mesures (BIPM) in Paris for a three month period commencing in February 1984. Measurements were made with both chambers at 14.65 MeV neutron energy.

Since returning to the UK, the performance of each chamber has been checked at the National Physical Laboratory with a strong  $^{252}\text{Cf}$  neutron source placed in carefully controlled conditions in a jig which allows its position with respect to the chamber to be accurately reproduced. Similar measurements with the same source and jig were made after the chambers returned from the National Bureau of Standards in mid 1983. The results show that there has been no deterioration in the performance of either chamber, and that the fissile content has remained constant to within the accuracy with which the relative strength of the  $^{252}\text{Cf}$  neutron source is known ( $\lesssim 0.2\%$ ).

In the autumn of 1984, a preliminary series of measurements was made in collaboration with C.A. Uttley and M.T. Swinhoe at Harwell using both chambers at 14.1 MeV neutron energy. A 500 kV Van de Graaff accelerator was used to provide neutrons through the  $^3\text{H}(\text{d},\text{n})$  reaction with a thick titanium tritide target. The measurements were made by the time-correlated associated particle method, and, as expected, excellent signal to background was obtained. It is planned to repeat these measurements at a later date with a thinner target to obtain a more accurate determination of the neutron sensitivity of the fission chambers.

The chambers were despatched in October 1984 to the Physikalisch-Technische Bundesanstalt (PTB) in Braunschweig for the next measurements in the series.

1.10D,I Studies of neutron induced charged particle reactions: development of a 'phoswich' detector (R.A. Jarjis (University of Birmingham) and D.B. Gayther)

A phoswich detector for the study of charged particle emission from neutron induced reactions on HELIOS was described last year (UKNDC(84)P111 p.61)). Since then, a second detector has been designed to enhance the energy range of detected alpha-particles and to demonstrate particle identification. Extensive measurements were conducted on the new detector using the Tandem Van de Graaff at Harwell. The detector consisted of a 0.02 mm thick NE-102A scintillator and a 10.0 mm thick CsI(Tl) scintillator. Fig. 1.8 shows a plot of the coincident light outputs  $\Delta L$  and  $L$  from the two scintillators for protons and alpha-particles at various energies.

Experiments are currently underway to detect (n, charged particle) events from an aluminium target exposed to neutrons generated from the  $^3\text{H}(\text{d},\text{n})^4\text{He}$  reaction using a 500 kV Van de Graaff accelerator. The detector and target are enclosed in a vacuum chamber which contains lead shielding to eliminate the background of charged particles.

To improve our understanding of the detector characteristics, the light output from a thin NE-102A scintillator was measured. Fig. 1.9 shows the luminescence data of a 0.02 mm thick NE-102A scintillator. The average energies were deduced from the known incident energies by taking into account the appropriate particle stopping power values. The stopping power data were obtained from experiments on a 0.01 mm thick NE-102A using a surface barrier detector.

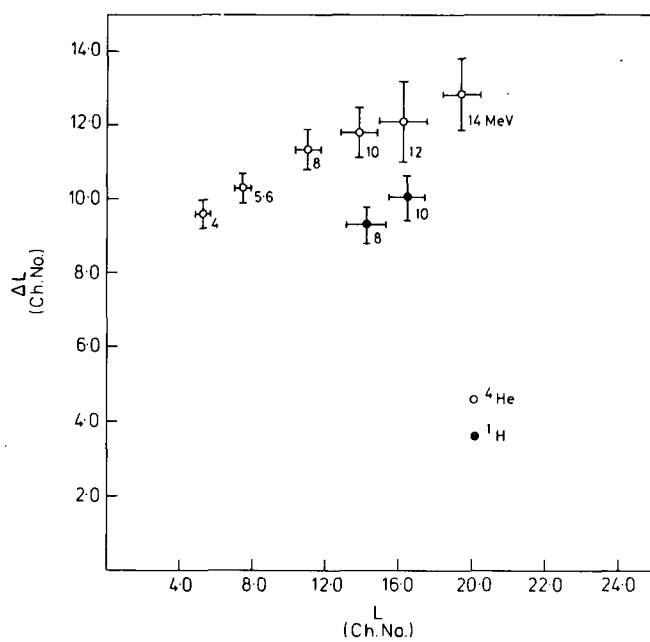


Fig. 1.8  $\Delta L$ - $L$  light output plot for a 0.02 mm thick NE-102A and a 10 mm thick CsI(Tl). The charged particle energies (in MeV) are shown

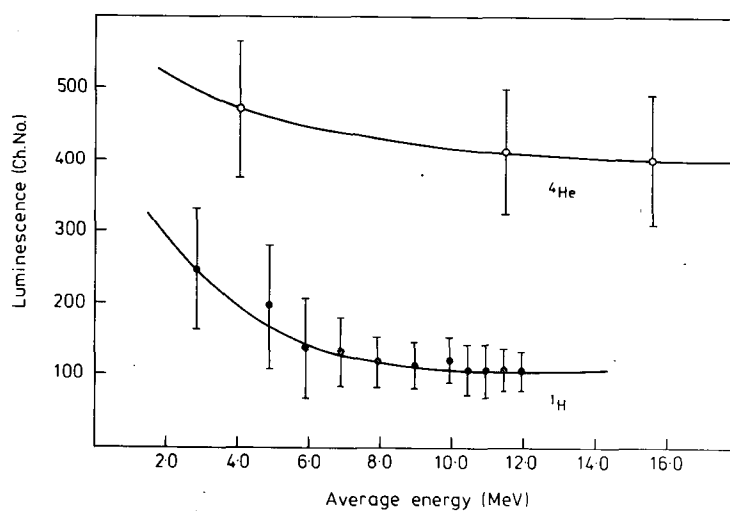


Fig. 1.9 Alpha-particle and proton luminescence data for a 0.02 mm thick NE-102A scintillator

1.11 Nuclear standard reference data (D.B. Gayther, B.H. Patrick and M.G. Sowerby)  
(WREMDA 949-956, 959)

Two papers were presented to the IAEA Advisory Group Meeting on Nuclear Standard Reference Data held at Geel on 12-16 November 1984.

One paper reviewed techniques for measuring the neutron spectra emitted by pulsed "white" neutron sources in the energy region from thermal to 20 MeV. Developments since the 1977 Symposium on Neutron Standards and Applications were emphasized. Neutron detection systems were discussed under two classifications: detectors with a flat response to neutron energy, and detectors which rely for their operation on standard neutron cross-sections.

In the other paper, the data on the  $^{235}\text{U}$  fission cross-section in the energy range 0.1 - 20 MeV published since the ENDF/B-V evaluation was performed were reviewed, and conclusions were drawn on the present status of the data and on future work required. The data on the fission fragment angular distribution over the same energy range obtained in the past two years were also considered.

1.12 Neutron energy standards (G.D. James)

The table of neutron energy standards (UKNDC(78)P88 p.45), originally formulated by an INDC sub-group, has again been revised with the advice of members of the sub-group. Changes are recommended to three of the standard energies and an oscillator level at 0.12 eV has been added to the table. A paper on this subject which includes a review of recent work on the determination of neutron energy is to be published in an IAEA Technical Report.

1.13 Nuclear data computer codes

1.13.1 The computer code NJOY (E.M. Bowey and D.W. Muir\*)

It was reported last year (UKNDC(84)P111 p.60) that the 10/81 version of the nuclear data processing system NJOY, written at Los Alamos National Laboratory, had been implemented on the Harwell IBM mainframe computer. It appeared subsequently that significant benefits in cost and running time would result from having the code system also available on the CRAY computer. Accordingly, steps have been taken to implement the latest NJOY version (6/83) on the CRAY.

---

\*On leave from Los Alamos National Laboratory, Los Alamos, New Mexico, USA.

### 1.13.2 FISPIN on the Harwell Computer (D.A.J. Endacott)

The FISPIN code<sup>(1)</sup> calculates the production and removal of three groups of nuclides: the actinide group, the fission product (FP) group, and the structural materials group. The code exists as several versions since several improvements to calculational methods and extra facilities have been made available. The most recent addition is version 6.

Major changes in version 6 from previous version 5.2<sup>(2)</sup> are

- (1) ability to read ENDF/B-V format,
- (2) energy production in structural materials,
- (3) gamma spectra energy boundaries may be input,
- (4) option for writing selected blocks of output to data files,
- (5) corrected treatment of FP isomer cross-sections,
- (6) correction of FP thermal cross-sections for reactor temperature,
- (7) optional condensed form of output,
- (8) multiple daughters of reactions,
- (9) alternative numerical method of solution.

Verification tests are not yet complete, so version 6, although available to users for trial runs, is not yet fully proved. The command macro<sup>(2)</sup> which generates the required job control language and data input file for execution of FISPIN has been modified to take advantage of these new facilities.

Two new condensed fission product data libraries have been added to the FISPIN facility:

UKFPTR3 - a thermal reactor library,

UKFPFR5 - a fast reactor library.

These libraries are generated from the following sources:

decay data from UKFPDD2<sup>(3)</sup>,

fission yield data from E.A.C. Crouch<sup>(4)</sup>,

(for the thermal reactor library, thermal energy yield values are used where available, for the fast reactor library, fast energy yield values are used where available),

cross-sections: thermal reactor 3-group for UKFPTR3<sup>(5)</sup>,

fast reactor one group for UKFPFR5.

Both libraries have 23 group gamma-ray spectra (earlier libraries have 12 group gamma-ray spectra).



- (1) R.F. Burstall, ND-R-328 (1979).
- (2) D.A.J. Endacott, The status of the FISPIN code and data libraries 1979-82 on the Harwell Computer (unpublished).
- (3) A. Tobias and B.S.J. Davies, CEGB report RD/B/N4942 (1980).
- (4) E.A.C. Crouch (1982) (unpublished).
- (5) A.L. Pope and J.S. Story, Winfrith report AEEW-M1234 (1973).

#### 1.14 Nuclear materials assay

##### 1.14.1 Fissile material assay by neutron interrogation (B.H. Armitage, T.E. Sampson\* and G. Edgar)

The assay of fissile material present in large matrices (for example 200 litre drums) is a difficult task. Much of the work described in this section is concerned with attempts to overcome problems associated with the presence of neutron moderating and absorbing matrices. An experimental study of matrix effects in a 200 l drum has been undertaken, and an assay procedure is proposed which does not require a prior knowledge of the matrix in which the fissile material is embedded. Monte Carlo computer calculations have been made of the spatial variation in response observed when fissile material is placed at different locations in a 200 l drum. Computational studies have also been made of problems posed by the use of 500 l drums. Through an external contract, an attempt is being made to produce a more long lived and reliable pulsed neutron source for waste assay.

##### 1.14.1.1 Matrix effects in the assay of fissile material in 200 l drums (T.E. Sampson and B.H. Armitage)

This work is concerned with the assay of fissile material in 200 l drums by means of the neutron die-away technique (UKNDC(84)P111 p.67). The measurements were made in a neutron die-away chamber consisting of a volume enclosed by graphite and polyethylene (CH<sub>2</sub>) walls containing a compact pulsed source of 14 MeV neutrons (Fig. 1.10a). Neutrons from the pulsed source are moderated and thermalized in the walls of the chamber. The thermal neutron flux produces fissions in the fissile material present in

---

\*Los Alamos National Laboratory

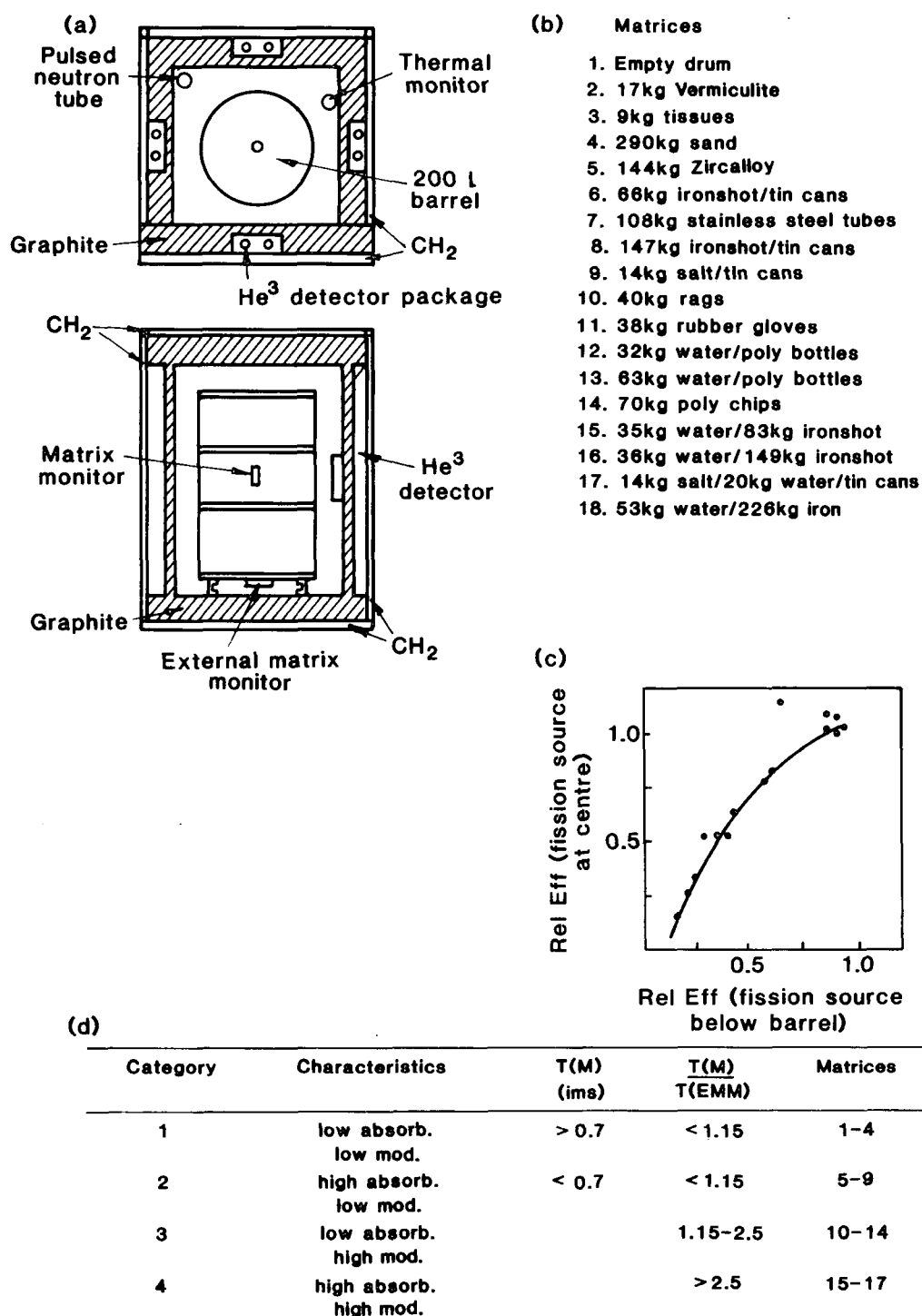


Fig. 1.10 (a) geometry of die-away chamber, (b) list of matrices, (c) data obtained with <sup>252</sup>Cf source, and (d) criteria for matrix categories

the chamber, and the ensuing fast fission neutrons are counted in thermally insensitive fast neutron detector packages embedded in the walls of the chamber. The detector packages are each composed of a 51 mm diameter  $^3\text{He}$  detector of 950 mm active length placed inside a 13 mm thick polyethylene cylinder and wrapped in 2.5 mm of cadmium.

The experimental study of matrix effects was undertaken with the eighteen matrices listed in Fig. 1.10b. The matrices were placed in 200 l drums each of which contained an axial aluminium tube which allowed access to the centre of the matrix. When a fissile sample (6g  $^{235}\text{U}$ ) was placed at the centre of any of the matrix filled drums, the fission neutron response of the detectors was modified. This modification is attributed to the product of two factors. The first factor is the number of fission reactions induced in the fissile sample; this is proportional to the thermal neutron flux at the centre of the drum, which in turn is a function of the moderating and absorbing properties of the matrix involved. The second factor is the detection efficiency for fast fission neutrons emitted from the sample; this again is a function of the moderating properties of the matrix.

The two factors have been studied independently. A small  $\text{BF}_3$  detector at the centre of each drum was used to obtain relative values of thermal neutron flux for each matrix (lowest section of Fig. 1.11). Relative values of detection efficiency for fission neutrons were obtained by placing a  $^{252}\text{Cf}$  source at the centre of each drum (middle section of Fig. 1.11). The fission neutron response obtained with the 6g  $^{235}\text{U}$  fissile sample is shown (as dots) in the highest section of Fig. 1.11.

The objective of the work is to define a procedure for the assay of the fissile content of a drum which does not require a prior knowledge of the matrix. Clearly, for real waste assay, access to the centre of the drum is unobtainable and detection efficiency measurements cannot be made directly. However, it is possible to place a  $^{252}\text{Cf}$  source underneath the drum, and the results of Fig. 1.10c demonstrate that such a measurement can be used to infer a value for the detection efficiency for a fission neutron source at the centre.

After the production of each pulse of 14 MeV neutrons the lifetime of thermal neutrons in the chamber was observed with a  $\text{BF}_3$  detector mounted on one of the inside walls of the chamber. In addition, similar measurements were made with a  $\text{BF}_3$  detector at the centre of the drum (matrix monitor) and

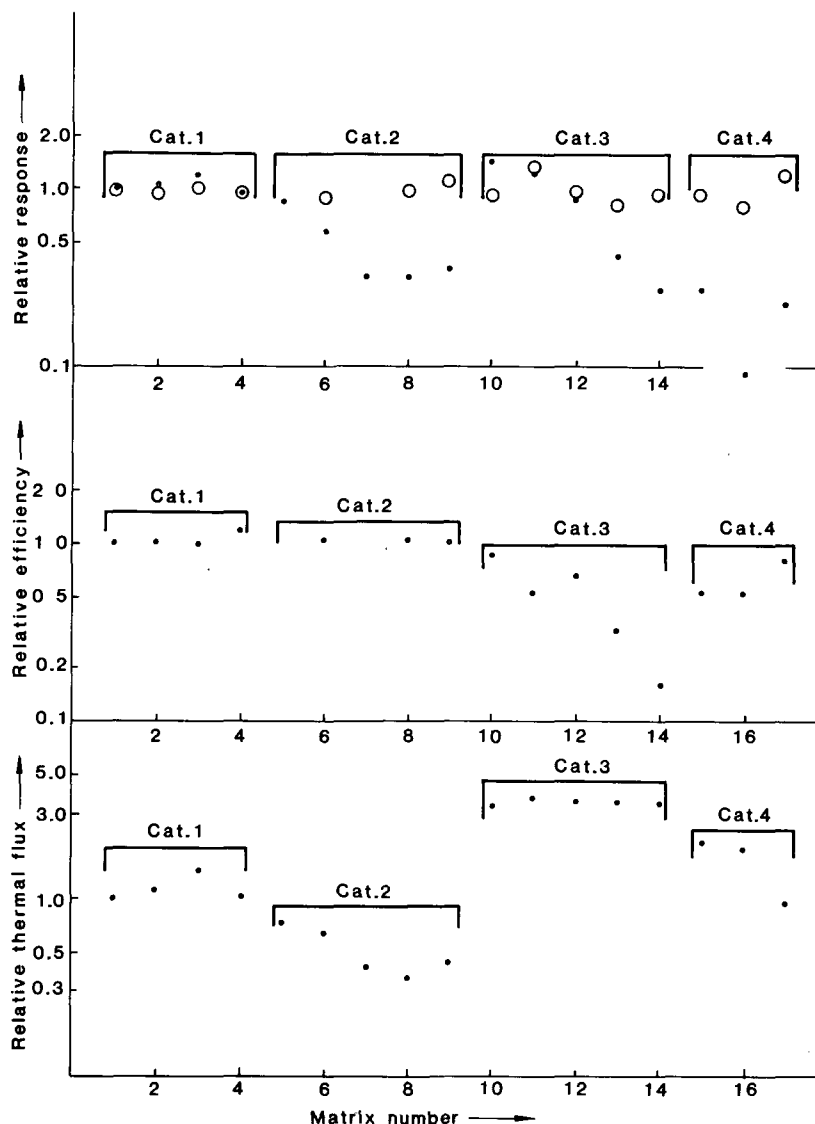


Fig. 1.11 Relative values of fission neutron response (dots) and matrix corrected fission neutron response (open circles) (highest section), detection efficiency (middle section) and thermal neutron flux (lowest section), for matrices listed in Fig. 1.10.

underneath the drum (external matrix monitor). These data (Fig. 1.10d) were used to place each of the matrices into one of four categories (see Fig. 1.10d) based on the measured lifetimes of thermal neutrons in the external matrix monitor T(EMM) and the wall mounted monitor T(M). Following this categorization, empirical analysis methods were used in each category to obtain matrix corrected responses. These are shown as open circles in the

highest section of Fig. 1.11. It can be seen that this method has been successful for seventeen out of the eighteen matrices examined. The one exception is that of the most absorbing matrix (226 kg of iron and 53 kg of water, matrix no. 18). In summary, this empirical approach has provided a waste assay method in cases where little or nothing is known about the matrix.

1.14.1.2 The assay of fissile material in 200 l drums: spatial variability of response (M.J. Cogbill\* and B.H. Armitage)

A limiting aspect of the experimental study described in sect. 1.14.1.1 is that it is confined to the observations of fissile material present at the centre of matrix filled 200 l drums. Clearly fissile material may be present anywhere within the drum, and the spatial variability of response must be taken into account. Accordingly, Monte Carlo calculations are being undertaken using a model die-away chamber. Considerable care is being exercised to try to ensure that the model chamber reproduces the features of the chamber used in the experimental study. As it is assumed that the drum is subject to continuous rotation during assay the azimuthal variation in response is not required, and the calculations are of radial and axial response alone. The calculations are being made with the computer code MORSE, which has been adapted for use on the VAX 11/750 computer by M.T. Swinhoe.

1.14.1.3 Monitoring 500 l drums by neutron interrogation (B.H. Armitage)

An initial assessment has been made of the implications of changing the disposal container size from 200 l to 500 l. The study so far completed has been concerned with neutron die-away interrogation of 500 l drums containing iron matrices at a variety of densities.

Calculations were carried out with the Monte Carlo computer code MORSE and required the modelling of a die-away chamber large enough to accommodate a 500 l drum. The model chamber retains the wall thickness and detection efficiency of the Harwell chamber. However, the lower limit of detection for fissile material is raised in a 500 l chamber for two main reasons. Firstly, the background count rate in the fission neutron detectors is increased due to a larger detector volume. Secondly, the larger chamber

---

\*Worcester College, Oxford

volume dilutes the interrogating thermal flux. The effect of these two factors is to raise the lower limit of detection from  $^{235}\text{U}$  from 3 mg to 9 mg for a matrix-free drum. More significantly, if the matrix density remains similar to that in 200 l drums, there may be a large reduction in response to the presence of fissile material due simply to an increase in matrix mass.

The results of calculations for 500 l iron matrices are given in Table 1.2. For a single piece of fissile material, there is a progressive deterioration in response as the matrix density increases within the range (1 - 2 g cm<sup>-3</sup>) likely to be encountered. Also, as the matrix density increases the response becomes more dependent on the location of the fissile material within the drum.

It is intended to extend these calculations to include other matrices, and to consider measures that might lead to a reduction in spatial variability.

Table 1.2

Response from neutron interrogation of 500 l iron filled drums

Iron matrix density (g cm <sup>-3</sup> )	Relative response (centre of drum)	Relative response (mean over drum)
0.0	1.0	1.0
0.5	0.2	0.3
0.88	0.05	0.2
1.1	0.015	0.08
1.7	0.002	0.02

#### 1.14.1.4 Pulsed neutron source development (B.H. Armitage and J.W. Leake\*)

A development programme with the objective of producing longer lived and more reliable pulsed neutron sources is being undertaken by Marconi Avionics (UKNDC(84)P111 p.71). A Marconi Avionics NK51 pulsed neutron generator has been in use at Harwell for over two years. It consists of a sealed tube within which deuterons are accelerated on to a tritiated erbium target, a separate high voltage transformer and a control unit.

---

\*Instrumentation and Applied Physics Division

The requirements of neutron interrogation are such that a slightly larger diameter canister than that currently in use may be used. This means that the high voltage characteristics of the sealed neutron producing tube may be improved, and anti-sputter guards and suppressor electrodes may be introduced.

Lifetime tests on tubes incorporating new features are an important part of this programme. Sealed tubes containing a new target material have been manufactured and successful lifetime testing undertaken. Sealed tubes utilizing low sputter coefficient materials have been manufactured and some of the life testing will be carried out at Harwell. Progress has also been made on the manufacture of sealed tubes incorporating an anti-sputter guard and suppressor electrode.

#### 1.14.2 Fast shuffler (E. Wood and A.R. Talbot)

Progress has been very limited this year due to shortage of manpower. The interference problems described last year (UKNDC(84)P111 p.71) have been eliminated by installing an electro-optic link between the shuffler detectors and the data collection system (some 50 metres away). The reliability of the system has been demonstrated by overnight runs.

It is hoped to progress further early in 1985.

#### 1.14.3 Evaluation of possible methods of monitoring the $^{235}\text{U}$ enrichment of centrifuge plants operating at low pressure (T.W. Packer and E.W. Lees)

This year the programme has been divided into two:

- (a) the use of a high resolution  $\gamma$ -ray spectrometer to determine the mass and the enrichment of uranium deposited on the inside of the pipe;
  - (b) the use of a high resolution  $\gamma$ -ray spectrometer and energy-dispersive X-ray fluorescence analyser to determine the enrichment of the  $\text{UF}_6$  gas in the pipe at the time of inspection.
- (1) Measurement of the enrichment and the mass of uranium deposited on the inside of product pipes

The previous progress report (UKNDC(84)P111 p.72) described how a high resolution  $\gamma$ -ray spectrometer had been used to determine the enrichment and mass of uranium deposited on the inside of pipes in centrifuge plants. The method is based on the measurement of the number of 186 keV  $\gamma$ -rays emitted by  $^{235}\text{U}$ , 84 keV  $\gamma$ -rays emitted by  $^{231}\text{Th}$  (a daughter of  $^{235}\text{U}$ ), and 63 keV  $\gamma$ -rays emitted by  $^{234}\text{Th}$  (a daughter of  $^{238}\text{U}$ ).

The enrichment and masses of the uranium deposit on eight product pipes at the centrifuge enrichment plant at Capenhurst that had previously been determined in 1983 have been remeasured. Good correlation was obtained between the enrichment measurements. It was also estimated that there had been an average increase in the mass of deposited uranium at an equivalent approximate annual rate of  $50 \mu\text{g}/\text{cm}^2 \text{ year}^{-1}$ . However, the latest results from the second enrichment plant described in UKNDC(84)P111 p.74 show that the plant can operate for several months without a significant mass of uranium being deposited.

Hence it has been concluded that it is unlikely that these measurements can be used to monitor the enrichment history of the cascade between inspection visits. However the ratio of the 84 and 63 keV  $\gamma$ -rays can be used to monitor the presence, or absence, of highly enriched uranium (HEU) in the pipework during the 24 hours prior to inspection.

Hence the effort has been concentrated on methods of detecting the presence, or confirming the absence, of HEU in the pipework at the time of inspection.

(2) Measurement of the mass of  $\text{UF}_6$  gas in the pipe at the time of inspection

In order to detect the presence of HEU in centrifuge pipework it is necessary to determine the mass (or pressure) of the  $\text{UF}_6$  gas in the pipe. Energy dispersive X-ray fluorescence analysis has been shown to be a suitable technique for approximately determining the pressure.

Characteristic uranium K X-rays (94.648, 98.428, 111.298 and 114.549 keV) are efficiently excited by 122 and 136 keV  $\gamma$ -rays emitted by a  $^{57}\text{Co}$  radioisotope source. However, due to the low  $\text{UF}_6$  gas pressure in the product pipes of centrifuges, the density of the  $\text{UF}_6$  gas is small ( $< 150 \mu\text{g}/\text{cm}^3$ ) and hence the number of excited U K X-rays is small compared with the number of scattered  $\gamma$ -rays. It is therefore necessary to use a high resolution semi-conductor detector, such as the GMX used in the  $\gamma$ -ray spectrometer, for resolving the X-rays. It is also necessary to limit the number of U K X-rays excited in the deposited uranium and also the number of  $\gamma$ -rays scattered from the aluminium walls of the pipe from being detected. A geometry has been developed that satisfies both of these requirements and which is also easily interchangeable with the one developed for the  $\gamma$ -ray spectrometry measurements.

The analyser was calibrated using a test rig and measurements were then



made on five product pipes which had uranium deposits in the range 200 to 700  $\mu\text{g}/\text{cm}^2$  on them. It was established that there was good correlation between the declared and measured gas pressure and there was no significant interference from the deposited uranium. It was estimated that the relative pressure measurements could be made to  $\pm 23\%$  (95% c.l.) in 600 s using a 7 mCi  $^{57}\text{Co}$  radioisotope source.

Having established that it was possible to measure the gas pressure, two methods were developed (in conjunction with workers in the USA) to detect if HEU was present in the pipe at the time of inspection.

(3) Method based on the measurement of the 186 keV  $\gamma$ -rays emitted by  $^{235}\text{U}$  and 63 keV  $\gamma$ -rays emitted by  $^{234}\text{Th}$

If the pipe being measured is producing HEU at the time of measurement there will be an excess number of detected 186 keV  $\gamma$ -rays (from  $^{235}\text{U}$ ) with respect to the number of detected 63 keV  $\gamma$ -rays (from decays of  $^{238}\text{U}$ ) compared with the number obtained if there was only LEU in the pipe. It has shown that, provided the pressure of  $\text{UF}_6$  gas in the pipework can be approximately determined ( $\pm 25\%$  relative) by an energy dispersive X-ray fluorescence measurement, it is possible to use the excess 186 keV  $\gamma$ -rays to estimate the excess enrichment of the gas (i.e. to confirm the presence or absence of HEU). Preliminary measurements have shown that under normal operating conditions at Capenhurst it should be possible to determine the "excess" enrichment of the  $\text{UF}_6$  gas to approximately  $\pm 3\%$  (absolute) in a total measurement time of 30 minutes.

(4) Method based on the determination of the 186 keV  $\gamma$ -rays emitted by  $^{235}\text{U}$  measured under two geometries

It has been shown that it is possible to determine the number of 186 keV  $\gamma$ -rays emitted by the gas and the deposited uranium with different relative efficiencies by making two passive  $\gamma$ -ray measurements under different geometries. This technique has the advantage that unlike the method described in (3) above it is independent of the enrichment of the deposited uranium. However as total measurement times of approximately 5 hours would be required to determine the  $\text{UF}_6$  enrichment to  $\pm 3\%$  (absolute) this technique is not recommended for routine inspections at Capenhurst.

1.14.4 The effects of neutron multiplication on neutron coincidence counter measurements (M.T. Swinhoe)

The amount of plutonium in various sample materials (metal, oxide, etc.) is often determined by measuring the spontaneous fission rate of

$^{240}\text{Pu}$ <sup>(1)</sup>. Since the neutrons from the spontaneous fission are often accompanied by neutrons produced by  $(\alpha, n)$  reactions in the sample, and since it is desirable to reduce the effects of background, the coincidence response rather than the total response of the detector assembly is used. The detector coincidence response is essentially proportional to the number of pairs of neutrons emitted per event, and since  $(\alpha, n)$  events emit single neutrons, this increases the signal to background ratio of the measurement.

When the sample is large enough to produce significant multiplication (i.e. when a fast neutron has a significant chance of inducing a fission in the sample) two problems arise. Firstly, the coincidence response of the detector assembly increases because there are on average more neutrons leaving the sample per spontaneous fission event, and secondly, events which begin with a single neutron can cause a coincidence response by inducing a fission.

The probability of inducing fission in various samples has been calculated using the Monte Carlo neutron transport code MORSE (AERE PR/NP 30 p.145). The response of an ideal neutron coincidence counter has been calculated as a function of sample multiplication, and has been compared both with previously made approximations and with some measurements (provided by F.J.G. Rogers of ANMCO). The results show that considerable improvement can be made to the commonly used correction techniques.

These correction methods all use a non-multiplying reference sample to calibrate the detector assembly. The small mass of the reference sample gives rise to a very low counting rate and in most nuclear plant situations, the high neutron background rates result in poor signal to background ratios. A new way of using the correction techniques has been proposed in which a larger multiplying reference sample is used. This can lead to much reduced errors in the corrected results and a reduced measuring time for the reference sample, which no longer suffers from a poor signal to background ratio. A report on this work is being prepared.

---

(1) N. Ensslin, M.L. Evans, H.O. Menlove and J.E. Swansen, Nuclear Materials Management 7 (1978) 43.

## 1.15 Neutron Diagnostics for JET\*

### 1.15.1 Neutron yield monitors (time resolved) (A.R. Talbot)

The detectors (see UKNDC(83)P109 p.64) are now installed at JET and are in regular use, being coupled to the JET computer system and automatically taking data. The stored data can be inspected and analysed with an appropriate software package. The results have been used in the determination of the plasma ion temperature and deuterium density.

### 1.15.2 Neutron yield calibration (E.W. Lees, M.T. Swinhoe, A.R. Talbot, O.N. Jarvis\*\*, J. Kallne\*\*, G. Sadler\*\* and P. Van Belle\*\*)

A 14 MeV pulsed neutron source as well as Am/Be and  $^{252}\text{Cf}$  neutron sources have been used to map out the response of the time resolved yield monitors as a function of neutron source position inside the JET vacuum vessel. The results for three identical detectors situated around the torus are up to a factor of two different, due to the construction of the machine and the presence of different diagnostic equipment. This shows the need for such a calibration.

An attempt to measure the response of the time integrated yield monitor directly, by activating a copper foil with neutrons from the 14 MeV pulsed source, gave a result with poor statistics. In order to get some information on the effect of scattering at the foil irradiation position, the neutron spectrum from an Am/Be source in the vacuum vessel was measured with an NE213 liquid scintillation detector placed at the irradiation position. The spectrum from the same source was then measured in the absence of any scattering material. The results are being analysed.

### 1.15.3I Time-integrated neutron yield monitor (G.B. Huxtable, J. Argyle, A.R. Talbot, P. Dixon<sup>+</sup> and P. Mills-Baker<sup>++</sup>)

This is a system for irradiating foils at positions close to the JET torus and analysing the induced gamma activity to provide an assessment of the neutron fluence over different neutron energy regions at that point. Neutron energies will extend from thermal up to a band around 14 MeV when

---

\* Joint European Torus, Culham, Oxon.

\*\*JET Joint Undertaking

<sup>+</sup> Engineering Projects Division

<sup>++</sup> Brunel University

JET starts d-t operation. Integrating JET output in this way ensures that the measurement can cope with unexpectedly intense bursts of neutron output or electrical noise, which can upset real-time neutron counting methods. By choosing materials which provide a combination of suitable neutron energy thresholds it should be possible to unravel the neutron spectrum into rather crude energy bands, and by using materials with known cross-sections the neutron dosimetry can be made absolute in terms of the fluence at the foils.

The system will also provide the transport mechanism for other diagnostic techniques used at JET such as the regular monitoring of neutron fluence using delayed neutrons from a uranium or thorium sample, and the exposure of photographic emulsions.

The sample transport system is a rather complex "rabbit" installation. Foils are placed in polythene capsules 25 mm in diameter and are driven pneumatically along polythene tubes to the irradiation positions (eight in all) around the torus. After one or more JET shots each foil is retrieved and sent to a radiation detector. At present one intrinsic germanium detector, one NaI and one delayed neutron counter are provided, but more are envisaged. At the hub of this system is a carousel, a turntable device allowing a capsule from any irradiation position to be sent to any detector, with a target time-delay of not much more than 10 s for this 100 m path. The carousel also allows new foils to be added to the system and old ones to be removed, and also allows foils to be stored while activities decay.

Control of the pneumatic system and the multichannel analyser used for spectrum analysis will be done by the JET computer system via JET's CAMAC interface: problems arise as this system is mainly intended to handle data acquired during a shot whereas in our case the data collection may not be complete until long afterwards. Limited manual control of the system will also be possible.

Most of this hardware has now been acquired and the pneumatic system has been assembled for testing in Hangar 7. It has been interfaced to JET's standard multiplexing hardware in a CAMAC crate, which is for the present being controlled by our own DEC LSI-11 computer instead of JET's NORD computer (both computers use FORTRAN). The pneumatic system (a one-off design built under contract in the USA) has been made operational, although a significant amount of work was needed to overcome teething troubles. It

has also been necessary to undertake much redesigning and manufacturing to achieve a system that will be sufficiently reliable in use at JET. The system has been operated over many thousands of capsule-transfer cycles under computer control, and this testing programme will be resumed when the design improvements have been completed.

In addition it has become necessary to redesign the control interface unit between the pneumatic system and the JET CAMAC hardware, partly because of additional requirements that have arisen to ensure safety from activities induced in the driving air, partly to achieve easier manual control, and partly because of shortcomings in the contractors' original design. This redesign is being done at present.

Engineering design of the mechanics of the system is largely complete. The most time-consuming problem has been agreeing with JET on details of pipework in the torus hall, and this is still not completely resolved. We aim to install the torus hall equipment during the JET shut-down in June 1985.

A Canberra 90 analyser has been acquired for collection and analysis of the gamma spectra. This will use pulse-processing electronics supplied by G. White of Instrumentation and Applied Physics. Using this system, an assessment of suitable activation foils has been performed on the basis of published cross-sections and on some measurements using d-d and d-t neutrons from our Van de Graaff. This has resulted in a list of foils recommended for use in various neutron fluences. Further work on the unfolding of the neutron spectra is planned.

The outstanding major task is to write the software for control and data-collection to run on the JET computer system.

#### 1.15.4 Neutron spatial emission profile monitor (M.T. Swinhoe and P. Dixon)

The nineteen NE213 detectors for this diagnostic have been delivered. Each has an integral  $^{22}\text{Na}$  source and LED for gain calibration. In order to achieve as high a count-rate as possible and use pulse shape discrimination, it has been decided to use the Link Systems 5020 PSD unit\*. This should shortly be available with a 0.25  $\mu\text{s}$  deadtime. The collimator/shield assemblies will shortly go to manufacturing tender.

---

\*Link Systems Ltd., Halifax Road, High Wycombe.

1.15.5 2.5 MeV neutron spectrometer for deuterium plasmas (M.T. Swinhoe, O.N. Jarvis\*, G. Sadler\* and P. Van Belle\*)

Some of the detectors for this device (UKNDC(83)P109 p.69) have been tested at JET, using the roof laboratory as the shielded enclosure. Using the  $^3\text{He}$  ion chamber it has been possible to measure the neutron spectrum emitted from an ohmically heated deuterium plasma in a single JET shot. This allows the determination of the plasma ion temperature. Neutron spectra have also been obtained with NE213 detectors, but with insufficient resolution to determine the ion temperature.

1.15.6 14 MeV neutron spectrometers for deuterium-tritium plasmas (C.A. Uttley, D. West and C.W. Thompson\*\*)

Of the three systems described in the last progress report (UKNDC(84)P111 p.76) and for which budgetary cost estimates were prepared for consideration by JET, the magnetic transport system, both in its original form and in an abbreviated (non-achromatic) version, has been rejected by JET as causing too drastic an effect on the layout of other equipment committed to the torus and diagnostic halls. The Si-diode and annular radiator recoil spectrometers, originally budgeted for use in a position just outside the torus hall, have had to be re-designed for location within the torus hall and also for operation in either of two positions since the choice of position must be delayed until after the equipment is produced. The systems will share a shielded enclosure more massive than would have been required in the diagnostics hall and the complications of remote handling have now to be catered for. A fixed price contract for a combination of the two systems capable of operating simultaneously is in active preparation.

1.15.6.1A,I Si diode spectrometer (D. West)

This spectrometer makes use of the  $^{28}\text{Si}(n,\alpha)^{25}\text{Mg}$  reaction in a Si detector. Various aspects of the behaviour of this form of spectrometer, important from a design point of view, have been investigated experimentally using the 500 keV Van de Graaff generator. The detectors were operated in air at atmospheric pressure inside a light-tight enclosure.

---

\* JET Joint Undertaking

\*\*Engineering Projects Division

### Radiation damage

Radiation damage limits the lifetime of the Si detector in the intense neutron radiation to which it must be subjected. No certain figures were available on the effects or the scale of the radiation damage. It was investigated directly for a commercial surface barrier detector of area 450 mm<sup>2</sup> and thickness 1 mm and for an ion implanted detector of area 100 mm<sup>2</sup> and 0.48 mm thickness prepared by J.H. Howes of Instrumentation and Applied Physics Division. For both detectors it was found that the width of the  $\alpha_0$  peak ( $\sim 120$  keV FWHM initially) was doubled by a fluence of 14 MeV neutrons of intensity  $2 \times 10^{12}$  neutrons cm<sup>-2</sup>. After a fluence of  $3 \times 10^{11}$  neutrons cm<sup>-2</sup>, the increase in width was barely perceptible. The results have been reported in ref. 1.

### Energy calibration

A thin source of mixed nuclides (<sup>239</sup>Pu, <sup>241</sup>Am and <sup>244</sup>Cm) was used. These nuclides have mean  $\alpha$ -particle energies of 5.148, 5.479 and 5.795 MeV. An air gap of 4.8 mm was needed to accommodate a collimator, and well resolved peaks at energies of 4.695, 5.048 and 5.381 MeV were seen in the counter (14 MeV neutrons deposit an energy of 11.346 MeV in the detector for the case of the ground state reaction).

### Induced activities

In addition to pulses from the ground state ( $n, \alpha_0$ ) reaction in <sup>28</sup>Si there are ( $n, \alpha$ ) reactions to excited states, ( $n, p$ ) reactions, and elastic and inelastic neutron scattering all of which give pulses in the detector. In fact only 1 in 170 of the pulses lies in the  $\alpha_0$  peak of interest. Consequently high count rates are inevitable, and so it is desirable to minimise additional counts from induced activity. One inevitable source is the 2.25 min. activity of <sup>28</sup>Al formed by <sup>28</sup>Si( $n, p$ ). In addition there are activities from <sup>29</sup>Al (6.6 mins., formed by <sup>29</sup>Si( $n, p$ )) and <sup>27</sup>Mg (9.5 mins., formed by <sup>30</sup>Si( $n, \alpha$ )). Fortunately all these activities are limited by the pulsed nature of the JET discharge - one pulse of 10 seconds duration every 15 - 20 minutes. The light-tight can surrounding the detector is a possible source of induced activity, and graphite containers were developed to minimise this.

### Detector size and source collimation

The important question of shielding the detector from neutrons other than those selected for examination by the precollimator is dealt with in section 1.15.6.3. However, the design of this shield is, in turn, dependent

on the acceptance of the precollimator.

Because of the complication involved in changing collimators, it is essential to have a range of sensitivities available for a given degree of collimation. Suitable Si detectors of areas  $450 \text{ mm}^2$ ,  $300 \text{ mm}^2$ ,  $100 \text{ mm}^2$ ,  $50 \text{ mm}^2$  and  $25 \text{ mm}^2$  are available and cover an intensity range of 18:1. The largest radius of the "pipe" of plasma which can be viewed without the field of view intersecting the central pillar of JET or the boundaries of the remote port is  $\sim 100 \text{ mm}$ . This determines the dimensions of the collimator for measurements having the greatest sensitivity. These dimensions coupled with the count rate restrictions in the Si diode result in a system which is appropriate for a neutron flux centred on a plasma temperature of 2.7 keV and covering the range from 1.9 to 3.7 keV. The intensity of the neutron flux is such that ten spectra per burst can be recorded, each containing sufficient counts to determine the plasma temperature (from the peak width), to  $\pm 10\%$  accuracy in the absence of background. At the bottom energy of the range for this collimator the  $450 \text{ mm}^2$  detector could be used for 32,000 shots, and at the top of the range the  $25 \text{ mm}^2$  detector would last for 2,100 shots or at least 40 working days with a pulse interval of 15 minutes. (These lifetime figures apply to all ranges.) Two other less sensitive ranges are chosen normally to overlap each other by a factor of  $\sqrt{2}$  in intensity. Again, because of the great inconvenience of changing collimators, should a persistent mode of operation of JET fall near the changeover between the basic range of collimators, two overlapping ranges are provided centred on the boundaries of the basic range of three collimators. These intermediate collimators will also take account of the considerable uncertainty in the estimates of neutron yield currently available. Some of the properties of the chosen collimators are listed in Table 1.3.

The extreme sensitivity ratio achieved by varying the collimators alone is 170:1, and when both collimators and detectors are varied it is  $170 \times 4 \times 4.5 = 3036:1$ .



Table 1.3

Plasma temperature ranges and dimensions of the collimators

Collimator identifier	Mid-radius of viewed cone of plasma (mm)	Plasma temperature (keV) at middle and extremes of range	Number of shots for a fluence of $3 \times 10^{11} \text{ n cm}^{-2}$ at the detector (mid-range plasma temperature)	Pre-collimator vertical semi-dimension at front face (mm)	Rear collimator vertical semi-dimension at outside face (mm)
1	100	2.7(1.9-3.7)	8,100	53.5	29.1
1.5	53	3.6(2.5-5.3)	8,400	31.3	19.9
2	28	5.2(3.4-8.2)	9,300	19.6	15.1
2.5	14.7	7.8(4.8-13.6)	11,000	13.3	12.5
3	7.7	13.1(7.3-28.6)	10,400	10.0	11.2

Count rate in the detector

The count rate in the detector will vary between  $70,000 \text{ s}^{-1}$  at the lowest (2 keV) plasma temperature and  $35,000 \text{ s}^{-1}$  at 20 keV. These rates would, as mentioned above, provide ten spectra per shot capable of defining the temperature from each spectrum to  $\pm 10\%$ . Of course only the  $\alpha_0$  region of the spectrum, containing 1/170 of the counts will be submitted for pulse height analysis. Direct checks of the broadening of the spectrum at high count rates have revealed less than 10% effect at rates of  $25,000 \text{ s}^{-1}$ . This is the maximum rate available from thin targets immediately to hand using the Cockcroft-Walton accelerator at maximum beam (120  $\mu\text{A}$ ) at 300 kV.

---

(1) D. West, report AERE-R 11481

1.15.6.2 Annular radiator proton recoil spectrometer (C.A. Uttley)

A basic unit of the spectrometer (see UKNDC(84)P111 p.78) is in the final stage of construction and consists of a  $6 \text{ mg cm}^{-2}$  polyethylene radiator of internal radius 7 cm and external radius 8 cm with a 1.5 cm radius HP Ge detector placed axially 40 cm behind the plane of the radiator. It will be used to check the calculated energy resolution for

recoil protons produced in the radiator by 14 MeV neutrons generated on a 0.5 MeV Van de Graaff accelerator using the d-t reaction. The energy resolution will differ slightly from that expected on JET due to the increased angle of incidence on the radiator of the lower intensity, laboratory generated neutrons.

An essential part of the spectrometer is the neutron collimator which defines the neutron beam incident on the radiator. The optimum collimator design to produce a minimum contamination of the direct flux by source neutrons scattered both from the front and from the inside surface of the collimator has been investigated. The basic principles involved have been applied to the design of the main collimator for the shielded enclosure in the torus hall and to the collimator to be used in the experimental tests on the basic unit of the spectrometer referred to above.

#### 1.15.6.3 Design of the shielded enclosure for both spectrometers (C.W. Thompson\*, C.A. Uttley and D. West)

Calculations of an effective shielded enclosure have been carried out by A.G. Sherwin of the National Radiological Protection Board using the computer program MORSE. There were three constraints: firstly the provision of internal volume so that the two spectrometers could be positioned vertically with a separation of 80 cm and to provide space for electronics and for cooling the Ge detectors: secondly, a shield material called PREMADEX<sup>(1)</sup> (an organo-lithium salt) was specified in order to make the enclosure as light as possible; and thirdly, the shield should attenuate the 14 MeV background flux to a factor of 1/16000 of the expected signal flux at a detector inside the enclosure from a 10 cm radius pipe of plasma. The result of the calculations is an enclosure with a front wall (facing the torus) 210 cm thick and side top and bottom walls 92 cm thick and of total weight ~ 65 tons, rising to ~ 70 tons allowing for the cladding of the PREMADEX. This is a substantial reduction in weight compared to a heavy concrete enclosure of similar neutron shielding effectiveness (~ 250 tons).

A neutron collimator for each spectrometer is inserted into the front wall of the enclosure which is some 13 m from the plasma centre. Thus the

---

\*Engineering Projects Division

(1) A.G. Sherwin, Radiol. Prot. Bull. 57 (1984) 19

volume of plasma viewed by each spectrometer will be defined by a precollimator placed as close as possible to the entrance port to the torus. The collimated neutron beams will suffer little attenuation in the spectrometers and will exit from the enclosure through two apertures in the rear wall and terminate in separate beam stops.

## 2. CHEMICAL NUCLEAR DATA

### 2.1 Introduction

During 1984 the Chemical Nuclear Data Committee held two meetings. A.L. Nichols (AEEW) took over from J.G. Cuninghame as Chairman of this committee with effect from June 1984, and R. Bett continued as Secretary. The Data Library Sub-committee (Chairman A. Tobias (CEGB), Secretary H.E. Sims (AERE)) also met twice in 1984.

Evaluation effort in the UK is now linked to the development and needs of the European Joint Evaluated File, and specific work for this project is identified with the Data Library Sub-committee. Members of the sub-committee have continued to monitor and assess the adoption of decay and fission yield data for the file (JEF-1). An agreed set of decay data has been assembled for issue in 1985, and proposals have been made for the inclusion of evaluated fission yield data that include isomer states.

A seven year programme formulated under the auspices of the IAEA has resulted in significant advances being made in establishing specialised laboratories and expertise for the measurement and evaluation of actinide half-lives and decay data. Recent UK measurements of decay data ( $^{231}\text{Pa}$ ,  $^{235}\text{U}$ ,  $^{239}\text{Pu}$  and others) have been published, and these data are being used to derive more accurate decay parameters than could previously be defined for these important nuclides.

Support for chemical nuclear data stands at between 1 and 2 scientist-years in the UK, and covers such diverse activities as measurement of actinide data and half-lives, neutron dosimetry studies, development of techniques for the measurement of decay data of short-lived fission products, measurement of neutron cross-section data and fission yields in PFR, as well as data evaluation and decay heat assessments.

### 2.2 Measurement work

#### 2.2.1 Nuclear reaction studies designed to test methods for the measurement of data for reactor development and isotope production (J.G. Cuninghame (AERE))

Future work on the measurement of quantities such as half-life, particle and radiation emission and cross-section for products with short half-lives in the range 1 s - 1 h will require the use of a panoply of sophisticated techniques, e.g.

- (a) on-line measurement of emitted particles and radiations,
- (b) very rapid removal of products from target room to a working area,
- (c) fast chemical separations of elements from the products so removed,
- (d) rapid sequential counting of (gamma-ray) spectra of the products,
- (e) multi-parameter event-by-event data acquisition,
- (f) automatic computer control and monitoring of all operations, and
- (g) fast and efficient methods for the analysis of data with as little operator intervention as possible.

Work has continued on the development of such methods with the aim of applying them to the study of decay data for fission products having half-lives in the range 1 s - 1 h and to the measurement of excitation functions needed for the production of isotopes.

Items (a), (b), (f) and (g) are now quite well advanced. During the past year work has concentrated on (d) and (e), with a little on (c). A succession of full gamma-ray spectra at 5 s intervals can now be obtained reliably from a rapidly decaying nuclide, and the spectra produced in a series of subsequent irradiations can be added to them until adequate statistics are obtained. During these operations all control is by computer, and the full details of all experimental parameters are recorded. Considerable effort has also been put into obtaining gamma-gamma coincidence data from two Ge(Li) detectors. A satisfactory electronic system, consisting of a fast-slow coincidence system feeding LeCroy ADCs, has been operated with a multi-parameter event-by-event programme on the PDP 11/34. This system is now working well.

#### 2.2.2 On-line chemical separations of short-lived nuclides in fission and other nuclear reactions (H.E. Sims (AERE); G.F. Blower, G.W.A. Newton, V.J. Robinson (Manchester University))

The main purpose of this study is the elucidation of decay properties of short-lived isotopes (half-life < 5 m) and especially the evaluation of absolute gamma abundances to allow yields to be measured from nuclear fission and nuclear reactions using Ge(Li) spectroscopy. The work was performed using the helium jet recoil transport facility (HJRT) at the Harwell Variable Energy Cyclotron (VEC).

Nuclear fission (and to some extent heavy ion reactions) result in products having a large spread of A and Z and a wide range of yields. As

the HJRT transports all products with equal efficiency, it makes the study of isotopes formed at low yield or with unknown decay systematics difficult. Due to this problem, ways of performing rapid chemical separations on line have been investigated with a view to developing an automated procedure. Two areas are of interest:

- (a) The light isotopes of Re, W and Ta are being studied for several reasons:
  - (i) the region is not easily accessible by mass separators, and
  - (ii) the compound nucleus  $^{181}\text{Re}$  is of interest as it can be made by several routes  $^{12}\text{C} + ^{169}\text{Tm}$ ,  $^{14}\text{N} + ^{167}\text{Er}$ ,  $^{16}\text{O} + ^{165}\text{Ho}$ ,  $^{22}\text{Ne} + ^{159}\text{Tb}$  having different angular momentum distributions, thus allowing us to examine how this affects the various modes of de-excitation.
- (b) The isotopes from Mo to As, which are formed in low yield by thermal neutron fission of  $^{235}\text{U}$ . This region is difficult due to the very short half-lives ( $< 1\text{ m}$ ) and very low yields and therefore requires automated procedures. To investigate the possibility of performing on-line chemical separation for these elements some separations for As, Tc, Ru have been performed using products from heavy ion reactions (where they are formed with higher yields).

Most of the initial work has been carried out on the light isotopes of Re as the decay properties of many of the products are not known. Therefore, it was necessary to establish half-lives, gamma energies, and gamma abundances for the isotopes of interest. A target of  $^{165}\text{Ho}$  was irradiated with a  $^{16}\text{O}$  beam at a series of energies from 184 MeV down to 90 MeV. The activity was collected using the HJRT. Chemical separations of Re isotopes were performed. The activity collected on the tape was washed off and precipitated as tetraphenylarsonium perrhenate. The decay of the rhenium isotopes was observed using a Ge(Li) detector. The time from the end of irradiation to the start of the count was around 50 seconds. This allows unambiguous identification of the gamma rays associated with the rhenium parent isotopes; from the resulting gamma ray excitation functions the mass numbers of the isotopes can be assigned. Previous work in this area has established decay data and absolute abundances for the mass chains 172 - 176 for Re, W and Ta. This work has been used to confirm the results for the isotope  $^{173}\text{Re}$  given below. Fig. 2.1 shows the Re gamma rays seen

from the precipitate using a beam energy of 160 MeV  $^{16}\text{O}$ ; this shows the effectiveness of the chemical separation.

$^{173}\text{Re}$  half-life and gamma ray energies

	Previous work	Present work
Half-life	2 m	1.6 m
Gamma ray energies	-	181.5, 190.7 keV

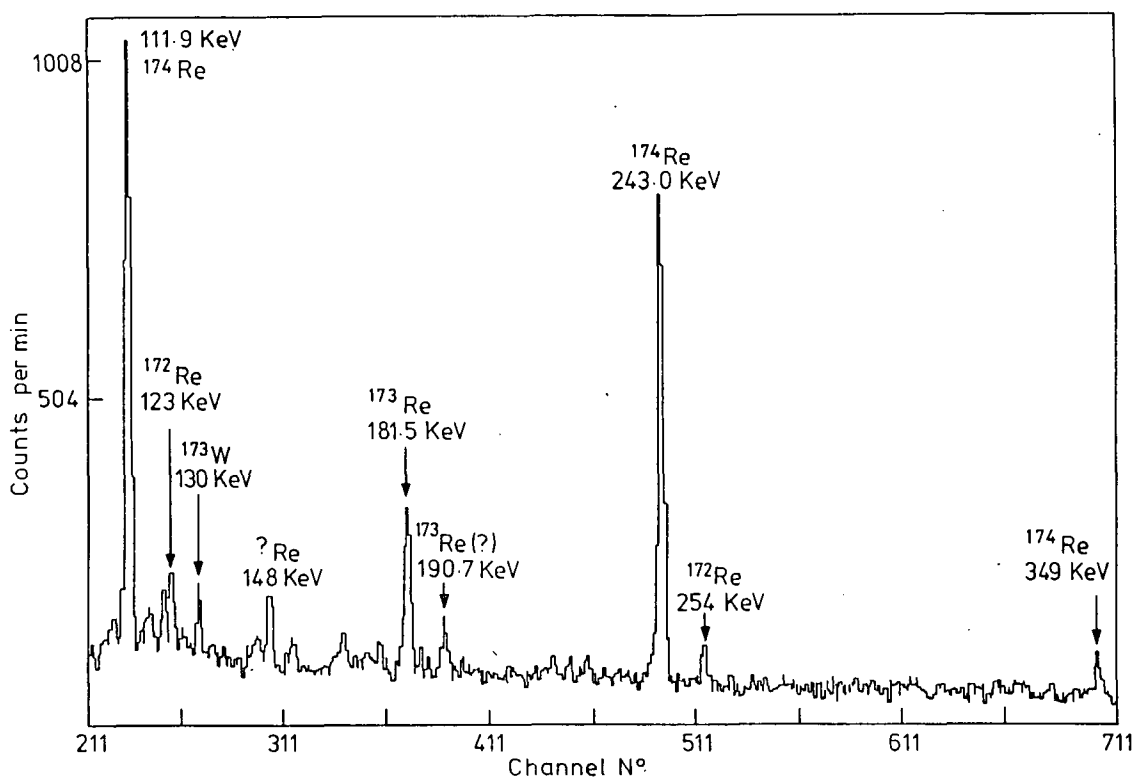


Fig. 2.1 Gamma-rays from a Re source prepared by fast chemical separation from recoils transported by helium jet system. The reaction used was  $^{16}\text{O} + ^{165}\text{Ho} \rightarrow ^{181}\text{Re}$ .

2.2.3 Transfer reactions in the system  $^{92}\text{Mo} + ^{16}\text{O}$  (H.E. Sims (AERE);  
G.W.A. Newton, G.P. Quirk, V.J. Robinson (Manchester University))

The reaction system  $^{92}\text{Mo} + ^{16}\text{O}$  has been studied using off-line Ge(Li) spectroscopy and on-line helium jet techniques. The targets were 97.37% isotopically pure and were rolled to  $3 \text{ mg cm}^{-2}$ . Cross-sections for as many reaction products as possible were measured, from compound nucleus products (e.g.  $^{102\text{m}}\text{Ag}$ ) to nuclides much lighter than the target (e.g.  $^{84\text{a}}\text{Y}$ ). Table 2.1 is a list of products measured and Table 2.2 gives excitation functions for a selection of these observed residual "target-like" products. Fig. 2.2 shows excitation functions for compound nucleus products. Figs. 2.3 - 2.5 show excitation functions for various transfer reactions. It can be seen that, in general, the cross-sections of transfer products more massive than the target peak and then fall off with increasing beam energy while the cross-sections of products lighter than the target continue to rise monotonically with beam energy. The data are being compared with various existing theories in an attempt to account for this behaviour.

Table 2.1

Residual products observed in the system  $^{92}\text{Mo} + ^{16}\text{O}$

$^{104\text{a}}\text{In}$ ,  $^{158\text{g}}\text{Tb}$   
 $^{102}\text{Cd}$ ,  $^{103}\text{Cd}$ ,  $^{104}\text{Cd}$   
 $^{101\text{g}}\text{Ag}$ ,  $^{102\text{g}}\text{Ag}$ ,  $^{103\text{g}}\text{Ag}$ ,  $^{104\text{g}}\text{Ag}$   
 $^{98}\text{Pd}$ ,  $^{99}\text{Pd}$ ,  $^{100}\text{Pd}$ ,  $^{101}\text{Pd}$  (21.4 C)  
 $^{96\text{g}}\text{Rh}$  (50.8 C),  $^{97\text{g}}\text{Rh}$  (69.6 C),  $^{98}\text{Rh}$  (46.2 C)  
 $^{99\text{m}}\text{Rh}$  (83.9 C)  
 $^{100\text{g}}\text{Rh}$ ,  $^{101\text{m}}\text{Rh}$   
 $^{94}\text{Ru}$  (52.3 C),  $^{95}\text{Ru}$  (113.9 C),  $^{97}\text{Ru}$  (99.0 I)  
 $^{92}\text{Tc}$ ,  $^{93\text{g}}\text{Tc}$  (171.0 C),  $^{93\text{m}}\text{Tc}$  (2.6 C),  $^{94\text{g}}\text{Tc}$  (118.9 I),  
 $^{95\text{g}}\text{Tc}$  (49.9 I),  $^{95\text{m}}\text{Tc}$ ,  $^{96\text{g}}\text{Tc}$   
 $^{90}\text{Mo}$  (37.5 C),  $^{93\text{m}}\text{Mo}$  (30.3 I)  
 $^{88\text{g}}\text{Nb}$  (13.0 C),  $^{89\text{g}}\text{Nb}$ ,  $^{90\text{g}}\text{Nb}$  (44.6 I)  
 $^{86}\text{Zr}$  (7.7 C),  $^{87\text{g}}\text{Zr}$ ,  $^{88}\text{Zr}$ ,  $^{89\text{g}}\text{Zr}$   
 $^{84\text{a}}\text{Y}$  (4.9 C),  $^{87\text{g}}\text{Y}$  (13.5 C),  $^{86\text{m}}\text{Y}$  (4.7 I),  $^{86\text{g}}\text{Y}$ ,  
 $^{87\text{m}}\text{Y}$  (23.9 C),  $^{87\text{g}}\text{Y}$   
 $^{85\text{g}}\text{Sr}$

Note: the value given after a nuclide is the cross-section in millibarns for the reaction  $^{92}\text{Mo} + 185 \text{ MeV } ^{16}\text{O}$ , C indicates a cumulative cross-section for that mass, and I indicates an independent cross-section.



Table 2.2

Some excitation functions for products of the reaction  $^{92}\text{Mo} + ^{16}\text{O}$ 

Nuclide	$^{16}\text{O}$ beam energy, MeV					
	185	177	161	144	126	115
$^{104}\text{Cd}$ C	-	-	-	2.6	12.4	54.0
$^{102}\text{gAg}$ C	-	-	29.4	86.6	117.4	91.5
$^{104}\text{gAg}$ C	-	-	4.9	24.7	32.6	112.7
$^{101}\text{Pb}$ C	21.4	-	122.5	147.6	99.9	169.4
$^{94}\text{Ru}$ C	52.3	62.7	61.2	28.4	20.7	20.5
$^{95}\text{Ru}$ C	113.9	128.5	180.5	73.5	40.1	48.7
$^{92}\text{Tc}$ C	-	43.2	40.1	27.8	6.7	7.2
$^{93}\text{gTc}$ C	171.0	175.0	177.9	103.7	60.2	61.8
$^{94}\text{gTc}$ I	118.9	127.0	117.0	62.2	47.8	44.4
$^{96}\text{gTc}$ I	11.5	10.9	12.4	-	-	-
$^{90}\text{Mo}$	37.9	33.9	27.7	13.9	6.2	4.9
$^{93}\text{mNb}$ I	30.3	24.8	22.7	15.7	7.2	4.8
$^{90}\text{gNb}$ I	44.6	33.3	27.7	13.9	6.2	4.9
$^{86}\text{Zr}$ C	7.7	7.6	4.8	1.0	0.8	-
$^{87}\text{mY}$ C	26.3	20.9	16.9	4.8	3.4	2.4
$^{84}\text{mY}$ C	2.6	2.7	2.0	-	-	-
$^{85}\text{gY}$ C	9.6	8.8	8.4	-	-	-

Note: cross-sections in millibarns,  
C = cumulative, I = independent.

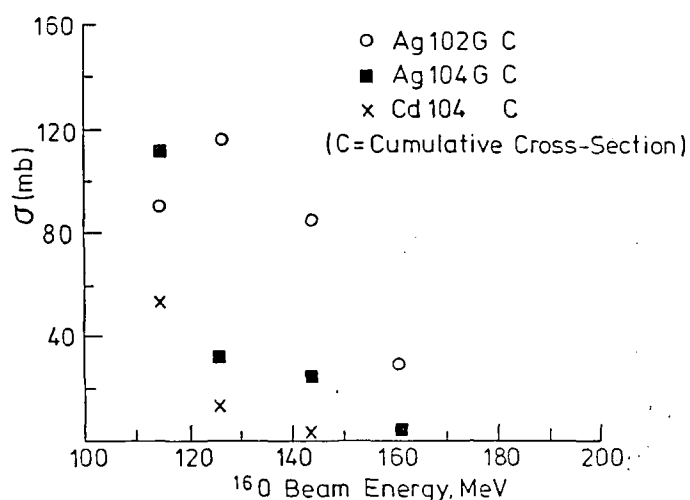


Fig. 2.2 Excitation functions for formation of compound nucleus products from the reaction  $^{16}\text{O} + ^{92}\text{Mo}$

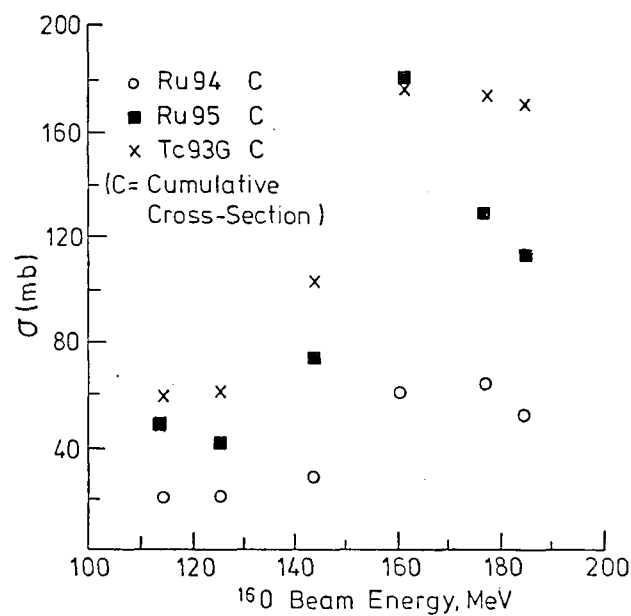


Fig. 2.3 Excitation functions for transfer reactions from the reaction  $^{16}\text{O} + ^{92}\text{Mo}$

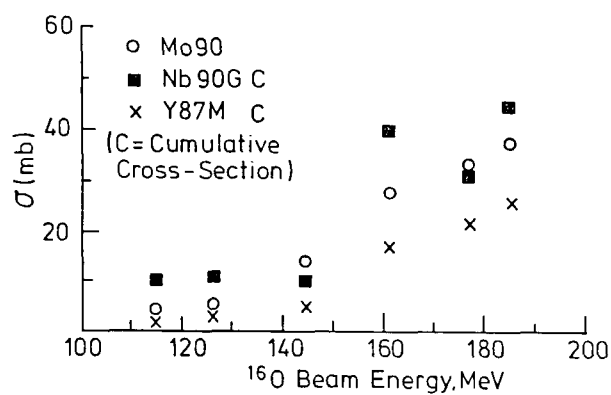


Fig. 2.4 Excitation functions for transfer reactions from the reaction  $^{16}\text{O} + ^{92}\text{Mo}$

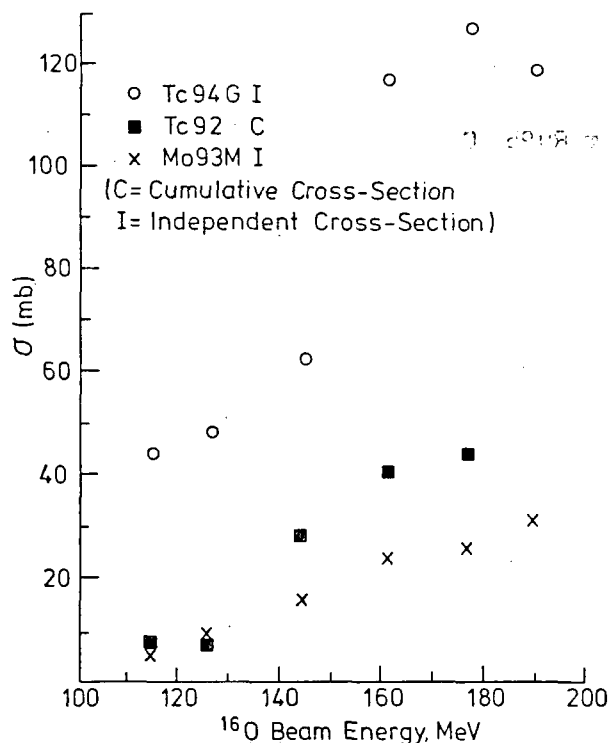


Fig. 2.5 Excitation functions for transfer reactions from the reaction  $^{16}\text{O} + ^{92}\text{Mo}$

#### 2.2.4 Direct transfer reactions in the heavy ion systems $^{12}\text{C}$ , $^{14}\text{N}$ and $^{16}\text{O}$ + $^{197}\text{Au}$ (H.E. Sims (AERE); G.W.A. Newton, V.J. Robinson, H.L. Wilkinson (Manchester University))

Single neutron transfer reactions in heavy ion systems were first observed in the 1950s. Because of their "direct" nature these reactions provide very useful tools for probing the nuclear structure of the two ions involved. The mechanisms of these reactions are however not yet fully understood. The purpose of this project is to measure the absolute yields of the single nucleon transfer products in the systems  $^{12}\text{C}$ ,  $^{14}\text{N}$  and  $^{16}\text{O} + ^{197}\text{Au}$  as a function of energy. This system has the following advantages:

- (a) most of the products are long lived (half-life  $> 1$  h) and may therefore be determined by foil counting, and
- (b) all the products have spin isomers, which allows some insight to be gained into the transfer of angular momentum.

The detectable products and the transfer reactions involved are shown in Table 2.3. Table 2.4 gives a list of the experiments performed.

Table 2.3

Target-like single nucleon transfer products in  $^{12}\text{C}$ ,  $^{14}\text{N}$  and  $^{16}\text{O} + ^{197}\text{Au}$ 

Isotope	Half-life	Spin/Parity	Transfer reaction
* $^{197g}\text{Hg}$	64.1 h	$\frac{1}{2}-$	p into, n out of target
$^{197m}\text{Hg}$	23.8 h	$13/2+$	"
$^{196g}\text{Au}$	6.18 d	$2-$	n out of target
* $^{196m1}\text{Au}$	8.2 s	$5+$	"
* $^{196m2}\text{Au}$	9.7 h	$\frac{1}{2}-$	"
$^{198g}\text{Au}$	2.7 d	$2-$	n into target
$^{198m}\text{Au}$	2.3 d	$\frac{1}{2}-$	"
$^{197g}\text{Pt}$	18.3 h	$\frac{1}{2}-$	p out of, n into target
$^{197m}\text{Pt}$	94 m	$13/2+$	"
* $^{198}\text{Hg}$	stable	$0+$	p into target
* $^{196}\text{Pt}$	stable	$0+$	p out of target
* $^{199}\text{Hg}$	stable	$\frac{1}{2}-$	p into, n into target
* $^{195}\text{Pt}$	stable	$\frac{1}{2}-$	p and n out of target

\*Undetectable

Table 2.4

Experiments performed

Beam	Energy (MeV)	Energy at target half-thickness	Irradiation time (hours)	Target/catcher counting arrangement
$^{16}\text{O}$	184.2	182.7	1.0	normal
	134.9	133.2	0.75	normal
	134.9	123.1	0.50	normal
	84.8	81.3	1.0	normal
$^{14}\text{N}$	148.6	147.4	0.67	separated
	151.2	141.5	1.0	normal
$^{12}\text{C}$	171.5	159.9	1.0	separated
	171.5	152.9	1.53	normal

The experimental technique used was off-line gamma-ray spectroscopy of the target foils. In some experiments the targets and the aluminium catcher foils were counted separately; this allowed an estimation of the linear momentum transfer.

Table 2.5 shows the cross-sections found; the only isotopes present in detectable quantities are:-

$^{197m}\text{Hg}$       1 neutron out of, 1 proton into target  
 $^{196g}\text{Au}$       1 neutron out of target  
 $^{198g}\text{Au}$       1 neutron into target

The 1 proton out of, 1 neutron into target exchange reaction was not observed. Fig. 2.6 shows one of the excitation functions obtained, that for the formation of  $^{196g}\text{Au}$ .

Table 2.5

Cross-sections for single nucleon transfer in the systems  
 $^{16}\text{O}$ ,  $^{14}\text{N}$  and  $^{12}\text{C}$  +  $^{197}\text{Au}$

Projectile	Energy (lab) (MeV)	Cross-sections (mb)		
		$^{197m}\text{Hg}$	$^{196g}\text{Au}$	$^{198g}\text{Au}$
$^{16}\text{O}$	183	$48.1 \pm 2.5$	$163.9 \pm 7.4$	$20.4 \pm 1.0$
	133	$30.4 \pm 1.3$	$124.7 \pm 5.3$	$7.2 \pm 0.3$
	123	$24.6 \pm 1.2$	$102.8 \pm 4.6$	$3.7 \pm 0.2$
	81		$6.8 \pm 0.4$	
$^{14}\text{N}$	147	$48.8 \pm 2.8$	$129.9 \pm 5.3$	$20.9 \pm 0.9$
	142	$49.4 \pm 3.2$	$135.2 \pm 6.1$	$23.2 \pm 0.9$
$^{12}\text{C}$	160	$44.4 \pm 2.9$	$174.2 \pm 7.4$	$15.2 \pm 0.8$
	153	$31.7 \pm 1.8$	$120.1 \pm 7.0$	$9.7 \pm 0.6$

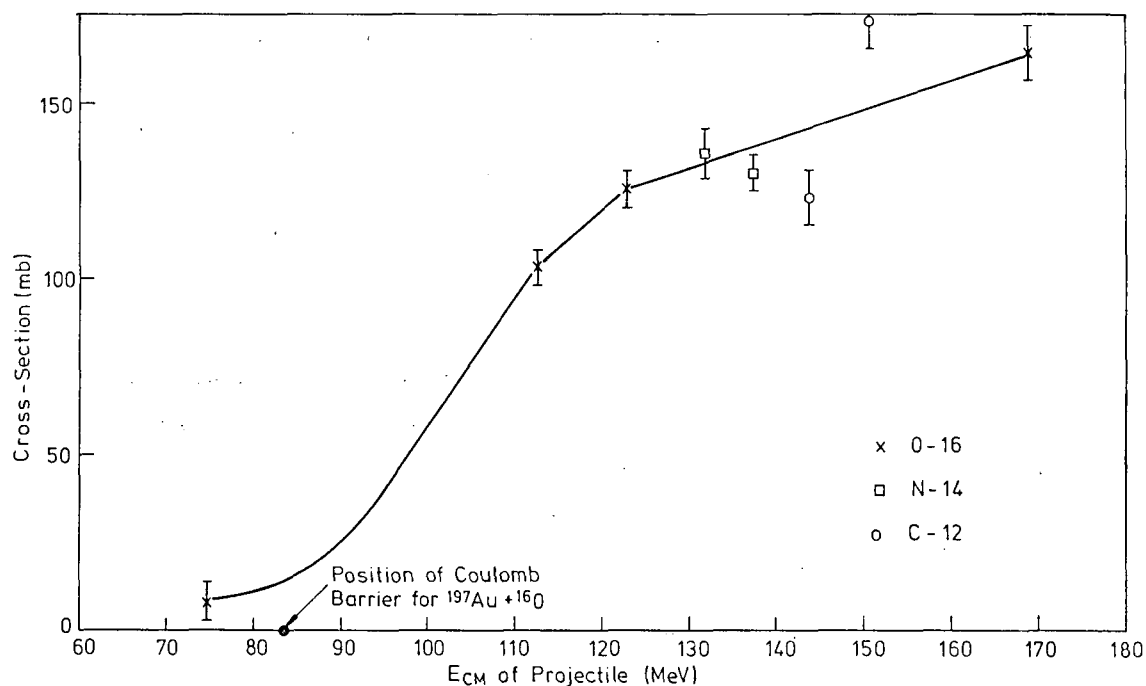


Fig. 2.6 Excitation functions for the formation of  $^{196g}\text{Au}$  from the reactions  $^{12}\text{C}$ ,  $^{14}\text{N}$  and  $^{16}\text{O}$  with  $^{197}\text{Au}$

The following tentative conclusions emerge:

- (i) the reactions are "direct" as shown by the monotonic excitation functions and by the fact that only one nucleon is involved. This means that there is only a small energy transfer;
- (ii) the mechanism involved in proton/neutron exchange is probably different from that involved in neutron only transfer since the latter reactions do not appear to involve large amounts of angular momentum transfer while the former does;
- (iii) the reactions may be qualitatively described by systematics which show the cross-sections to be dependent on the height of the energy barrier to a transfer reaction;
- (iv) the excitation functions, in particular at energies near to the Coulomb barrier, need further work. Once this is complete an attempt can be made at using the results to model the reaction mechanism.

2.2.5 Integral nuclear reaction rate measurements of transactinium nuclides in defined neutron spectra (R.A.P. Wiltshire, W. Snooks, D. Anstee and R. McCrohon (AERE))

Measurement of the capture and fission product nuclides produced from known quantities of transactinium nuclides after irradiation in characterised neutron spectrum positions in reactors has enabled reaction rates to be calculated for these nuclides. As well as providing a useful check on calculated rates and differential cross sections, those data are often the only experimental data available for the estimation of nuclear waste production. Capsules containing 100 µg to 1 mg quantities of  $^{238}\text{U}$ ,  $^{239}\text{Pu}$ ,  $^{241}\text{Am}$ , and  $^{243}\text{Am}$  were irradiated in mid- and outer-core regions of the Prototype Fast Reactor (PFR) at Dounreay. Mass, alpha-particle, and gamma-ray spectrometry have been used to measure the plutonium and curium products and the fission product  $^{137}\text{Cs}$ . This work has been completed and is in process of publication.

Multi-gram quantities of  $\text{Am}_2\text{O}_3$ ,  $\text{Cm}_2\text{O}_3$  and mixed rare earth, americium and curium oxides have been irradiated in PFR to a significant burn-up as part of a joint USA/UK actinide nuclear incineration programme. Some of this material is expected at Harwell shortly and will be analysed for reaction products. Again, the data will be used to check calculated reaction rates in the fast reactor neutron spectra used.

2.2.6 Participation by AERE Harwell in the IAEA Co-ordinated Research Programme on the Measurement and Evaluation of Transactinium Nuclear Decay Data (A.J. Fudge (AERE))  
(WRENDA 1072)

Measurements of the gamma-ray emission probability  $P_\gamma$  and the half-life  $t_{1/2}$  for a number of nuclides continued in collaboration with other establishments. Recalculation of some earlier measurements of  $P_\gamma$  has been necessary so that they are now compatible with measurements made using the IAEA agreed standards data. Theoretical and experimental work on the half-life of  $^{241}\text{Pu}$  and a re-examination of previous measurements made at Harwell is changing many of the previously reported values.

$^{232}\text{U}$

Measurements of  $P_\gamma$  have been made on freshly separated  $^{232}\text{U}$ . The results, shown in Table 2.6, have been sent to the evaluators for inclusion in the Co-ordinated Research Programme (CRP) compilation.

Table 2.6

 $P_{\gamma}$  values for  $^{232}\text{U}$  decay (daughters excluded)

Energy (keV)	$P_{\gamma}$
57.70	$0.001992 \pm 0.000012$
129.03	$0.000681 \pm 0.000004$
270.27	$0.0000317 \pm 0.0000002$
328.05	$0.0000284 \pm 0.0000002$

 $^{237}\text{U}$ 

This nuclide was prepared by irradiation of high purity  $^{236}\text{U}$  and purified by ion-exchange from fission products. Samples taken from the bulk stack have been sent to the National Physical Laboratory for assay by  $4\pi\beta\gamma$  coincidence counting and also, in collaboration with Harwell, for half-life measurement.  $P_{\gamma}$  measurements have been carried out, but so far only on a relative basis, using a range of gamma and X-ray detectors.

 $^{231}\text{Pa}$  and  $^{237}\text{Np}$ 

The results of the  $P_{\gamma}$  measurements previously obtained on these nuclides have been revised by using a new method of estimating the detector efficiencies and the IAEA recommended values for the calibration nuclides. These results have also been sent to the evaluators for inclusion in the CRP data set.

 $^{241}\text{Pu}$ 

Measurements of the half-life of this nuclide have been of concern because of the discrepant values from different laboratories. In particular, the measurements carried out by Cabell and Wilkins at Harwell have, for no obvious reason, resulted in half-life values significantly larger than more recently measured values. Experimental investigations indicate that the sensitivity of  $^{241}\text{Am}$  in a surface ionisation mass spectrometer is significantly greater than that for  $^{241}\text{Pu}$ . Thus a possible reason for a longer half-life could be the incomplete, but reproducible, separation of  $^{241}\text{Am}$  from the plutonium isotopic mixture before mass spectrometry. This aspect is being investigated further. Measurements carried out on the same isotopic mixture since 1977, but on which extra care was taken to ensure the



complete removal of  $^{241}\text{Am}$  prior to mass spectrometric ratio measurements, are resulting in a half-life of  $14.4 \pm 0.1$  years, but the results are based on a limited number of observations. A theoretical assessment of the chemical bonding influences on nuclear beta decay rates carried out by M.R. Harston and N.C. Pyper of the University of Cambridge indicates that it can account for no more than 0.3% change in the half-life of  $^{241}\text{Pu}$ . This work is to be published shortly.

#### Half-life measurements of $^{242}\text{Cm}$ and $^{237}\text{Pu}$

Re-evaluations of the data obtained for the above nuclides using more rigorous curve fitting techniques have resulted in values of  $162.98 \pm 0.16$  days and  $45.86 \pm 0.10$  days for the above nuclides.

Work is continuing also on  $P_\alpha$  and  $t_{1/2}$  measurements on  $^{237}\text{Np}$  and  $^{244}\text{Cm}$  as well as  $P_\gamma$  for  $^{233}\text{Pa}$ ,  $^{239}\text{U}$  and  $^{239}\text{Np}$ .

#### 2.2.7 Transactinium half-life, alpha energy and emission probability measurements (R.A.P. Wiltshire, M. King and B. Whittaker (AERE)) (WRENDA 1072)

Measurements of the half-lives, alpha energies and alpha particle emission probabilities of a range of actinide nuclides of importance to the nuclear fuel cycle continue to be made, using the radiochemical expertise built up over many years in Chemistry Division. The progress is dictated by the availability of both manpower and materials, and also in some cases by the need to develop improved measurement techniques.

#### Half-life measurements

A final value of  $163.00 \pm 0.16$  days has been obtained for the half-life of  $^{242}\text{Cm}$  which agrees well with the recent evaluated value of  $162.94 \pm 0.06$  days by H. Okashita (JAERI) as part of a Coordinated Research Programme of the IAEA. Measurements over four half-lives of the nuclide  $^{237}\text{Pu}$  which decays by electron capture have been made. The value obtained of  $45.86 \pm 0.10$  days is significantly longer than the recently evaluated value of  $45.17 \pm 0.06$  days. More detailed examination of the data indicates the presence of a long-lived impurity. Measurements will continue in order to obtain a correction factor. Measurements of the half-life of the 396 day  $^{235}\text{Np}$  nuclide have been started using  $^{241}\text{Am}$  as an internal standard. This work is continuing.  $^{237}\text{Np}$  is of considerable importance in a number of aspects of the nuclear industry. Its half-life, although claimed to be known to high accuracy, has been measured only once in the past 30 years.

Consideration is now being given to the re-measurement of the half-life of this nuclide together with its associated decay scheme. No direct decay measurement is possible because of its very large value, so it will be attempted via a specific activity measurement.

#### Alpha particle energy measurements

Highly accurate alpha particle energy values are of considerable importance to detailed decay scheme analysis and alpha spectrometry measurements. This work is being carried out in conjunction with A. Rytz of BIPM using a high precision magnetic spectrometer. Measurements are in progress on  $^{236}\text{Pu}$ ,  $^{252}\text{Cf}$ ,  $^{243}\text{Am}$  and  $^{212}\text{Po}$ .

#### Decay scheme emission probability measurements

As well as providing data for detailed decay scheme measurements of nuclides, the emission probabilities of decay modes are vitally important to assay by radiometric analysis since they directly limit its accuracy. Many values are either only known with poor accuracy or have been measured with unrealistic uncertainties. The X-ray and alpha particle emission probabilities have been measured for  $^{235}\text{Np}$ , which is a nuclide of increasing importance as an environmental tracer, in conjunction with Campbell of the University of Guelph.  $P_{\alpha}$  measurements on  $^{237}\text{Np}$  are constrained by the lack of adequate resolution of the alpha particle energies at present. Even the improved resolution detectors now being examined are unlikely to be adequate for this work. Investigations into the use of computer codes to fit the energy peaks as used in gamma-ray spectrometry is in progress in collaboration with Bortells of CBNM.

### 2.3 CNDC Data Library Sub-Committee

(Current membership: A. Tobias (Chairman, BNL), H.E. Sims (Secretary, AERE), A.L. Nichols (AEEW), M.F. James (AEEW), and B. Aldred (BNFL)).

#### 2.3.1 Data library development

The current status of the UKCNDL data libraries is summarised in Table 2.7. There has been little change to the available data libraries during the past 12 months, but work has progressed towards future revisions of them.

Table 2.7

UK Chemical Nuclear Data Libraries status

Data	Present status	File development
1. Fission Product Decay Data	Exists as UKFPDD-2 (ENDF/B-IV format); replaces UKFPDD-1. Total no. of nuclides = 855 Radioactive nuclides = 736 Ground state = 175 1st excited state = 133 2nd excited state = 5 Nuclides with spectra = 390 Total no. of $\gamma$ lines = 11978 Total no. of $\beta^-$ lines = 3592 Total no. of $\beta^+$ lines = 91	Data acquisition for future revision. Some data have been converted to ENDF/B-V format. Adoption of delayed neutron emission probabilities from Reeder (BNL))
2. Activation Product Decay Data	Available in ENDF/B-IV and V format for 91 nuclides as UKPADD-1. Now includes detailed K x-ray spectra.	60 nuclides have been evaluated for UKPADD-2; 56 are in ENDF/B-V format. Temporarily suspended.
3. Heavy Element and Actinide Decay Data	Completion of UKHEDD-1 including spontaneous fission data in June 1982 Data in ENDF/B-V format for: Total no. of nuclides = 125 Ground state = 111  1st metastable state = 13 2nd metastable state = 1 Total no. of $\alpha$ lines = 767 Total no. of $\beta^-$ lines = 527 Total no. of $\beta^+$ lines = 39 Total no. of $\gamma$ lines = 3475 Total no. of discrete electrons = 6755 Total no. of X-rays = 381	AEW-R 1407 References are being brought together for evaluation of nuclides in the 4n series. $^{231}\text{Pa}$ , $^{234}\text{U}$ and $^{239}\text{U}$ decay data and $^{242\text{m}}\text{Am}$ half-life have been evaluated. On completion of IAEA-CRP document decay data for ~ 20 nuclides will be incorporated to form UKHEDD-2.
4. Fission Yields	Available in ENDF/B-V format, based on James/Crouch data called Crouch 4A (adjusted) and Crouch 4U (unadjusted).	Crouch's data files and programs have been used (in ENDF/B-V-IV and V formats) to produce updated libraries of both unconstrained and constrained yields including uncertainties. These will also generate most of the necessary documentation. Also included in ternary fission and the work described in CNDC 85(P3) and CNDC 85(P4). Further development will be in collaboration with Birmingham University.

Spectral data from the decay data files may be accessed via the retrieval system described by Tobias (CEGB report RD/B/517QN81 (1981)).

### Heavy elements (A.L. Nichols (AEEW))

Important decay data have been evaluated for  $^{231}\text{Pa}$ ,  $^{234}\text{U}$ ,  $^{239}\text{U}$  and  $^{242\text{m}}\text{Am}$ . This work was undertaken to assist in the IAEA Co-ordinated Research Programme (CPR) on the Measurement and Evaluation of Transactinium Isotope Nuclear Decay Data. All re-evaluations associated with this international exercise will be incorporated into an updated version of the UKCNDP heavy element and actinide decay data file UKHEDD-2.

#### $^{231}\text{Pa}$

Adjusted gamma-ray emission probabilities were received in mid-October 1984 from Banham of AERE. These final data show small differences from the original data<sup>(1)</sup>, particularly for the low energy gamma emissions. Some minor adjustments have been made to the uncertainties of the low energy emissions to bring them within the accepted limits defined by the CRP participants.

#### $^{234}\text{U}$

The alpha and gamma decay data have been evaluated for this nuclide. CRP measured data have been reported by Vaninbroukx et al<sup>(2)</sup> and H. Okashita<sup>(2)</sup>, and they have been evaluated against equivalent data from earlier publications. The half-life of this nuclide has been re-assessed in conjunction with recent proposals arising from alpha and neutron cross-sections studies<sup>(3,4)</sup>.

#### $^{239}\text{U}$

Adjusted gamma-ray emission probability data were received at the beginning of November 1984 from MacMahon of Imperial College. The initial measurements from this source were presented<sup>(5)</sup> using detector calibration data from ref. 6. These preliminary data differed from the values reported in ref. 7. The data have been adjusted further after additional discussions and the adoption of the calibration standards given in ref. 8. The half-life of this nuclide has also been evaluated.

#### $^{242\text{m}}\text{Am}$

The total and alpha half-lives have been evaluated following the recent measurements by Zelenkov et al<sup>(9)</sup>, and a reassessment of the data published by Barnes et al<sup>(10)</sup>. The spontaneous fission half-life has also been recalculated using the latest values for the total half-life and the branching fraction to  $^{242}\text{Cm}$ ; this involved an adjustment of the data measured by Caldwell et al<sup>(11)</sup>.

Specific decay data for 26 actinides have been measured and evaluated

under the auspices of the CRP. A final report is being prepared for publication, and all of the new and improved data from this source will be used to produce UKHEDD-2. When this has been completed work will begin on the development of UKPADD-2, which was temporarily suspended in late 1983.

#### Fission products (A. Tobias (CEGB/BNL))

The decay data processing code COGEND<sup>(12)</sup> was modified so that it would provide details of all K-shell X-rays arising in a decay scheme in preference to the 'average' K-shell value previously derived. The data base for this revision was taken from ref. 6.

The literature search for decay data of short-lived fission products has continued. Attention was focussed on those nuclides for which no data were previously available. Due to the work towards the JEF1 decay data file there has been no further progress towards UKFPDD-3. It is now anticipated that it will evolve from JEF1 for which the provisional UKFPDD-3 data form a major contribution.

---

- (1) M.F. Banham and R. Jones, Int. J. Appl. Rad. Isot. 24 (1984) 1225.
- (2) Submitted to Int. J. Appl. Rad. Isot.
- (3) W.P. Poenitz and J.W. Meadows, ANL/NDM-84.
- (4) M. Divadeenam and J.R. Stehn, Annals Nucl. Energy 11 (1984) 375.
- (5) S.P. Holloway et al., Proc. Int. Conf. Nucl. Data Sci. Tech., Antwerp, 1982 (ed. K.H. Böckhoff) p.287 (Reidel, 1983).
- (6) Table of Isotopes (ed. C.M. Lederer and V.S. Shirley), 7th ed. (Wiley, 1978).
- (7) S.P. Holloway, thesis (1983), Imperial College.
- (8) INDC(NDS) - 145/GEI.
- (9) Zelenkov et al., Atomnaya Energiya 47 (1979) 405.
- (10) V. Barnes et al., J. Inorg. Nucl. Chem. 9 (1959) 105.
- (11) Caldwell et al., Phys. Rev. 155 (1967) 1309.
- (12) CEGB report RD/B/N4147.

#### 2.3.2 Fission yields

An extensive revision of the fission yield evaluation is planned. This will include the development of new models for the prediction of unmeasured

yields and the construction of appropriate covariance error files which will describe the uncertainties of, and correlations between, the final results. This work will be undertaken by a Research Fellow at the University of Birmingham under the combined sponsorship of CEGB, UKAEA and BNFL.

### 2.3.3 Joint Evaluated File (JEF)

Much of the Data Library Sub-Committee's efforts have been towards establishing the decay data component of JEF1 in collaboration with the CEA in France. The selection of decay data for JEF1 from UK and French sources was proposed by Nichols and Tobias<sup>(1)</sup> on the basis of a decay scheme consistency check for each nuclide. The UK contribution towards this consists of decay data for 411 nuclides and has been assembled in the internationally agreed ENDF/B-V format. It has been tested using standard ENDF/B-V checking codes. A preliminary version of the French contribution has been received and examined. The final version of this should be available shortly and will then be merged with the UK contribution. It is anticipated that JEF1 decay data will be available for use by Spring 1985 following appropriate testing and validation.

---

(1) A.L. Nichols and A. Tobias CNDC(83)P19.

### 2.3.4 CASCADE (G. Evangelides (Daresbury Laboratory))

There have been no further developments to the CASCADE suite of programs. Most of the CASCADE reports have been edited following critical review by the Data Library Sub-Committee and are now approaching their final form. It is hoped that this work will be completed by mid-1985.

3. REACTOR PHYSICS DIVISION, AEE WINFRITH  
(Division head: Dr. J.R. Askew)

3.1 Nuclear data evaluation and validation

3.1.1 Fission product data (M.F. James and S. Whitworth)

3.1.1.1 Fission product yields

The evaluation programs by Crouch (recently retired from AERE Harwell) have been implemented at Winfrith, and further developed. Using the last database of yield measurements produced by Crouch, a revised evaluation has been made. Two libraries of independent yields and their standard deviations are available in ENDF/B-V format: C4U, containing unadjusted data from a straightforward evaluation of measured yields; and C4A, containing data obtained from a least-squares adjustment, forcing yields to satisfy several conservation laws. Yields of isomeric states are included. Data files of the covariance matrices will be prepared for the adjusted set C4A. A draft report describing the evaluation has been written, and testing of the libraries, including comparison with the currently recommended set C3I and with the ENDF/B-V library, is under way.

3.1.1.2 Decay heat

Further studies (primarily of the sensitivity of decay heat to branching ratios and to fission product isomer yields) have confirmed the difficulty of explaining all of the discrepancies between calculated and measured decay heat in terms of deficiencies in the decay data or yield libraries. Revised calculations using the new yield library C4A will be made shortly.

3.1.2 IAEA Coordinated Research Programme on transactinium decay data  
(A.L. Nichols)

In support of the IAEA coordinated research programme the decay data evaluation for  $^{234}\text{U}$  has been completed and the evaluations for  $^{231}\text{Pa}$  and  $^{239}\text{U}$  should be available in early 1985.

3.1.3 Few-group capture cross-sections of  $^{231}\text{Pa}$  and  $^{230}\text{Th}$  in FISPIN  
(R.W. Smith)  
(WRENDA 834,862,863)

An in-depth review of the three group (thermal, resonance and fast) capture cross-sections of  $^{231}\text{Pa}$  and  $^{230}\text{Th}$ , as used in FISPIN, has been completed. Significant changes to some of the existing data are proposed, and error estimates have been derived by comparing the calculated values with an evaluation of all available experimental data.

#### 3.1.4 Three-group actinide cross-sections (Mrs. C.R. Eaton and C.J. Dean)

A library of irradiation independent actinide cross-sections (129 actinides) has been produced for use in FISPIN to predict isotope inventories and activities in irradiated MAGNOX reactor fuel.

#### 3.1.5 Benchmark testing of the JEF1 library (Miss C. Biles, C.J. Dean and M.J. Grimstone)

Benchmark testing of this library has continued during 1984.

### 3.2 Theoretical methods

#### 3.2.1 Level statistics in the unresolved resonance region (M.F. James)

Existing methods of generating ladders of resonances from statistical populations (e.g. GENEX, RESP and TIMS) do not assume any correlation between spacings of neighbouring resonances, although it has been known for some time that a strong correlation exists. A study has shown that the diagonalisation of relatively small random matrices (e.g. of order 50 x 50) will generate populations of levels that satisfy all statistical tests that appear relevant to the production of shielded multigroup cross-sections, and be still sufficiently rapid for practical purposes.

### 3.3 Cross-section processing codes

#### 3.3.1 NJOY/SIGAR (R.W. Smith)

During 1983 the implementation of the SIGAR7 option in NJOY for the generation of Doppler broadened cross-sections was completed and tested. A comparison of NJOY and SIGAR7 broadened data has been made using the data files in the ENDF/B-V dosimetry library, and the results, constituting stage 2 of the IAEA intercomparison exercise, are being sent to the IAEA in Vienna.

#### 3.3.2 NJOY/ACER (Miss C. Biles)

Extensive modifications have been made to the ACER module of NJOY on the ICL 2976 in order to produce cross-section data for UK Monte Carlo codes.

#### 3.3.3 Code implementation and testing on the Harwell computers (Mrs. C.R. Eaton and S. Whitworth)

TIMS has been successfully implemented on both the CRAY and IBM computers at AERE Harwell. Difficulties in running NJOY on the CRAY, due to problems of character handling, are the subject of current studies.



4. DIVISION OF RADIATION SCIENCE AND ACOUSTICS  
NATIONAL PHYSICAL LABORATORY

(Superintendent: Dr. K.C. Shotton)

4.1 Californium neutron source emission rate intercomparisons  
(organised by BIPM\*)

NBS Source SR144 (coordinator: E.J. Axton (NPL, BIPM))  
(Emission rate  $\sim 4.5 \times 10^7 \text{ s}^{-1}$  at start of intercomparison)

Final results have been received from participants who received this source. These will be analysed in early 1985. An NPL source has also been sent to BARC and to IAE, to allow them to participate.

Source SR225Z (coordinator: W.G. Alberts (PBT))  
(Emission rate  $\sim 10^9 \text{ s}^{-1}$  at start of intercomparison)

There has been no further progress.

4.2 Fast neutron fluence intercomparisons  
(organised by BIPM)

Transfer method using the  $^{115}\text{In}(n,n')^{115\text{m}}\text{In}$  reaction at 14.8 MeV  
(coordinator: H. Liskien (CBNM))

Studies are in progress of the corrections for target-scattered and room-scattered neutrons.

Transfer method using  $^{115}\text{In}(n,\gamma)^{116\text{m}}\text{In}$  reaction at 0.144 and 0.565 MeV  
(coordinator: T.B. Ryves (NPL))

Final results have been received from five laboratories (CBNM, ETL, NPL, NRC and PTB) and the remaining measurement, by IAE, should be completed early in 1985.

Transfer method using twin  $^{235}\text{U}$  and  $^{238}\text{U}$  fission chambers  
(coordinator: D.B. Gayther (AERE))

(See section 1.9)

4.3 Investigation of the  $^{45}\text{Sc}(p,n)^{45}\text{Ti}$  reaction (J.B. Hunt, M. Cosack\*\* and H. Lesiecki\*\*)

The  $^{45}\text{Sc}(p,n)$  neutron yield curve at  $0^\circ$  has been determined as a function of the incident proton beam energy using both conventional DC-beam and time-of-flight techniques using the 3 MV NPL Van de Graaff. For the DC-beam measurements, the neutron yield was measured with NPL long counters calibrated previously. In order to increase the energy resolution of the measurements, very thin scandium metal targets of approximately  $5 \mu\text{g cm}^{-2}$ , corresponding to an energy loss of about 0.3 keV for incident proton

---

\*See UKNDC(84)P111 p.96 and UKNDC(82)P105 p.71 for abbreviations

\*\*Physikalisch-Technische Bundesanstalt, W. Germany

energies near the reaction threshold of 2.908 MeV, were used. For the time-of-flight measurements two lithium glass scintillators were used for neutron detection.

The neutron yield curves measured by the two methods agree very well, and exhibit very pronounced resonances with little neutron production between the lines. The independent determinations of the neutron energies agree to within 0.1 keV for neutron energies below 20 keV, to within 0.5 keV at 27.4 keV, and to within 1.3 keV at higher energies. The final values of the neutron energies at  $0^\circ$  at the observed resonances are 8.15, 9.1, 10.9, 13.2, 14.4, 16.7, 19.4, 20.2, 23.3, 25.2, 27.4, 33.4 and 36.7 keV.

The resonances at 8.15 keV, 16.7 keV and 27.4 keV are well suited for detector calibrations. With these three resonances the neutron energy can be varied continuously from 2 keV to 27.4 keV using only angles from  $0^\circ$  to  $80^\circ$ . Neutrons with an energy of 0.5 keV can be produced at an angle of  $120^\circ$ . From the variation of neutron yield with emission angle it is inferred that the angular distributions are isotropic in the centre of mass frame.

The absolute neutron yields from individual resonances have been determined with a calibrated DePangher long counter. For a target  $10 \mu\text{g cm}^{-2}$  thick, bombarded by a proton beam of  $50 \mu\text{A}$ , they vary from about  $3 \times 10^4 \text{ sr}^{-1} \text{ s}^{-1}$  at 2.0 keV to about  $10^5 \text{ sr}^{-1} \text{ s}^{-1}$  at 8.15 keV and at 27.4 keV.

4.4 Neutron yield from the spontaneous fission of  $^{252}\text{Cf}$  (E.J. Axton, A.G. Bardell)  
(WREND 1367-1369)

The average number of neutrons emitted per spontaneous fission of  $^{252}\text{Cf}$  has been derived from separate measurements of the fission and neutron emission rates from different samples of californium. The fission rates were determined by fission-fission coincidence counting<sup>(1)</sup> and the neutron emission rates were measured by the manganese sulphate bath method<sup>(2)</sup>. An account of this work has been accepted for publication in Metrologia with the following abstract:

The average number of neutrons ( $\bar{\nu}$ ) emitted per fission event in the spontaneous fission of  $^{252}\text{Cf}$  has been determined by separate absolute measurements of the fission rate and the neutron emission rate per mg of a solution of californium chloride. The fission rate was determined by a hitherto untried method based on fission-fission coincidences, and

the neutron emission rate was determined by the well known manganese sulphate bath technique. The measurements were carried out during the period 1968 to 1972, and several provisional values of  $\bar{\nu}$  have been released from time to time. The results have now been subjected to a rigorous statistical treatment in which correlations were treated by covariance matrices. The value for  $\bar{\nu}$  (total) for  $^{252}\text{Cf}$  is  $3.7509 \pm 0.0107$  neutrons per fission. This value supersedes all previously released provisional values.

---

- (1) E.J. Axton, A.G. Bardell, and B.N. Audric, J. Nucl. Energy 23 (1969) 457.
- (2) E.J. Axton and A.G. Bardell, Metrologia 18 (1982) 97.

4.5 The ratio of the hydrogen to manganese thermal neutron capture cross-sections and its impact on the measurement of neutron source emission rates by manganese bath techniques (E.J. Axton, A.G. Bardell, S.J. Felgate and E.M.R. Long)

Following the discovery of significant impurity levels in the NPL manganese sulphate bath measuring system<sup>(1)</sup>, the solution was replaced with very pure material and a re-measurement of the hydrogen to manganese thermal neutron capture cross-section ratio was undertaken by a dilution method. The neutron emission rates of the UK national standard Ra-Be ( $\gamma, n$ ) source and of a  $^{252}\text{Cf}$  spontaneous fission source were also measured. The results have been prepared for submission for publication in Metrologia with the following abstract:

The neutron emission rates of the United Kingdom national standard Ra-Be photoneutron source and a  $^{252}\text{Cf}$  spontaneous fission source have been re-measured by the manganese sulphate bath technique. The measurements were performed as part of a dilution experiment in which the hydrogen to manganese capture cross-section ratio was determined following replacement of the original manganese sulphate by purer material. The data have been subjected to rigorous analysis in which the correlations were treated by covariance matrices. These measurements confirm the re-evaluation of previously determined source emission rates published in 1982. A value for the hydrogen to manganese capture cross-section ratio of  $0.02480 \pm 0.00005$  is recommended for use with other manganese baths and other neutron source spectra.

---

- (1) E.J. Axton and A.G. Bardell, Metrologia 18 (1982) 97.

#### 4.6 The thermal neutron capture cross-section of $^{55}\text{Mn}$ (E.J. Axton)

A value for the thermal neutron capture cross-section of  $^{55}\text{Mn}$  has been derived from a recent accurate measurement of the hydrogen to manganese capture cross-section ratio<sup>(1)</sup>, other published values<sup>(2,3)</sup> of this ratio, and published values for the capture cross-sections of hydrogen and manganese<sup>(4)</sup>. The result has been accepted for publication in the Annals of Nuclear Energy with the following abstract:

The ratio of the thermal neutron capture cross-sections of hydrogen and manganese can be measured with high accuracy in the course of measurement of neutron source emission rates in manganese bath systems in which the chemical concentration of the manganese sulphate solution is varied. Three recent measurements of this ratio are used in conjunction with the capture cross-sections for hydrogen and manganese taken from the latest Brookhaven compilation to produce a value for the manganese cross-section with significantly reduced uncertainty. The recommended value is  $13.41 \pm 0.04$  b. A simultaneous evaluation of all standard thermal neutron capture cross-sections would enable some of the improvement in the uncertainty for manganese to influence the values and uncertainties of other cross-sections.

---

(1) E.J. Axton and A.G. Bardell, submitted to Metrologia.

(2) E.J. Axton and A.G. Bardell, Metrologia 18 (1982) 97.

(3) J.R. Smith, S.D. Reeder and R.J. Gehrke, report EPRI-NP-3436 (1984)

(4) S.F. Mughabghab, M. Divadeenam and N.E. Holden, Neutron Cross-Sections 1 (Part A) (Academic Press, 1981).

#### 4.7 Nuclear decay scheme measurements<sup>+</sup> (P. Christmas, W. Gelletly\*, S.M. Judge, R.A. Mercer, D. Smith, S. Waters\*\*, M.J. Woods, S.A. Woods\* Half-lives)

The measurements have been continued for  $^{152,154}\text{Eu}$ , the provisional results now becoming  $4938 \pm 4$  d and  $3139 \pm 2$  d respectively.

$^{237}\text{Np}$

A collaboration is under way with Manchester University to obtain

---

<sup>+</sup> This work forms part of a collaboration with the Medical Research Council (MRC)

\* Schuster Laboratory, University of Manchester.

\*\*MRC Cyclotron Unit, Hammersmith Hospital.

improved decay data for  $^{237}\text{Np}$  by means of  $\gamma$ -ray and  $\beta$ -ray spectrometry. A multi-wire proportional counter and a Bergqvist-type multi-element source have been developed to facilitate conversion electron studies on the NPL iron-free  $\beta$ -ray spectrometer.

$^{207}\text{Bi}$

Measurements are in progress of relative rates of  $\gamma$ -ray and conversion electron emissions from the 570, 1064 and 1770 keV transitions in the decay of  $^{207}\text{Bi}$  with a view to obtaining more precise internal conversion coefficient values.

$^{82}\text{Rb}$

Measurements have been made of the probabilities of positron emission and electron capture in the decay of  $^{82}\text{Rb}$ , and of the emission probability for the 776 keV  $\gamma$ -ray. Provisional values are

positron emission probability        =  $95.73 \pm 0.24\%$

electron-capture probability        =  $4.27 \pm 0.24\%$

776 keV  $\gamma$ -ray emission probability =  $15.66 \pm 0.13\%$

5. DEPARTMENT OF PHYSICS RADIATION CENTRE, UNIVERSITY OF BIRMINGHAM  
(Director: Professor J. Walker)

5.1 Delayed neutron measurements (J.G. Owen, J. Walker, D.R. Weaver and S.J. Chilton)  
(WREND 979)

5.1.1 Further delayed neutron spectrum measurements

The Birmingham Dynamitron accelerator has been used at 3 MV to generate intense neutron fluxes from the  $\text{Be(d,n)}$  reaction for the bombardment of a sample of  $^{235}\text{U}$ . Delayed neutron spectra have been measured by pulsing the deuteron beam, variation of the timing cycle being used to emphasise different groups within the Keepin scheme<sup>(1)</sup>. Once analysed, these measurements should provide new information on delayed neutron group spectra.

5.1.2 Comparison of existing data

Analysis of delayed neutron spectra measured at different incident neutron energies and reported previously (see UKNDC(84)P111, p.101 and ref.2) has been extended to include the calculation of covariance matrices after the spectra have been normalised and then rebinned to give a standard energy grouping. Previously, each of our spectra had been presented in energy groups determined by the experimental conditions and was therefore different for each incident neutron energy. In order to make a detailed comparison of the results, it is necessary to reallocate the individual spectra to fixed energy groups; a 30 keV width with the first group starting at 30 keV has been chosen because it matches the resolution obtained in the experiments. The reallocation of intensity was done by a straightforward linear reapportionment between the initial and final group structures. The rebinned spectra have been subtracted from each other to produce difference distributions, and the calculations of the full covariance error matrices for these distributions are nearly complete. The matrices are required to determine the significance of variations between the original spectra.

5.1.3 Improved utilisation of data from delayed neutron measurements

When measuring delayed neutron spectra with  $^3\text{He}$  spectrometers, both pulse amplitude and rise-time have been recorded (see UKNDC(84)P111, p.101 and refs. 2 and 3). In this way, events which correspond to  $^3\text{He}$  recoils (and therefore have short rise-times) may be separated from genuine  $^3\text{He(n,p)}^3\text{H}$  events which have longer rise-times in general. Unfortunately,

in discarding the recoil events some  $^3\text{He}(n,p)^3\text{H}$  events are also lost; this is a problem in experiments with low count-rates. A new method is being developed to parameterise the response of the detector including the recoil distribution and hence to unfold the total data set. It is likely that the optimum analysis will combine both the old and new methods, the combination being determined by the balance between the reduction in statistical uncertainty as a result of additional data and the increase in unfolding errors produced by the more complicated response function when recoil events are included.

---

- (1) G.R. Keepin, Physics of Nuclear Kinetics, (Addison Wesley, 1965).
- (2) J. Walker, D.R. Weaver and J.G. Owen, Proc. Int. Conf. Nucl. Data Sci. and Technol., Antwerp, 1982 (ed. Böckhoff) p.265 (Reidel, Dordrecht, 1983).
- (3) J.G. Owen, D.R. Weaver and J. Walker, Nucl. Instr. Meth. 188 (1981) 579.

6. DEPARTMENT OF PHYSICS, UNIVERSITY OF BIRMINGHAM

6.1 The use of a deuterated scintillator for in situ neutron spectrometry  
(T. Williams and M.C. Scott)

Deuterated scintillators (organic scintillators in which the hydrogen is replaced by deuterium) have been used for studies of deuterium break up by nuclear structure physicists but have not previously been used for in situ neutron spectrometry. Unlike proton recoil distributions, deuterium recoil distributions are forward peaked; consequently, it appears possible that, because the resulting response matrix would be more nearly diagonal, the detector might have advantages for in situ spectrometry, where unfolding is required.

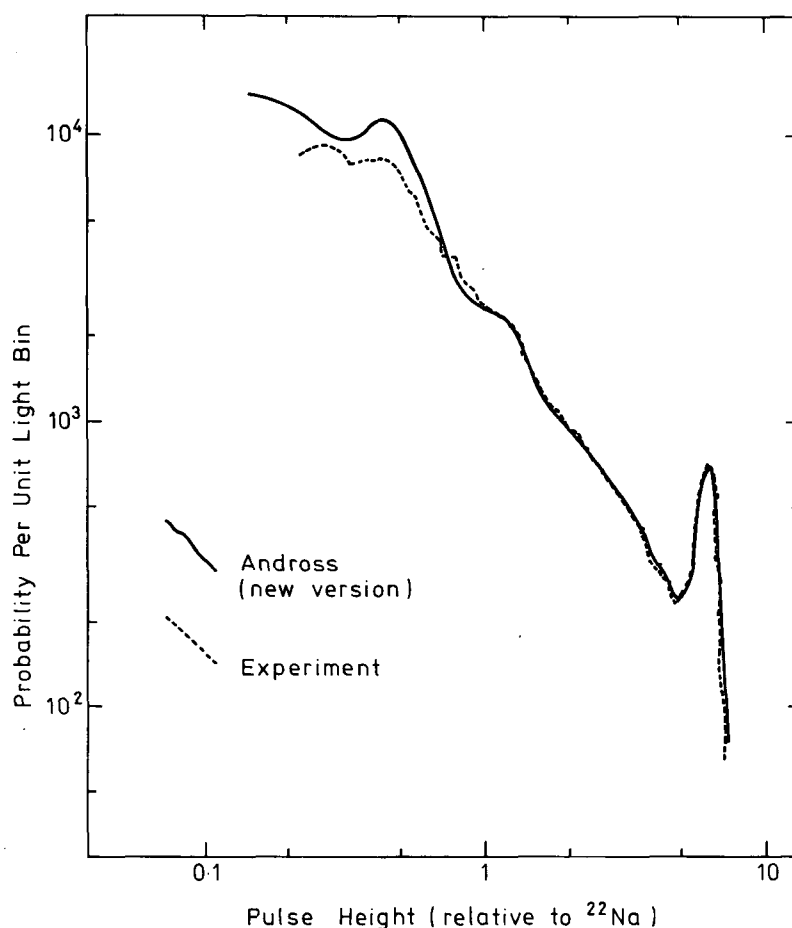


Fig. 6.1 A comparison between an experimental measurement and a response function generated by the new version of the ANDROSS computer program for 14.3 MeV neutrons in deuterated NE213.



Deuterated NE213 was used for the present work, because it had the greatest light output and lowest hydrogen content of the commercially available scintillators investigated. In order to predict the response functions needed for unfolding using the matrix unfolding code FERDOR, the ANDROSS Monte Carlo code<sup>(1)</sup> was used. However comparison between a measured and calculated 14 MeV response function revealed a number of significant differences, as a result of which modifications were made. These were: changes to the  $^{12}\text{C}(n,3\alpha)$  routine; allowance for wall effects; modification of the  $^{12}\text{C}(n,\alpha)^9\text{Be}$  differential cross-sections; and the incorporation of a new deuterium light curve. The resulting agreement between measurement and prediction is good except at low energies, as can be seen from Fig. 6.1. A 14.3 MeV response function was then unfolded using FERDOR and, as may be seen from Fig. 6.2, there was evidence of some systematic bias down to 5 MeV, and the characteristic FERDOR oscillations below this.

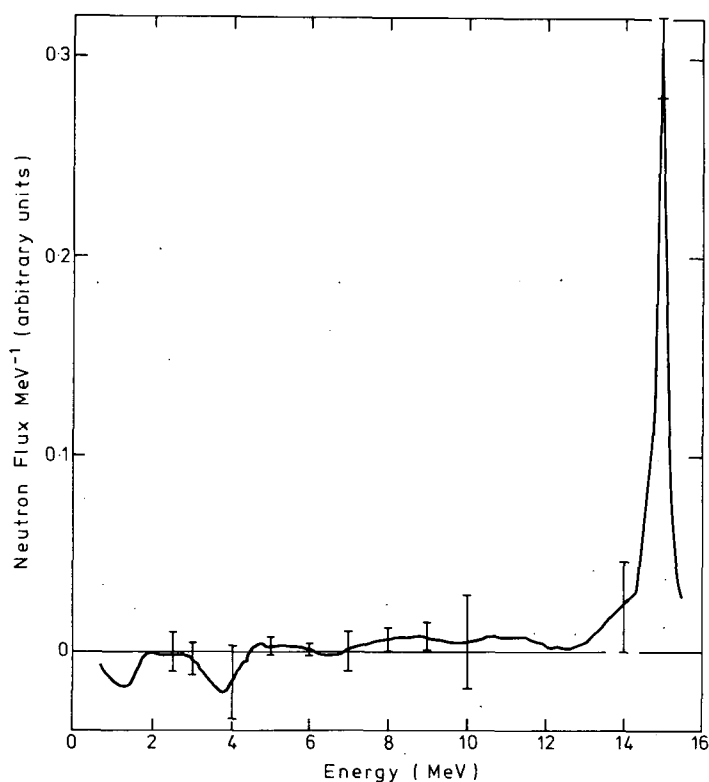


Fig. 6.2 A 14.3 MeV monoenergetic response measured with the new detector and unfolded using FERDOR.

The detector used in these studies, a miniature 1.5 cm<sup>3</sup> glass cell fitted to a 50 cm quartz light pipe, was used for a series of measurements in a LiF fusion reactor assembly consisting of six slabs of aluminium encapsulated LiF each of dimensions 0.9 x 0.9 x 0.15 m with an external <sup>3</sup>H(d,n) neutron source. For comparison purposes, measurements were also made using a very well studied normal (hydrogenated) NE213 scintillator of similar dimensions on a quartz light guide. Both sets of results were unfolded using FERDOR, and the results are shown in Fig. 6.3, where it can be seen that there is reasonable agreement over the peak region and down to 10 MeV or so, but that the deuterated scintillator flux then becomes very oscillatory. The reason for this is not clear, although it is thought to be related to the effect of low energy response function uncertainties.

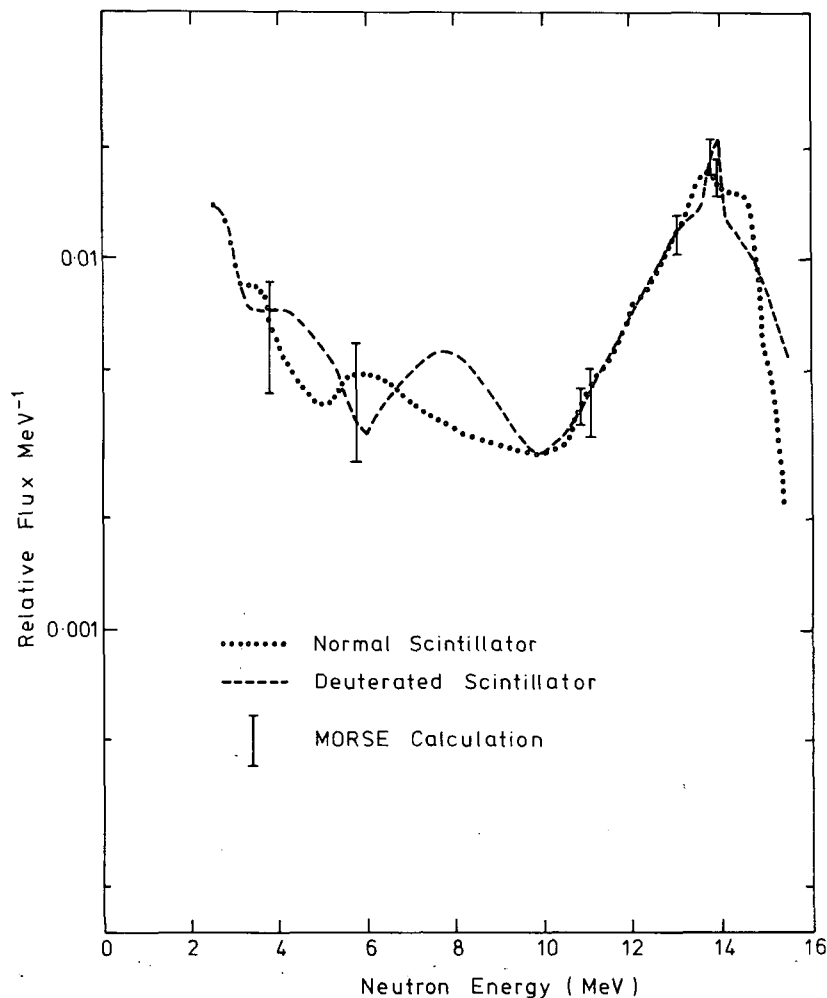


Fig. 6.3 A comparison of the two measurements and the MORSE calculation of neutron spectra for the LiF assembly.

It is concluded that, with the present uncertainties in response function, the deuterated NE213 is marginally less satisfactory for in situ neutron spectrometry than normal NE213. Whether additional effort could be justified to obtain more adequate response functions and to realise the apparent potential of the deuterated scintillator is not clear.

---

(1) C.O. Blyth et al., University of Birmingham report 82-02 (1982).

7. DEPARTMENT OF MATHEMATICS AND PHYSICS, UNIVERSITY OF  
ASTON IN BIRMINGHAM

7.1 Multiple neutron scattering effects in  $^7\text{Li}$  (A.J. Cox and P.C. Warner)  
(WRENDA 51,55))

Future fusion reactors will use lithium as a blanket material in order to breed tritium. Knowledge of the gamma ray production cross-sections associated with 14 MeV neutron interactions in lithium are therefore important for local heating and biological shielding calculations and neutron energy degradation studies. In the present work, the differential cross-sections have been measured for the production of 0.478 MeV gamma rays following the inelastic scattering of 14 MeV neutrons in large samples of LiF. The neutrons were produced using the  $^3\text{H}(\text{d},\text{n})^4\text{He}$  reaction, the deuterons being accelerated by a 150 kV SAMES type accelerator. In order to reduce the background level, the gamma ray signal was gated using a time-of-flight technique based on the alpha particle associated with neutron production. The gamma ray detector was a 3 x 3 inch NaI(Tl) scintillator coupled to a 56AVP photomultiplier.

Scattering samples were positioned 25 cm from the tritium target, and gamma rays were detected at scattering angles between  $30^\circ$  and  $90^\circ$ . Samples of five different thicknesses were used, the thinnest being 4 cm thick. The scattering samples consisted of powdered LiF contained in aluminium containers. LiF was chosen for its non-corrosive properties and because the energy levels in the fluorine nucleus were well separated from those of the lithium, enabling the gamma ray spectra from the two nuclei to be easily resolved.

Fig. 7.1 shows a typical LiF spectrum. The only gamma ray emitted from  $^7\text{Li}$  is due to the prompt de-excitation of the 0.478 MeV level directly to ground state. All other levels decay directly to ground state by particle emission when excited by 14 MeV neutrons. The 0.478 MeV photopeak is the most prominent feature of the LiF spectrum and is well separated from the fluorine lines which are indicated. Although  $^6\text{Li}$  is a natural isotope of lithium, its abundance is only 7.42% and no gamma rays from this were observed. The angular distribution data were fitted by the even order series  $d\sigma/d\Omega = A_0 + A_2 \cos^2\theta + A_4 \cos^4\theta$  which is consistent with the predictions of the statistical model of the nucleus. The values of the coefficients for 4 and 9 cm thick samples are given in Table 7.1. Isotropy remains even when the sample thickness increases.

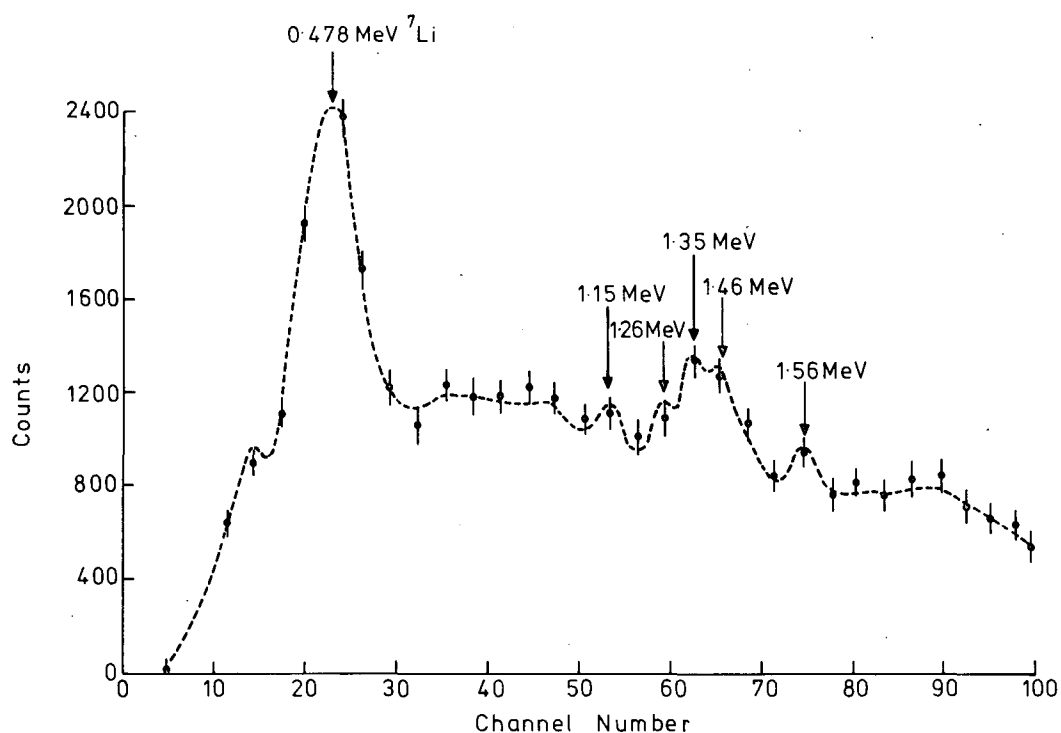


Fig. 7.1 Photon spectrum at 90° for the 9 cm thick LiF sample

Table 7.1

Fits to angular distributions

Coefficients	Sample thickness	
	4 cm	9 cm
$A_0$	$9.2 \pm 2.1$	$11.3 \pm 0.8$
$A_2$	$-1.7 \pm 5.6$	$1.3 \pm 1.5$
$A_4$	$3.9 \pm 7.3$	$-3.2 \pm 2.9$

A comparison between the experimental results for the variation of gamma ray production cross-section at 90° with increasing sample thickness and the predictions of the Monte Carlo computer code MORSE<sup>(1)</sup> is shown in Fig. 7.2, agreement to within  $\pm 11\%$  being achieved. In addition a phenomenological expression was found which is capable of predicting the variation in cross-section with thickness due to multiple scattering effects

to within  $\pm 12\%$ ; the expression is

$$d\sigma/d\Omega = (d\sigma_m/d\Omega - d\sigma_0/d\Omega)(1 - \exp(-\sum_T b)) + d\sigma_0/d\Omega$$

where  $d\sigma/d\Omega$  is the differential gamma ray production cross-section for thickness  $b$ ,  $d\sigma_m/d\Omega$  is the differential gamma ray production cross-section for a theoretically infinitely thick sample,  $d\sigma_0/d\Omega$  is the differential gamma ray production cross-section for a theoretically zero thickness sample, and  $\sum_T$  is the macroscopic total cross-section. The derivation of the above is given by Warner<sup>(2)</sup>. The fitting parameters for the present work were  $d\sigma_m/d\Omega = 19.3$  and  $d\sigma_0/d\Omega = 4.3 \text{ mb sr}^{-1}$ .

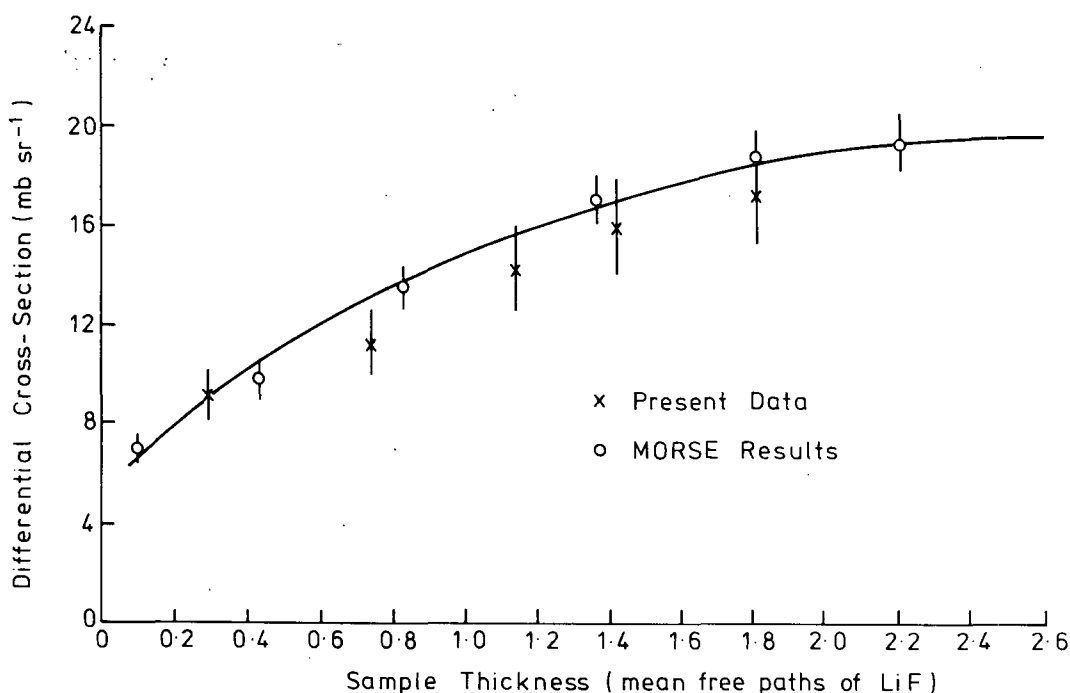


Fig. 7.2 Comparison of the present results with MORSE predictions. The line is the fit to the MORSE predictions described in the text

All other published work concerning the <sup>7</sup>Li gamma ray production cross-section assumes isotropy for the 0.478 MeV gamma ray, and results are only available at 90°. When making comparisons it must be noted that the thinnest sample used in present work (4 cm thick, 0.31 mean free paths) was too thick to exclude multiple scattering. However, Day<sup>(3)</sup> has shown that

multiple scattering is negligible below about 0.2 mean free paths. Hence, by extrapolating the curve of Fig. 7.2 to 0.2 mfp, a comparison between the present datum and those of other workers may be made. Table 7.2 illustrates this. Overall the results agree with each other to within the quoted experimental uncertainties. The results of ORNL<sup>(4)</sup> seem a little high in comparison to our average value of 6.6 mb sr<sup>-1</sup>. One possible reason is that thick samples of LiF were used in this work and the effects of multiple scattering were undercorrected.

Table 7.2

Comparison of thin sample gamma ray production cross-sections at 90°

Reference	$d\sigma/d\Omega$ (mb sr <sup>-1</sup> )
Morgan <sup>(5)</sup>	5.3 ± 0.6
ORNL <sup>(4)</sup>	8.0 ± 1.6
ENDF/B-IV	6.0 (no error quoted)
Present work	6.6 ± 0.9

- 
- (1) MORSE Manual, ORNL-4972 (1975).
  - (2) P.C. Warner, Ph.D. thesis (1984), University of Aston in Birmingham.
  - (3) R.B. Day, Phys. Rev. 102 (1956) 767.
  - (4) J.K. Dickens et al., ORNL-TM-4538 (1974).
  - (5) G.L. Morgan, ORNL-TM-6247 (1978).

## 8. DEPARTMENT OF PHYSICS, UNIVERSITY OF EDINBURCH

### 8.1 The polarization and differential cross-section for elastic scattering of 3 MeV neutrons (R.B. Galloway and H. Savalooni) (WRENDA 1004,1005)

The programme of measurements of the angular dependence of polarization due to elastic scattering and of the elastic differential cross-section for 3 MeV neutrons is continuing (see UKNDC(84)P111, p.109). The measurements are made at 7° intervals from 20° to 167° using the 24 detector fast neutron polarimeter<sup>(1)</sup>. Measurements have been made during the past year on Sn, Sb, I, Te and In. These measurements along with previous measurements on U, Bi, Pb, Tl, Hg and W are being compared with the results of optical model, Hauser-Feshbach and coupled channels calculations.

---

(1) J.E.M. Annand and R.B. Galloway, Nucl. Instr. Meth. 206 (1983) 431.

### 8.2 Polarization of neutrons from the ${}^7\text{Li}(d,n){}^8\text{Be}$ reaction (R.B. Galloway and A.M. Ghazarian)

This work (see UKNDC(84)P111, p.109) has been completed and an account of it has been published<sup>(1)</sup>.

---

(1) R.B. Galloway and A.M. Ghazarian, Phys. Rev. C 29 (1984) 2349.

### 8.3 2.5 MeV neutron elastic and inelastic differential scattering cross-sections (M.N. Erduran and R.B. Galloway) (WRENDA 660,812)

These measurements using proton recoil spectrum unfolding (see UKNDC(84)P111, p.109) have provided elastic and inelastic differential cross-sections at 10° intervals from 20° to 150° for Bi, Hg, I, Sn and In. Final stages of the analysis and of comparison with previous measurements and with model calculations are in progress.

### 8.4 Inelastic scattering of 14 MeV neutrons by Bi (R.B. Galloway and J. Rahighi)

An associated particle time-of-flight system has been developed using neutrons from the  ${}^3\text{H}(d,n){}^4\text{He}$  reaction for 14 MeV neutron scattering studies. The flight path is 13 m long with a large volume time-compensated neutron detector to provide adequate efficiency to measure differential cross-sections of a few mb sr<sup>-1</sup>. The energy resolution at 14 MeV is 250 keV. Measurements of the differential cross-section for scattering by Bi for states up to 8 MeV excitation energy are in progress.



## 9. NUCLEAR PHYSICS LABORATORY, UNIVERSITY OF OXFORD

### 9.1 Neutron inelastic scattering

#### 9.1.1 The inelastic scattering of neutrons by $^{238}\text{U}$ (P.E. Hodgson and A.M. Kobos)

This work, described last year (UKNDC(84)P111, p.111) is being published in Nuclear Science and Engineering.

#### 9.1.2 The inelastic scattering of neutrons by $^{232}\text{Th}$ (A.M. Street and P.E. Hodgson)

The method previously used to analyse the inelastic scattering of neutrons by  $^{238}\text{U}$  by separating the cross-sections into compound nucleus and direct interaction components has been applied to the corresponding data for  $^{232}\text{Th}$ . The fission and capture channels are now included explicitly. The excitation functions for eighteen states up to 2.5 MeV were analysed, together with two angular distributions at 2.5 MeV. A paper describing this work has been submitted to Nuclear Science and Engineering.

### 9.2 The neutron optical potential (P.E. Hodgson)

The review paper described last year (UKNDC(84)P111, p.111) has been published<sup>(1)</sup>.

A paper<sup>(2)</sup> has been written with the following abstract:

The present status of the phenomenological neutron optical potential is briefly reviewed, with particular attention to the dependence on the nuclear asymmetry. It is shown that the conventional parametrisation is inadequate and some possible improvements are discussed. These improvements are of two types: firstly a more flexible global parametrisation and secondly some ways of incorporating data relating to each particular nucleus. Two ways of doing this are proposed, using the RMS matter radius to improve the real potential and the nuclear level density to improve the imaginary potential.

---

(1) P.E. Hodgson, Rep. Prog. Phys. 47 (1984) 613-654.

(2) P.E. Hodgson, Conf. on Neutron-Nucleus Collisions - A Probe of Nuclear Structure, Ohio, Sep. 1984.

### 9.3 Neutron reaction cross-section calculations (D. Wilmore (AERE Harwell) and P.E. Hodgson)

#### 9.3.1 Neutron scattering and reactions on $^{59}\text{Co}$ from 1 to 20 MeV

A report<sup>(1)</sup> has been written with the following abstract:

The cross-sections of all the more important reaction channels for neutrons on  $^{59}\text{Co}$  are calculated and the results compared with the experimental data. The optical model with standard parameters is used to obtain the differential elastic scattering cross-section, and the total and reaction cross-section. The Weisskoff-Ewing, Hauser-Feshbach and Feshbach-Kerman-Koonin theories are used to evaluate the compound and statistical multistep pre-compound contributions to the inelastic scattering cross-section. Several other reaction channels, in particular the (n,2n), (n,p) and (n, $\alpha$ ), are also calculated using one or more of these theories, and the sensitivities of the cross-sections to the input parameters are discussed.

---

(1) D. Wilmore and P.E. Hodgson, Harwell report AERE-R 11439.

#### 9.3.2 Neutron scattering and reactions on $^{93}\text{Nb}$ from 1 to 20 MeV

An analysis is being made of neutron reactions on  $^{93}\text{Nb}$  using the methods previously applied to  $^{59}\text{Co}$ .

### 9.4 Pre-equilibrium processes

#### 9.4.1 Pre-equilibrium processes in the reactions of neutrons on $^{59}\text{Co}$ and $^{93}\text{Nb}$ (G.M. Field, R. Bonetti\* and P.E. Hodgson)

The statistical multistep compound (SMC) and statistical multistep direct (SND) theories of Feshbach, Kerman and Koonin (FKK) are being used to analyse the energy and angular distributions of neutrons inelastically scattered by  $^{59}\text{Co}$  and  $^{93}\text{Nb}$  in the energy range 8 - 14 MeV. In all cases an acceptable fit to the experimental data is obtained, essentially without arbitrarily adjusted parameters. The cross-section of the (n,p) reaction is also calculated, and while the energy spectra are in good accord with the data, there is still some uncertainty about the absolute magnitudes.

---

\*Istituto di Fisica Applicata Generale, Milano, Italy

9.4.2 Pre-equilibrium processes in nuclear reactions (P.E. Hodgson,  
G.M. Field, H. Gruppelaar\* and P. Nagel\*\*

A paper<sup>(1)</sup> is being written with the following abstract:

The semi-classical and quantum mechanical theories of pre-equilibrium processes in nuclear reactions are reviewed, with special attention to the exciton, unified and hybrid models, and the Feshbach-Kerman-Koonin quantum mechanical theory. The results of the 'International Nuclear Model and Code Comparison of Pre-equilibrium Effects' carried out under the auspices of the NEA Data Bank are presented and the physical bases and approximations of the models are discussed. The quantum mechanical theory is described and compared with the semi-classical models.

Selected data for pre-equilibrium processes in  $^{59}\text{Co}$  and  $^{93}\text{Nb}$  are analysed using both the semi-classical models and the quantum mechanical theory and their reliabilities for fitting and prediction are compared. The future development of analyses of pre-equilibrium processes is discussed with particular reference to the scopes of the various models and their optimum areas of applicability.

---

(1) Int. Conf. on Nucl. Data for Basic and Appl. Sci., Santa Fe, May 1985.

---

\*Netherlands Energy Research Foundation ECN, Petten, Netherlands

\*\*NEA Data Bank, Gif-sur-Yvette, France

## 10. DEPARTMENT OF PHYSICS, UNIVERSITY OF LIVERPOOL

### 10.1 Nuclear data evaluation (P.D. Forsyth and N.J. Ward)

Data evaluation work at Liverpool continued as usual during the early part of the year. In April the Nuclear Structure and Decay Data (NSDD) Advisory Group Meeting was held at Karlsruhe, West Germany. At this meeting Liverpool regretfully relinquished its responsibility for the mass-chains  $A = 65 - 74$  primarily because of insufficient man-power. It was proposed to continue evaluating mass-chains in the rare-earth or cerium regions on an ad hoc basis, subject to the agreement of the evaluation centre with responsibility for the particular mass-chain concerned.

The mass-chain  $A = 66$  was published early in 1984 and the evaluation of  $A = 65$  was submitted for publication in September. This marked the completion of the first cycle of evaluations of the mass range  $A = 65 - 74$  since the NSDD network was started. It also marked a halt in evaluation activities at Liverpool, at least for the time being, owing to the resignation of Dr. N.J. Ward, the one full-time evaluator.